MEASURING AND MODELING STREAM AND AIR TEMPERATURE

RELATIONSHIPS IN A MULTI-LAND USE WATERSHED OF THE CENTRAL

UNITED STATES

_____

A Thesis Presented to the

Faculty of the Graduate

School at the University of

Missouri

_____

In Partial Fulfillment of the

Requirements for the Degree

Master of Science

_____

by

SEAN J. ZEIGER

Dr. Jason A. Hubbart, Thesis Supervisor

JULY 2014

The undersigned, appointed by the dean of the Graduate School, have examined the

thesis entitled

MEASURING AND MODELING STREAM AND AIR TEMPERATURE RELATIONSHIPS IN A MULTI-LAND USE WATERSHED OF THE CENTRAL UNITED STATES

presented by Sean J. Zeiger,

a candidate for the degree of Master of Science,

and hereby certify that, in their opinion, it is worthy of acceptance.

_____

Dr. Jason A. Hubbart

_____

Dr. Stephen H. Anderson

_____

Dr. Michael C. Stambaugh

DEDICATION

I dedicate this thesis to my wife, Bonnie S. Zeiger, and my son, Asher J. Zeiger.

You are the most special people in my life and I appreciate all that you have sacrificed so

that I could complete this work.

ACKNOWLEDGMENTS

TABLE OF CONTENTS

LIST OF FIGURES

LIST OF TABLES

MEASURING AND MODELING STREAM AND AIR TEMPERATURE
RELATIONSHIPS IN A MULTI-LAND USE WATERSHED OF THE CENTRAL
UNITED STATES

Sean J. Zeiger

Dr. Jason A. Hubbart, Thesis Supervisor

ABSRACT

A nested-scale experimental watershed study design approach was used in an urban watershed of the central U.S. to investigate stream water temperature (T_w) variability during water year's 2011, 2012, and 2013. Drought conditions were observed during water year 2012 when total annual precipitation was approximately 340 mm less than the 30 year record. Sudden increases of >1 °C within a 15 minute time interval in T_w (T_w surges) following summer thunderstorms were observed at urban sites. Differences in mean T_w between gauging sites were significantly ($p=0.02$) correlated to urban land use and downstream distance as discharge increased. Linear and nonlinear regression analyses were performed between T_w and air temperature (T_a) data at time scales ranging from 15 minute to seasonal time steps. Additionally, the linear T_w model used in the Soil and Water Assessment Tool (SWAT), and a new processed based T_w model that accounts for hydrology were evaluated. Significant ($p>0.05$) differences in model efficiency were not found between the linear T_w model used in SWAT and the new process based T_w model. Results from this study will provide land managers with quantitative information and T_w models needed to make informed management decisions and improve water quality in urban watersheds.

CHAPTER I

INTRODUCTION

THE IMPORTANCE OF STREAM WATER TEMPERATURE

Stream water temperature (T_w) is an important water quality variable because of its effects on nearly all aspects of aquatic ecosystems (Subehi et al. 2010). Temperature affects physical and chemical properties of water, and biological processes in aquatic ecosystems (Bogan et al. 2004). For example, temperature affects the physical state, density, pressure, conductivity / resistivity, and solubility of water. Additionally, chemical / biochemical reaction rates (e.g. redox reactions) in aquatic systems are dependent on T_w. Thus, T_w affects nearly every biological process in aquatic systems including cell growth, reproduction, digestion, photosynthesis, respiration. Stream water temperature also affects the absorption, distribution, metabolism, and excretion of chemicals (including toxins) in aquatic organisms (Subehi et al. 2010).

Many water quality parameters are directly or indirectly influenced by T_w including, but not limited to, suspended / dissolved solids, nutrient concentrations, dissolved oxygen (DO), and biological oxygen demand (BOD) (Webb et al. 2008, McClain et al. 1998). As an example, the effect of increased T_w on dissolved oxygen supply due to decreased solubility of water coupled with increased microbial activity is a classic example of a water quality problem affected by increased T_w.

According to Henry's law, T_w regulates the amount of DO water can hold. Dissolved oxygen concentrations decrease with increases in T_w. Microbial activity also increases with increased T_w (McClain et al. 1998). Too much heat, however, can denature

proteins in microbial cells leading to disruption of microbial activity or even cell death (McClain et al. 1998). As microbial activity increases, microbial communities require more DO to meet BOD. When increased microbial activity results in DO levels lower than BOD, aquatic communities become stressed for DO. Low DO levels can cause reproductive problems ranging from birth defects to mortality in heterotrophic aquatic species (Cox, 2003). Additionally, heterotrophic aquatic species can asphyxiate without enough DO (Anka-Lufford et al. 2007).

When T_w reaches 32 to 40 °C most North American freshwater fish species will perish (Nelson and Palmer, 2007; Beitinger et al. 2000). A Thermal Maximum (TM) water quality T_w standard of 32 °C has been used for many states in the U.S.A. (Gu et al. 1999). Dinan (1992) justified a threshold of 35 °C as a temperature that is closer to Critical Thermal Maximum (CTM) than the 32 °C standard for many fish species in Platte River, Nebraska (Gu et al. 1999). At CTM ectotherms experience muscular spasms that they cannot escape from leading to the organism's death (Hutchison, 1961). It is important that T_w does not exceed TM because of the relationship between aquatic ecosystem health and elevated T_w. It is therefore critical to understand the independent and interacting natural processes and anthropogenic impacts that affect T_w regimes for effective management and sustainability of aquatic ecosystem health (Caissie, 2006).

IMPACTS ON STREAM WATER TEMPERATURE REGIMES

Natural processes that affect T_w regimes

Stream water temperature (T_w) regimes are affected by four primary factors including meteorological conditions (i.e. solar radiation, air temperature, etc.),

topography, stream discharge, and streambed interactions (e.g. hyporheic exchange) (Figure 1). Meteorological conditions usually account for the majority of heat inputs (Webb et al. 2008; Caissie, 2006). For example, T_w regimes are governed by seasonal and diel (i.e. 24 hour) cycles in solar radiation input (Erickson and Stefan, 2000). Seasonal cycles of solar radiation input are a result of the tilt of the Earth's axis (Zachos et al. 2001), while diel cycles in solar radiation input are largely a result of the rotation of the Earth (Wahr, 1988). Other factors that affect solar radiation regimes include the Earth's movement and position relative to the Sun (Bennett, 1990).

The relationship between solar radiation regimes and T_w has been studied to better understand the physical processes that affect T_w regimes. Studies by Webb and Zhang (1997, 1999) quantified heat fluxes that control T_w fluctuations. Results showed that solar radiation accounted for more than 70% of stream water heating. Sensible heat flux between the stream water and the atmosphere was also a significant source of energy that contributed 10.3% of advected heat inputs and 13.6% of non-advected heat inputs.

Topography is also important for influencing T_w primarily because they influence atmospheric conditions. A review by Ward (1985) discussed the importance of topographic factors including longitude and altitude on temperature regimes. Further, a study by Webb et al. (1995) concluded that valley and channel morphology, riparian vegetation, and geology, can influence stream exposure to atmospheric conditions including wind and solar radiation. Topography and atmospheric conditions also affect stream discharge.

Meteorological Conditions	Topography
solar radiation	upland shading
air temperature	riparian vegetation
wind speed / humidity	geology (bedrock)
precipitation (rain / snow)	aspect (stream orientation)
evaporation / condensation	latitude / altitude
phase change (e.g. melting)	

Stream Water Temperature

Stream Discharge	Streambed Interactions
volume of water	conduction (sediment)
slope / water falls	longwave radiation (sediment)
turbulence	hyporheic exchange
inflow / outflow	goundwater input
friction (streambed)	

Figure 1. Four primary factors that affect stream water temperature regimes recreated after Caissie, 2006.

Stream water temperature regimes are controlled by meteorological conditions (e.g. solar radiation, and T_a), particularly during low flow periods. But, hydrologic factors (e.g. volume of water, source of water) dominate during high flow periods. As discharge increases, streams are more thermally stable and less responsive to changes in meteorological conditions, in part, because of the high specific heat capacity of water (4.184 J/g °C). Additionally, residence times decrease as flow rates increase. Decreased

residence times decrease stream interaction with the atmosphere (Erickson and Stefan, 2000).

Heat exchange processes at the stream / streambed interface can be important inputs and outputs of stream heat fluxes. Friction between the stream and the bed / banks can affect T_w regimes especially where large amounts of topographic shading and steep channel slopes are present (Webb et al. 2008). Webb and Zhang (2004) showed friction accounted for the majority of stream heat inputs during winter months in four streams located in South-West England. Groundwater inflows affect T_w regimes, generally increasing T_w in winter months and decreasing T_w in summer months (Webb et al. 2008).

Anthropogenic impacts that affect T_w regimes

Anthropogenic impacts on T_w regimes of aquatic ecosystems include (but are not limited to) deforestation (Doyle and Shields, 2012), flow alteration (Sinokrot and Gulliver, 2000), and thermal pollution (Mohseni et al. 1999, Herb et al. 2008). For example, deforestation of riparian zones has been shown to alter T_w significantly ($P<0.05$), particularly during summer months, when T_w can increase as much as 8.8 °C (Webb et al. 2008; Gomi et al. 2006). The vegetation canopy in riparian zones attenuates radiation that can lead to stream heating by increasing net radiation at the stream surface (Moore et al. 2005; Webb et al. 2008). For example, a recent study by Bulliner (2011) in a central U.S. hardwood forest concluded that any thinning of forested riparian zones could result in stream water heating by increasing net radiation.

Flow alteration / reduction associated with increased impervious surfaces can alter T_w regimes. Sinokrot and Gulliver (2000) noted during a four year study (summer 1991

to summer 1994) in Platte River at Shelton, Nebraska [population 1,074 (USCB, 1012)] that as discharge decreased the number of days T_w was above 32 °C increased by approximately 4 days per 5.6 m^3/s (Sinokrot and Gulliver, 2000). Stream water temperature exceeded the 32 °C thermal maximum (threshold for potential mortality of North American freshwater fishes) and the 35 °C "critical thermal maximum" at four hydrometeorological stations for an average of 57 days, and 14 days, respectively. One of four hydroclimate stations in the study recorded a maximum of 101 days during which T_w was above 32 °C, and 26 days above 35 °C. Stream water temperature was shown to be inversely proportional to stream discharge when heat capacity of water (4.184 J/g °C) and heat input were held constant (Gu et al. 1999). Stream water temperature can exceed 32 °C particularly during hot dry summer months when incoming solar radiation is high and base flow rates are low (Sinokrot and Gulliver, 2000).

Previous studies showed that independent and interacting physical hydrologic and land use practices impact aquatic ecosystems with thermal pollution (Webb et al. 2003; Nelson and Palmer, 2007; Webb et al. 2008; Kaushal et al. 2010). For example, increases in impervious surfaces were shown to increase T_w (Webb et al. 2008; Kaushal et al. 2010) in part due to re-emitted heat energy from those surfaces heating stormwater runoff. Additionally, urban heat island effects on local climate can increase surrounding air temperature (T_a) by as much as 6 °C (Lin et al. 2008). A study by Akyuz et al. (2004), showed "a distinct urban influence" on T_a where the difference in monthly maximum T_a ranged from 1.5 to 3.5 °C between urban and rural sites in Columbia, Missouri, U.S.A. Another study in Columbia, Missouri, U.S.A., by Hubbart et al. (2014) showed an urban heat island effect on local climate during 1995 to 2013 where significant differences

(p<0.001) in mean air temperature and relative humidity ranged from 13.47 °C and 12.89

°C, and 69.11% and 72.51% in urban and rural sites, respectively.

Studies showed heated stormwater runoff from impervious surfaces following

summer thunderstorms cause sudden increases (surges) in T_w (Hester and Baumen, 2012;

Rice et al. 2011; Anderson et al. 2011; Nelson and Palmer, 2007). The surges in T_w were,

attributed to reduced shading associated with deforestation, and the conduction of heat

energy from impervious surfaces to stormwater runoff. Rice et al. (2011) showed during

January 2007 to October 2010, in Boone Creek (a headwater stream) in the Town of

Boone, North Carolina, U.S.A., that increased impervious surfaces from 13.7 to 24.3%

caused an increase of summer and winter T_w by 4 to 5 °C and 3 to 4 °C, respectively.

There were 44 sudden rises (surges) in T_w from heated stormwater runoff (>1 °C increase

within 15 minutes) recorded showing mean T_w surges that ranged from 1.9 to 3.7 °C with

a mean surge duration of more than 3 hours. Another study in Boone Creek, North

Carolina, USA, by Anderson et al. (2011) showed 71 temperature surges with a mean T_w

surge of 2.39 °C and a maximum increase of 6.36 °C during four summers of years 2006,

2007, 2008, and 2010. Nelson and Palmer (2007) used multiple regression techniques to

model the effects of T_w increases due to summer thunder storms in urbanizing watersheds

in a three year study (summers of 2002, 2003, and 2004) within the Piedmont region of

Maryland north of Washington DC. Thirty-seven sudden rises in T_w were detected

subsequent to summer thunder storm generated stormwater runoff (>2 °C increase in 30

minutes) with an average T_w surge and surge duration of 3.7 °C and 2.8 hours,

respectively. Maximum T_w surge and surge duration was 7.4 °C and 7.6 hours

respectively. Hester and Baumen (2012) measured T_w surges at a stormwater outfall at

Stroubles Creek located in Blacksburg, Virginia U.S.A. during June to August 2009. A

total of 15 T_w surges showed a mean T_w surge of 2.8 °C, a maximum T_w surge of 8.1 °C,

and a peak surge temperature of 25.2 °C. Mean surge duration was approximately 2

hours.

MODELING STREAM WATER TEMPERATURE

A considerable amount of research has been conducted to develop predictive

models to foretell future effects of natural and anthropogenic impacts (including

urbanization and global warming) on T_w regimes. Caissie (2006) and Benyahya et al.

(2007) reviewed three main groups of models used for T_w predictions, including: 1)

deterministic models; 2) stochastic models; and 3) regression models.

Deterministic T_w models include physical models that use an energy balance

approach to quantify heat transfer between a stream and its surrounding environment.

Deterministic models, while robust and highly transferable, require measurements of all

physical hydroclimate parameters making model development expensive because of costs

associated with instruments (sensors, data loggers, etc.) and labor (installation,

maintenance, etc.) (Caissie, 2006; Benyahya et al. 2007).

Stochastic models have been used to analyze long term (annual) and short term

(diel) T_w fluctuations (Webb and Walling, 1993; Caissie, 2006). Stochastic models have

been shown to predict T_w reliably at daily intervals, generally within 2 °C, but are

computationally demanding (Caissie, 2006). Regression models (e.g. simple linear

regression or nonlinear regression) are stochastic models that can be created using the

least squares method (Dong et al. 1998). The least squares method minimizes the sum of

squared deviations for each individual observed y value from a best fit line or curve.

Stream water temperature linear regression models, developed using the least squares

method generally follow a format as follows (Caissie, 2006; Caissie et al. 2007):

$$T_w = b_0 + b_1 * x \qquad (1)$$

where T_w is stream water temperature, b_1 is the independent variable (e.g. T_a), b_0 is T_w at

the y-intercept, and x is the slope of the linear relationship between the dependent

variable and the independent variable.

    Nonlinear regression models are more arithmetically complex than simple linear

regression models making them potentially more difficult for land managers to create and

utilize. Nonlinear regression models can be used to model nonlinear T_w / T_a relationships

with the following equation (Mohseni et al. 1998; Webb et al. 2003):

$$T_w = \mu + \frac{\alpha + \mu}{1 + e^{\gamma(\beta - T_a)}} \qquad (2)$$

where T_w is stream water temperature, T_a is air temperature, α is maximum T_w, μ is

minimum T_w, β is T_a at the inflection point of the function, γ is the steepest slope of the

function, and e (Euler's number) is 2.71828. The nonlinear equation shown in Figure 2 is

an s-curve function characterized by two curves. The inflection point separates the two

curves in the function. Below the inflection point, the curve is positive increasing from

left to right. Above the inflection point, the curve is negative decreasing from left to right.

The steepest slope of the function γ is a function of the slope $tan\theta$ at the point of

inflection:

$$\gamma = \frac{4 \, tan\theta}{\alpha - \mu} \qquad (3)$$

where γ is the steepest slope of the function, α is maximum T_w, and μ is minimum T_w.
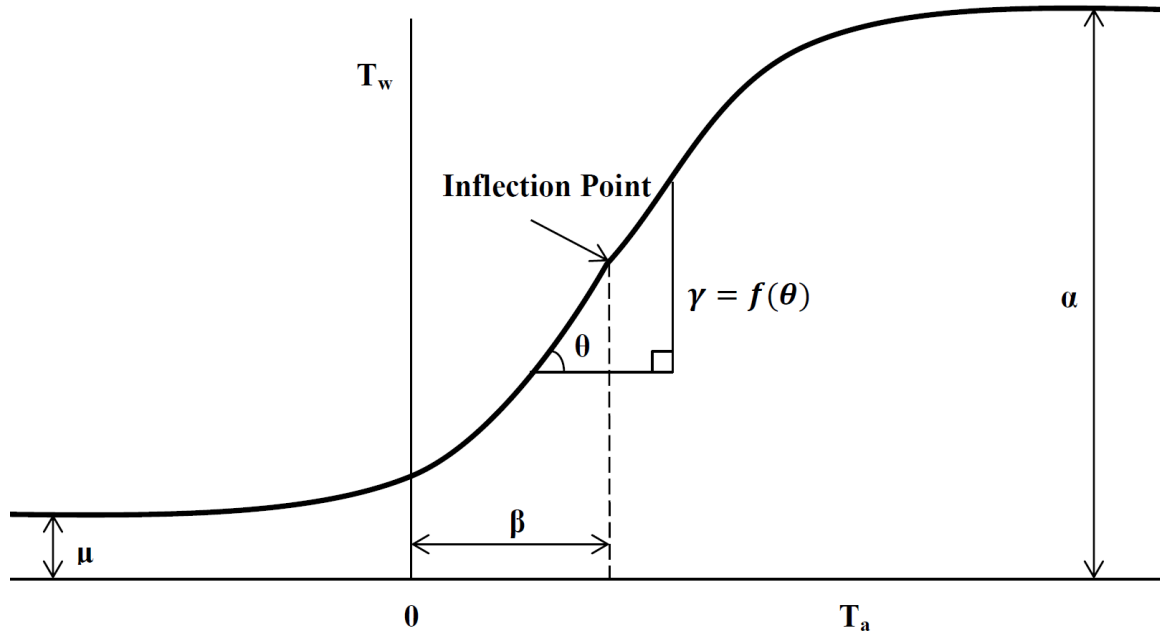
Figure 2. Representation of nonlinear stream and air temperature equation recreated after Mohseni et al. (1998).

Stream and air temperature relationships

After a T_w regression model is created, the model can be used to predict T_w by imputing the appropriate independent variable (e.g. T_a) into the model and then solving the model equation. Observed stream water temperature data are rare and more difficult to obtain compared to air temperature (Stefan and Preud'homme, 1993). Given its availability, and significant correlation with T_w, T_a is commonly used as an independent variable to predict T_w with regression modeling techniques (Caissie, 2006). Mohseni (1999) made the following statement that supports the use of T_a data to predict T_w:

> *"Regressions between water temperatures at individual stream gauging stations and air temperatures at nearby weather stations provide the easiest practical method to estimate stream temperatures for the entire United States."*

While linear and nonlinear T_w regression models dependent on only T_a are attractive because of ease of use and availability of data, there are limitations. For example, T_w regression models do not work as well at sub-daily time steps, or when air temperature is >25 °C. Stream and air temperature relationships are affected by time scale (Erickson and Stefan, 2001).

Stream water temperature regression models have been used to predict T_w at hourly, daily, weekly, monthly, and seasonal time steps (Stefan and Preud'homme, 1993; Erickson and Stefan, 2000; Webb et al. 2003). Erickson and Stefan (2000) showed time scale affected stream and air temperature relationships. The range of the data sets decreased when averaged. Meaning, the maximums decreased and the minimums increased. Air temperature had a greater diel and seasonal range than T_w mainly because of the specific heat capacity of water. Thus, T_a is affected more by averaging causing a slight counter clockwise rotation of the best fit line in linear regression analyses (Erickson and Stefan, 2000). Therefore, the slope of the best fit lines (linear coefficient *a*) increased and the y-intercept (linear coefficient *b*) decreased as time step increased.

Time lag has also been shown to affect stream and air temperature relationships. "Time lag" is a term used to describe the lagged response of T_w relative to T_a. Stream water temperature lags behind fluctuations in T_a (Figure 3) due to the time it takes water to absorb thermal energy from its surroundings (i.e. thermal inertia) (Stefan and Preud'homme, 1993). Webb et al. (2003) showed that accounting for time lag improved r^2 values by 3.6 to 8.5% in regression analysis. Time lag was shown to increase with watershed scale by a range of 2 hours (h) to 6 h, because as volume of water increases so does stream thermal capacity, thereby affecting the response time of T_w to changes in

surrounding T_a (Webb et al. 2003). Stefan and Preud'homme (1993) used regression analysis techniques for 11 streams in the Mississippi River Basin to predict T_w with T_a data at daily and weekly time intervals. Time lag increased with stream depth from hours to days in length. Accounting for time lag slightly increased r^2 values by 0.03 to 0.07, and decreased the mean standard deviation of predicted T_w by 0.04 degrees at daily intervals. There was not a time lag effect for weekly intervals. Stefan and Preud'homme (1993) concluded that time lag was directly proportional to average stream depth. Ultimately, accounting for time lag has been shown to improve model accuracy when investigating T_w / T_a relationships at timescales less than weekly intervals.
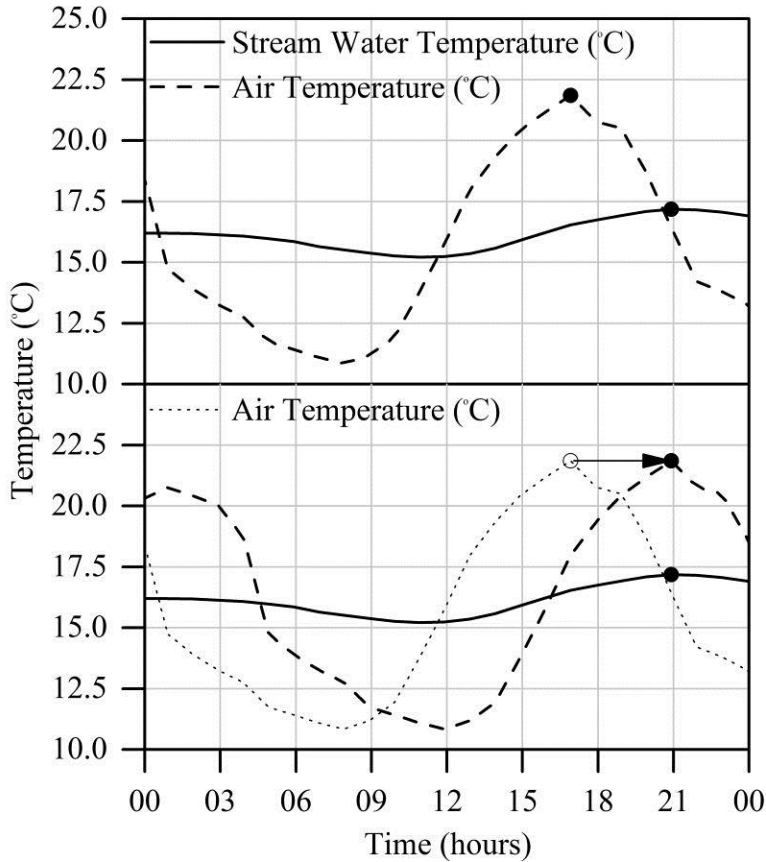
Figure 3. An example of time lag between stream water temperature and air temperature and how the temperature time series can be synchronized is shown. The black points denote peak temperatures. On top, air temperature peaks at 17:00 hours and stream water temperature peaks at 21:00 hours. The two time series were synchronized by shifting the air temperature time series forward by 4 hours.

Accounting for latent heat exchange has also been shown to improve model accuracy. The relationship between T_w / T_a is linear between 5 and 20 °C, but energy required for phase change of water causes departure from linearity (Mohseni et al. 1998; Mohseni et al. 1999; Webb et al. 2003). For example, nonlinear relationships in T_w / T_a regressions are, in part, attributable to latent heat exchange at the stream surface at temperatures above 20 °C, (latent heat of vaporization), and below 5 °C (latent heat of fusion).

Previous studies showed that using nonlinear T_w / T_a regressions to account for the effects of latent heat exchange result in slightly greater level of explained variance than simple linear relationships (Mohseni et al. 1998; Webb et al. 2003). Mohseni et al. (1998) fitted nonlinear regression models to weekly T_w / T_a data collected from 584 USGS stream gauging stations and nearby weather stations located in the contiguous United States. Results showed an average coefficient of determination of 0.93 ± 0.01 for 89% of the stream gauging stations. Webb et al. (2003) showed nonlinear T_w / T_a regressions at hourly time steps with increased r^2 values of 1.3 to 0.8%. At daily and weekly time steps, however, there was not significant evidence to support a nonlinear T_w / T_a relationship.

The effects of discharge

Discharge can affect T_w (as previously presented) and T_w / T_a regression analyses. Webb et al. (2003) used regression modeling techniques to study the T_w / T_a relationship and modulation by discharge in the United Kingdom. Reduced flow was usually found to increase levels of explained variance in T_w / T_a regression analyses at hourly, daily, and weekly time steps for all study catchments considered by an average of 1.7, 7.7, and 4.7%, respectively. While reduced flow greatly affected levels of explained variance for T_w / T_a regression analyses in smaller catchments, larger catchments were only slightly affected by reduced flow. For example, r^2 values decreased by 0.8% in T_w / T_a regression analyses at hourly time steps for the River Barle catchment (128 km^2) and only slightly increased by 0.6% the River Exe catchment (601 km^2). Webb et al. (2003) explained that reduced discharge decreases stream thermal capacity (i.e. specific heat capacity), which

in turn increases stream response to temperature changes of the surrounding environment (Stefan and Preud'homme, 1993; Webb et al. 2003). Heat exchange rates at both the stream water-atmosphere and stream water-streambed interfaces are influenced by stream width to depth ratios, which affect surface area (i.e. stream / air surface interface) to volume ratios (Brown et al. 2005; Poole and Berman, 2001). Other previous studies investigated the effects of stream boundaries and inflows (e.g. reservoirs and groundwater inflows) on the relationship between T_w and T_a.

Erickson and Stefan (2000) showed that T_w / T_a relationships are affected by various factors including, but not limited to, impoundments and reservoirs, groundwater interaction, and thermal effluent (e.g. hydroelectric dams, and wastewater). The T_w / T_a relationship is lost when the temperature and volume of inflows from impoundments and reservoirs, groundwater sources, and thermal effluent are drastically different from stream conditions. Impoundments and reservoirs have stratified water temperature. Water at the surface in the epilimnion (i.e. the upper layer of water in a thermally stratified lake) is affected by meteorological conditions, but not water below the surface in the hypolimnion (the denser bottom layer of water in a thermally stratified lake). Therefore, the T_w / T_a relationship downstream can be weakened when impoundments and reservoirs release large volumes of water from the hypolimnion. Residence times can also affect T_w / T_a relationships because stream interaction with the atmosphere decreases as residence time decreases (Erickson and Stefan, 2000). Stream water temperature regression models need to account for hydrology.

MODELING STREAM WATER TEMPERATURE WITH SWAT

The Soil and Water Assessment Tool (SWAT) is a physically based, daily time step, deterministic model that uses commonly available input data (i.e. topography, soils, land use, and meteorological data) and regression modeling techniques (e.g. linear regression) to predict long term impacts of land management practices on water yield, sediment yield, and chemical agriculture yields (Neitsch et al. 2005). SWAT simulates components of watershed hydrology including snowmelt, groundwater flow, soil water lateral flow, discharge, and surface water runoff. SWAT was designed to simulate management strategies in large ungauged basins thereby saving time and money making the model an economical choice for land managers (Arnold et al. 2012). To test the SWAT models capability of simulating streamflow in ungauged basins, Srinivasan et al. (2010) used SWAT to simulate streamflow in the Upper Mississippi River Basin (UMRB) without calibration. Results showed r^2 ranged from 0.78 to 0.99 on an annual scale and 0.29 to 0.81 on a monthly scale.

To model in-stream water quality and biological processes, SWAT requires daily estimates of T_w. The currently available 2012 version of SWAT (SWAT 2012) uses a linear regression T_w model, developed by Stefan and Preud'homme (1993), to predict T_w:

$$T_w(t) = 5.0 + 0.75 T_a \tag{4}$$

where T_w is stream water temperature (°C), T_a is air temperature (°C), and t is time (daily).

Equation 4 was generated using average coefficients from linear regression analyses that were performed by Stefan and Preud'homme (1993) using stream water temperature data collected from 11 streams in the Mississippi River basin and

corresponding T_a data collected from weather stations ranging in distances of 0 to 144 miles from the rivers.

Stefan and Preud'homme (1993) showed the average standard deviation between observed and simulated T_w was 2.7 °C using equation 4. The average standard deviation was 2.1 °C using equations derived for each stream individually. Thus, it was reported advantageous to develop an equation for each stream individually, or to use a relationship calculated for a stream of similar size and climate.

Stefan and Prud'homme (1993) showed lower standard deviations between observed and simulated T_w were obtained from smaller rivers (rivers with lower discharge). For example, average discharge of Straight River was 1.3 m^3/s and the standard deviation between observed and simulated T_w was 1.8 °C, while average discharge at Mississippi River was 317 m^3/s and standard deviation between observed and simulated T_w was 4.4 °C.

A major limitation associated with Equation 4, the original SWAT T_w regression model, was linear regression models do not account for the damping temperature amplitudes caused by thermal inertia of water as discharge increases. Another limitation reported by Ficklin et al. (2012) was that the original SWAT T_w model does not consider the effects of watershed hydrology (e.g. snowmelt, groundwater flow, soil water lateral flow, discharge, and surface water runoff) on T_w.

Ficklin et al. (2012) proposed a new process based SWAT T_w model that accounts for T_a, snowmelt, groundwater flow, soil water lateral flow, discharge, and surface water runoff. All of the input data required to run the Ficklin et al. (2012) T_w model is generated by SWAT 2012. Three components are considered including T_w and amount of

17

the local water contribution within the subbasin, the temperature and volume of inflows from upstream subbasin(s), and heat transfer at the stream surface during the streamflow travel time in the subbasin. Stream water temperature and the amount of local water contribution within the subbasin are derived with the following equation:

$$Tw_{local} = \frac{(T_{snow}sub\_snow)+(T_{gw}sub\_gw)+(\lambda T_{air.lag})(sub\_surq+sub\_latq)}{sub\_wyld} \quad (5)$$

where *sub_snow* is snowmelt volume ($m^3\ d^{-1}$), *sub_gw* is groundwater flow ($m^3\ d^{-1}$), *sub_surq* is surface water runoff ($m^3\ d^{-1}$), *sub_latq* is soil water lateral flow ($m^3\ d^{-1}$), and *sub_wyld* is total water yield within the subbasin. Lambda (λ) is a calibration coefficient relating $T_{air.lag}$ and sub_latq and sub_surq. $T_{air.lag}$ is the average daily T_a with lag (°C). T_{snow} is the temperature of inflows from snowmelt (0.1°C), and T_{gw} is groundwater temperature (°C) (Ficklin et al. 2012).

The temperature and amount of inflow from upstream subbasin(s) is derived with the following equation:

$$Tw_{initial} = \frac{(Tw_{upstream}(Q_{outlet}-sub\_wyld)+Tw_{local}sub\_wyld}{Q_{outlet}} \quad (6)$$

where *$Tw_{upstream}$* is water temperature of streamflow entering the subbasin (°C), *Q_{outlet}* is discharge at the outlet ($m^3\ d^{-1}$). For headwater streams *$Tw_{initial}$* equals *Tw_{local}* (Ficklin et al. 2012).

The heat transfer at the stream water surface during the streamflow travel time in the subbasin is derived with the following equations:

$$T_w = Tw_{initial} + (T_{air} - Tw_{initial})K(TT) \quad \text{if} \quad T_{air} > 0, \quad (7)$$

$$T_w = Tw_{initial} + [(T_{air} + \varepsilon) - Tw_{initial}]K(TT) \quad \text{if} \quad T_{air} < 0, \quad (8)$$

where T_{air} is the mean daily temperature (°C), K (1/h) is a bulk coefficient of heat transfer ranging from 0 to 1, TT is travel time (hourly) of water through the subbasin, and ε is a coefficient that accounts for T_w pulses when T_{air} is less than 0 °C (Ficklin et al. 2012).

The Ficklin et al. (2012) T_w model and the original SWAT T_w model were tested on seven streams located in the costal and mountainous regions of western United States (Washington, Oregon, Idaho, and northern California). The Ficklin et al. (2012) T_w model showed better predictions than the original SWAT T_w model. The Ficklin et al. (2012) T_w model produced a seven stream average Nash-Sutcliffe efficiency coefficient (NSE) and mean error (ME) of 0.81 and -0.69 °C, respectively, during the calibration period and 0.82 and -0.63 °C, respectively, during the validation period. The original SWAT T_w model (equation 4) produced a seven stream average NSE of –0.27 and ME of 3.21 °C during the calibration period and a NSE of -0.26 and ME of 3.02 °C during the validation period. NSE values range from -∞ to 1 where a value of 1 corresponds to a perfect match of modeled output and observed data. The lower the NSE value the less accurate the model. NSE values >0.50 are considered sufficient when simulating at a monthly time step (Moriasi et al. 2007). Lower ME values are desirable with a ME value of 0 corresponding to a perfect score.

STATEMENT OF NEED

Research is needed to improve mechanistic understanding of the relationships between natural and anthropogenic processes that control T_w (Webb et al. 2008), and ultimately the relationship between T_w and T_a (Caissie, 2006). Such an understanding is increasingly important as urban land use continues to alter aquatic ecosystem health

(Anderson et al. 2011). There is, however, a lack of long term high resolution data in low order urban streams mainly because of the difficulty of maintaining gauging sites in "flashy" urban catchments (Anderson et al. 2011; Nelson and Palmer, 2007). Validated T_w models that are useful in urban streams are needed to aid in the protection of water quality, thereby providing local land managers with the knowledge to make informed management decisions in the central United States. Practical T_w regression models dependent on T_a are an attractive choice, but there is controversy on the accuracy of T_w regression model output as discharge increases and time scale decreases. Therefore, T_w regression model outputs need to be evaluated against observed T_w data and the effect of increased discharge and land use on the T_w / T_a relationship needs to be quantitatively characterized. Stefan and Preud'homme (1993) showed the magnitude of error associated with daily and weekly T_w regression models dependent on T_a, but there remains a need to investigate the error associated with T_w regression models at sub-daily time scales because information showing diel variation of T_w can be important in ecologic modeling and water quality investigations. Finally, the Ficklin et al. (2012) T_w model produced better predictions than the original SWAT T_w model in seven coastal and mountainous regions of the western United States; however, the models have not been tested in the central United States where hydrogeological and land use interactions may be different.

OBJECTIVES

The overall objective of the following research was to investigate T_w variability due to land use and validate T_w models using time series data collected in a multi-land use urbanizing watershed in the central United States. Sub objectives included: 1) test for

20

significant differences in T_w between five stream gauging sites each with different land uses, 2) compare T_w / T_a relationships between five stream gauging sites each with different land uses, 3) compare T_w / T_a relationships at 15 minute, hourly, daily, weekly, monthly, and seasonal time scales, 4) quantitatively characterize the significance of the effects of discharge in the T_w / T_a relationship, 5) test the daily T_w model utilized in the SWAT 2012, and the new T_w model developed by Ficklin et al. (2012) with observed hydroclimate data from five stream gauging sites each with different land uses, and 6) test sub-daily T_w linear and nonlinear regression models with observed hydroclimatic data from five stream gauging sites each with different land uses.

HYPOTHESES

1.) H_o: T_w will not be significantly different (CI=95%) between land use types.

H_a: T_w will be significantly different (CI=95%) between land use types.

2.) H_o: T_w / T_a relationships will not be significantly different (CI=95%) between study stream sites.

H_a: T_w / T_a relationships will be significantly different (CI=95%) between study stream sites.

3.) H_o: T_w / T_a relationships will not be significantly different (CI=95%) as time step increases.

H_a: T_w / T_a relationships will be significantly different (CI=95%) as time step increases.

4.) H_o: T_w / T_a relationships will not be significantly different (CI=95%) as discharge increases.

H_a: T_w / T_a relationships will be significantly different (CI=95%) as discharge increases.

5.) H_o: Model evaluation results from the sub-daily linear T_w models and the nonlinear T_w models will not be significantly different (CI=95%).

H_a: Model evaluation results from the sub-daily linear and nonlinear T_w models will be significantly different (CI=95%).

6.) H_o: Model evaluation results from the original SWAT T_w model utilized in SWAT 2012 and the new T_w model developed by Ficklin et al. (2012) will not be significantly different (CI=95%).

H_a: Model evaluation results from the original SWAT T_w model utilized in SWAT 2012 and the new T_w model developed by Ficklin et al. (2012) will be significantly different (CI=95%).

CHAPTER II

METHODS AND MATERIALS

STUDY SITE

The study watershed for the following research was the Hinkson Creek Watershed

(HCW), located in the Lower Missouri Moreau River Basin (LMMRB, HUC 10300102)

(Figure 4). The HCW is approximately 22,790 ha in size. The headwaters of HCW are

primarily rural agricultural lands and forested areas; however, the lower reaches are

mostly urbanized. Approximately 60% of the city of Columbia, Missouri is located in the

lower elevations of the HCW (MDNR, 2011). The study period for this research included

the 2011, 2012, and 2013 water years. A water year dates from October 1st to September

30th and the year of the water year corresponds to the year at the end of the water year on

September 30th. The population of Columbia, Missouri was estimated to be 113,225 as

per 2012 census results (USCB, 2012). The locations of five hydroclimate monitoring

stations that provided data used for this research are provided in Table 1 and shown in

Figure 4. The reader is referred to Hubbart et al. (2010) for additional information about

the watershed and experimental design. Land use information for the study site is

provided in Table 2.

Table 1. Locations of five nested hydroclimate stations in Hinkson Creek Watershed
located in central Missouri, U.S.A.

Gauging site	Location (meters)
Site #1	922460W 3902363N
Site #2	922793W 3898230N
Site #3	923053W 3894818N
Site #4	923398W 3892783N
Site #5	924001W 3891411N

Table 2. Cumulative contributing area of sub-basins and land use type in the Hinkson Creek Watershed, central Missouri, USA. LULC percent areas are shown in parentheses. All LULC data were obtained from the MSDIS website. The LULC data were collected in 2005.

Subbasin	Total Area (km^2)	Stream Length (km)	Stream Width (m)	Urban (km^2)	Pasture / Crop (km^2)	Forested (km^2)	Wetland/ Water (km^2)
Site #1	77	20	12.2	3.9 (5)	43.9 (57)	27.7 (36)	1.5 (2)
Site #2	101	27	16	6.1 (6)	56.6 (56)	36.4 (36)	2.0 (2)
Site #3	114	32	13.4	12.5 (11)	58.1 (51)	41.0 (36)	2.3 (2)
Site #4	180	40	18.4	28.8 (16)	82.8 (46)	64.8 (36)	3.6 (2)
Site #5	206	49	14.1	47.4 (23)	84.5 (41)	70.0 (34)	4.1 (2)
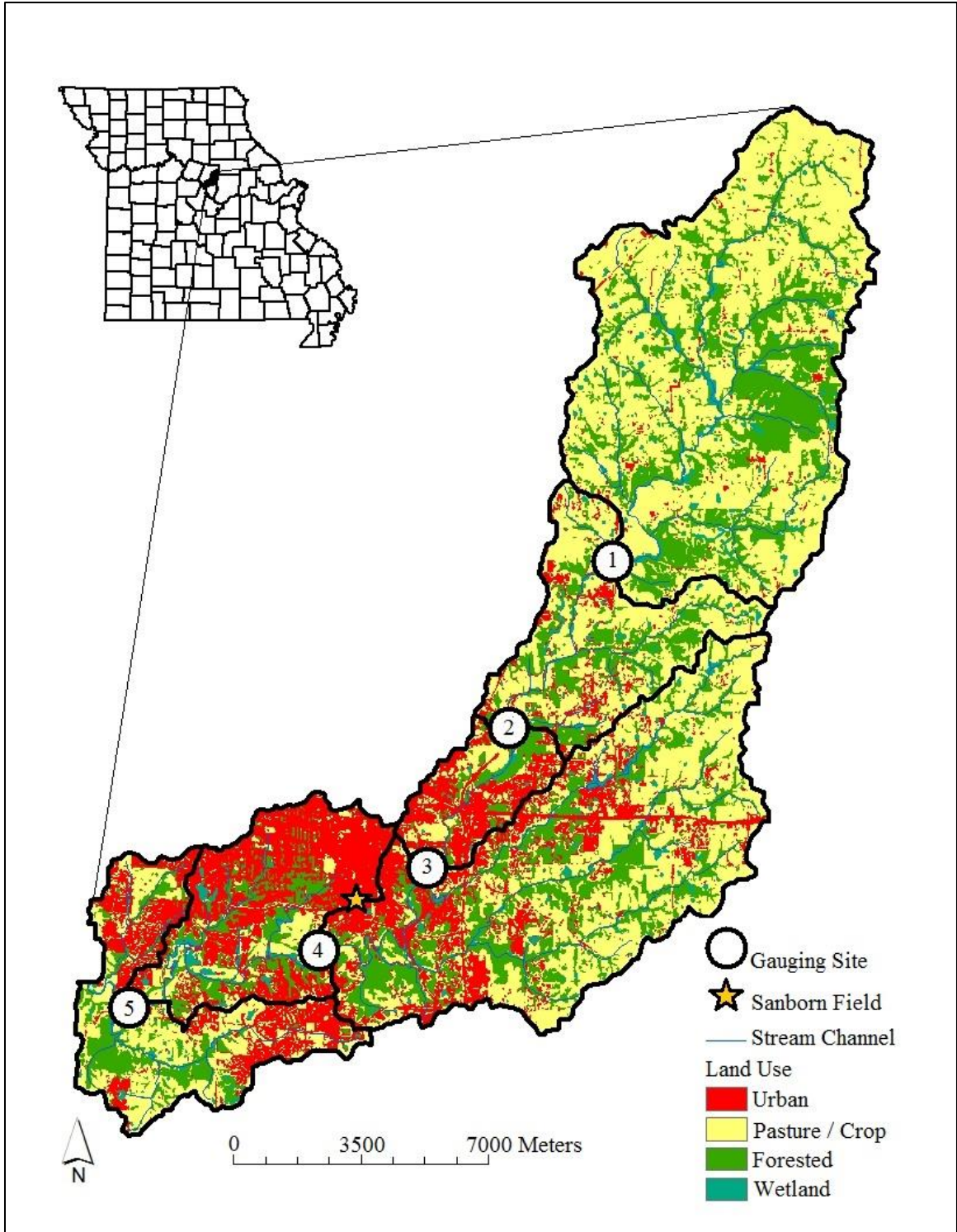
Figure 4. Location of hydroclimate monitoring sites and respective subbasins containing various land use types of the Hinkson Creek Watershed, central Missouri, USA. Sanborn Field meteorological monitoring station is located on the University of Missouri campus.

Climate

Climate in Missouri is dominated by maritime and continental tropical air masses in the summer and continental polar air masses in the winter (Nigh and Shroeder, 2002, Hubbart et al. 2010). Average annual total precipitation was 1082 mm and average annual T_a was 14 °C (30 year record) (Hubbart and Zell, 2013). Data from Sanborn Field climate station (located on University of Missouri campus) indicated average annual total precipitation, mean T_a and total daily solar radiation of 1037 mm, 13.4 °C and 14.5 MJ/m^2, respectively, from 2000 through 2013 in Columbia (14 year record). The wettest months in Missouri are March through June, while the driest months are November to March (Hubbart et al. 2013).

Hydrology

Hinkson Creek (HC) is approximately 42 linear kilometers in length; flowing southwesterly from the headwaters in Hallsville, Missouri through Columbia, Missouri to its confluence with Perche Creek. After its confluence with Perche Creek, Hinkson Creek flows approximately 18 kilometers (including meandering) through Perche Creek to its confluence with Missouri River. Elevation of Hinkson Creek ranges from 274 m above mean sea level in headwater to 177 m above mean sea level at the confluence of Perche Creek (Hubbart et al. 2010; Freeman, 2011). Stage of Hinkson Creek has been intermittently monitored since 1967 at a U.S. Geological Survey gauging station (#06910230) located 122 m downstream of Providence Road in the city of Columbia, MO. U.S. Geological Survey gauging station (#06910230) corresponds to site #4 (Figure 4). Mean annual discharge from 1967-1981, 1986-1991, and 2007-2013 was 1.73 m^3/s.

Four other stream gauge stations, co-located with meteorological sites, were installed in winter 2008 (see sub section "*Nested Hydroclimate Stations*" below for more information.

Soil and vegetation

Soils in the HCW are comprised of poorly drained to well drained prairie-forest transitional soils (Perkins, 1995). Soils in the headwater portion of HCW are loamy loess with an underlying claypan, while soils in the lower reaches of HCW are composed of silty and sandy clay (Chapman et al. 2002). Floodplain alluvial soils in the lower reaches have infiltration rates that vary dramatically from agricultural sites (porosity = 0.5 g/cm^3, bulk density = 1.33 g/cm^3) to bottom land hardwood forest sites (porosity = 0.51 g/cm^3, bulk density = 1.31 g/cm^3) ranging from 0.1 to 126.0 cm/hr, respectively (Hubbart, 2011). Soils outside of the alluvium in the lower reaches are composed of a cherty clay solution residuum corresponding to the Weller-Bardley-Clinkenbeard (CBC) association (Hubbart and Zell, 2013). Upland hardwood forests in the HCW are dominated by oak species. Bottomland hardwood forests in the HCW are dominated by woody species including *Acer saccharinum* (silver maple), *Acer negundo* (boxelder), *Ulmus americana* (American elm), *Populus deltoides* (eastern cottonwood), and *Juglans nigra* (black walnut) (Hubbart et al. 2011), *Salix spp.* (willows), *Betula spp.* (birches), *Platanus occidentalis* (sycamores), *Tilia spp.* (basswoods), and woody shrubs (MDNR 2006).

Water quality

Approximately 39 km of Hinkson Creek was listed as impaired under section 303(d) of the federal Clean Water Act in 1998 (Hubbart et al. 2010). While the pollutant resulting in initial 303(d) listing is listed as *unknown*, the stream is currently deemed impaired for protection of warm water aquatic life (EPA, 2011). Urban land use is suspected to have caused the majority of impairment (EPA, 2011). In 2011 a TMDL was developed for Hinkson Creek that used "storm water runoff as a surrogate for multiple pollutants and stressors associated with urban storm water" (EPA, 2011). Given the lack of understanding pertaining to impairment, further investigation is greatly needed to validate the assumption that stormwater reduction will remediate the water quality problems in HCW. This research investigated T_w because of its known importance pertaining to water quality and aquatic ecosystem health.

Nested-scale experimental watershed study design

Hinkson Creek Watershed was instrumented with a nested-scale experimental watershed study design in fall of 2008 that partitioned the HCW into five subbasins (Hubbart et al. 2010). Each subbasin was characterized by different dominant land use types (e.g. site #1 is mainly agricultural, while site #5 is mainly urban). Hydroclimate stations monitor solar radiation, T_w, T_a, and a suite of additional variables in each subbasin (Hubbart et al. 2013). At the time of the current study, site 1, the largest subbasin at 77 km^2, and site #2 were mostly rural subbasins, while sites #3,# 4, and #5 were primarily urbanized subbasins (see Table 2 above) (Hubbart et al. 2010).

DATA COLLECTION

Hydroclimate data

Solar powered hydroclimatic stations were installed at the top of the stream bank at each gauging site. Data loggers were housed in an air tight box located >2 m above the top of the stream bank. Rechargeable desiccant bags were placed inside the air tight boxes to keep water vapor from damaging the electronic data loggers. Desiccant bags were changed approximately once every two months. Solar panels and sensors that measure meteorological variables (i.e. rain gauge, pyrometer, anemometer, and T_a / Rh sensors) were installed on steel (pipe) masts three meters above the ground at all sites. In-stream T_w and stage sensors were installed inside of conduit to protect the cables from any potential damage. The conduit for the T_w and stage sensors were buried 10 cm below the soil surface and covered with soil and rip-rap (large rock). The tips of the T_w and stage sensors were located under and over each other (respectively) low enough to record the lowest expected stage. All the instruments required for the current research are described in Table 3. Hydroclimate data were sensed every 30 seconds, and averaged and logged (i.e. stored in Campbell Scientific CR-1000 data loggers) at each site every five minutes.

Table 3. Instrumentation installed at gauging sites along Hinkson Creek, Missouri, USA, and associated variables sensed, necessary for the current work.

Instrument	Measurement	Accuracy
TE525WS Rain Gauge	Precipitation in mm	+1% at 1 in/hr rainfall rate to -3.5% at 2 to 3 in/hr rainfall rate
LI200X, LICOR pyrometer	Solar Radiation in W/m^2	±5%
MET1 034B	Wind speed in m/s and wind direction in degrees	±0.11 m/s at < 10.1 m/s to ±1.1% at >10.1 m/s
Sutron Accubar® Constant Flow Bubble Gauge/Recorder 560133	Water stage in mm	0.02% at 0-25 ft to 0.05% at 26-50 ft
Campbell Scientific, Inc. Model HMP45C Temperature and Relative Humidity Probe with radiation shield	Air temperature in °C and relative humidity in %	±0.2 °C at 20 °C to ±0.5 at <-40 °C and >60 °C
Campbell Scientific, Inc. Model 107 Temperature Probe	Water temperature in °C	±0.2 °C
Thermochron iButtons	Water temperature in °C	±0.1 °C

Sudden rises in T_w due to summer thunderstorms

To investigate urban land use effects on stream heating, Thermochron iButtons (temperature sensors) were deployed during summer 2009 (June 1st to August 31st). Thermochron iButtons are digital temperature sensors that can log up to 2048 data points from 1 to 255 time intervals (Hubbart et al. 2005). The temperature sensors were small (about the size of a stack of five dimes), durable, and produced accurate (±1.0 °C) temperature results making them well suited for hydrologic and water quality research (Hubbart et al. 2005). The temperature sensors were programmed to log T_w data at each location every 15 minute. Each temperature sensor was placed in a 2" by 4" piece of PVC

pipe that was anchored in stormwater drains so that the pipe was oriented with flow. The

PVC pipes served as a radiation shield.

Stage Data and Rating Curves

Each nested hydroclimate station was equipped with a Sutron Accubar® Constant

Flow Bubble Gauge and Recorder designed to measure stage. Stage was measured every

second (Sutron, 2008). One second data were averaged and stored every five minutes.

Rating curves were used to accurately estimate stream discharge by developing a

relationship between stage and equivalent manually measured stream discharge (Dottori

et al. 2009). In the development of a rating curve, stage is the independent variable, and

stream discharge is the dependent variable. For the current research, the incremental cross

section method was used to manually measure stream discharge in order to develop rating

curves. In the development of rating curves, a power function is commonly used (Yu,

2000). A power function was fit to the measured stage and stream discharge data. The

power function is as follows:

$$Q = ah^b \tag{9}$$

where *Q* and *h* are instantaneous stage and stream discharge values and *a* and *b* are

constants (Yu, 2000). Polynomial functions are also commonly used when developing a

rating curve (Herschy, 1985; Krashnikikov, 1987):

$$Q' = \beta_0 + \beta_1 H^1 + \beta_2 H^2 + \cdots + \beta_m H^m \tag{10}$$

where *Q'* is discharge, *β* is a fitted parameter, *H* is stage, and *m* is the exponent of the

polynomial function. A piecewise approximation of stage and flow rate regressions is

recommended when the relationship of stage and flow rate become too complex

(Shiklomanov et al. 2005). In this study, recent rating curves formulated by Freeman (2011), and Scollan (2011), were used to calculate estimates for total stream discharge, and stream discharge statistics (Table 4) (Shiklomanov et al. 2005). Additional cross section data collected in the spring of 2013 were used to update current rating curves.

Table 4. Rating equations for five gauging stations in Hinkson Creek, Missouri, USA. Variables α_0 are constants, α_1 to α_3 are regression coefficients, and κ are exponential constants used in regression equations.

Equation	HCW #1	HCW #2	HCW #3	HCW #4	HCW #5
Linear	(0-0.552)	(0-0.464)	(0-0.120)	(0-0.303)	--
α_1	0.0472	0.4163	1.35902	0.8286	--
Polynomial	(0.552-max)	(0.464-max)	(0.120-0.363)	(0.303-max)	--
α_3	12.794	4.3007	17.57	0.7788	--
α_2	17.502	21.944	7.0615	17.908	--
α_1	10.57	20.288	3.94	9.249	--
α_0	2.6548	4.4526	0.238	1.1784	--
Power	--	--	(0.363-max)	--	(0-max)
α_1	--	--	15.061	--	5.136
κ	--	--	2.5797	--	1.8118

Backwatering

Backwatering in Hinkson Creek was observed during WY 2011 when stage in Missouri River rose above 8.5 m at Booneville, Missouri located approximately 30 km west of Columbia, Missouri. Missouri River discharge was 7363.2 m^3/s at Booneville, Missouri. Measured discharge at HCW site #5 was affected for 111 days (Figure 5) during that time period. The affected discharge data at site #5 were interpolated using measured discharge data from the nearest upstream gauging site, site #4 (USGS gauging station). First, the affected discharge data at site #5 were delineated and deleted in Excel.

Next, a power regression analysis was performed in Excel to calculate the relationship

between discharge data at site #4 and site #5. Finally, the discharge data at site #5 were

interpolated using the following equation from the power regression analysis (n=70)

$(r^2=0.92)$:

$$y = 2.1391x^{0.9014} \qquad (11)$$

where y is discharge at site #5 and x is discharge at site #4.
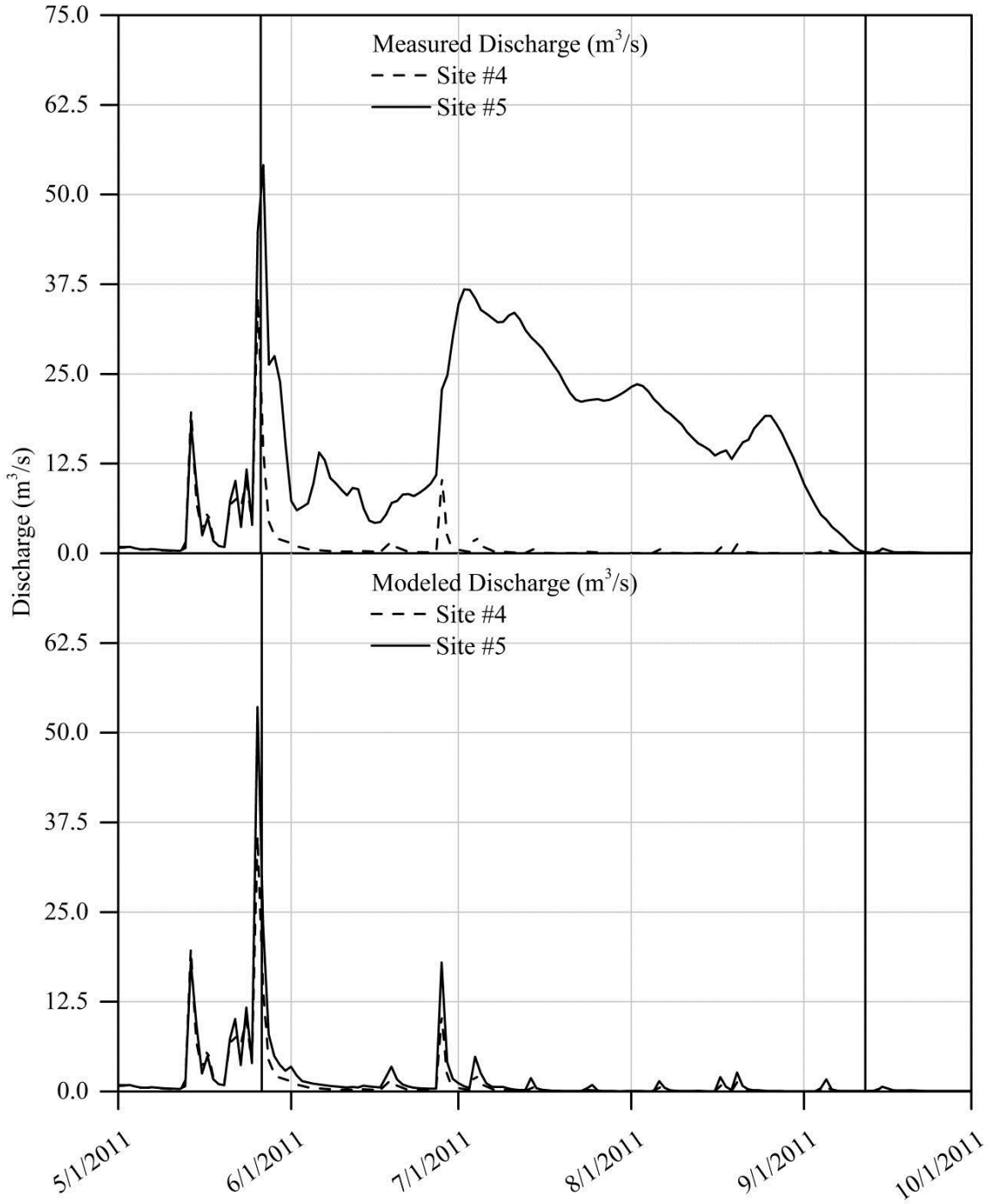
Figure 5. Backwatering phenomenon observed during 111 days of summer 2011 recorded at site #5 located in Hinkson Creek Watershed, Missouri, USA. Black vertical lines delineate a period of back watering that was modeled out using discharge data from site #4 (USGS gauging station number 06910230).

Land use data

Silva and Williams (2001) used an earlier version of ArcGIS (ArcView) to study

land use effects on river quality. For the current study similar analyses methods were

performed, using ESRI© ArcGIS10 software, to determine subbasin areas and land use

cover classes. The Missouri Spatial Data Information Service (MSDIS) website

(http://www.msdis.missouri.edu) contained all necessary LULC data for this project. The

most recent available LULC data (LULC data created in 2005) on the MSDIS website

were used. LULC data are presented in Table 5.

Table 5. Land use land cover (LULC) data for the current research. All LULC data were
obtained from the MSDIS website with the exception of the SSURGO soils data set. The
SSURGO soils data set was acquired from online from NRCS.USDA.gov.

Data	Projected Coordinate System	Feature Class	Units	Year Created
Hydrology	NAD 1983 State Plane Missouri central FIPS 2402	Arc	Meter	2003
LULC	NAD 1983 State Plane Missouri central FIPS 2402	Arc	Meter	2005
County	NAD 1983 State Plane Missouri central FIPS 2402	Arc	Meter	2003
DEM	NAD 1983 UTM Zone 15N	Raster	30 Meter	2003
Soils	NAD 1983 UTM Zone 15N	Raster	30 Meter	2011
State	NAD 1983 UTM Zone 15N	Polygon	Meter	2003

To determine subbasin areas in HCW a point shape file was created from XY

coordinates (Table 1) of the gauging sites in HCW. ESRI© ArcGIS10 spatial analyst

hydrology tools were used to delineate the HCW and its subbasins. Land use/land cover

data were extracted by mask to the extent of a polygon representing the delineated subbasins within the HCW. Finally, tables containing the quantity of each LULC type within each subbasin were exported for further analysis.

DATA ANALYSIS

Hydroclimate data analysis

Hydroclimate data including T_w, T_a, and stream discharge from the 2011, 2012, and 2013 water years were reduced (by averaging the time series data into several time steps) and graphed. The time steps considered were 15 minute, hourly, daily, weekly, monthly, seasonal, and water year. The seasonal time step divided the water year into three seasons; October 1st – January 31st, February 1st – May 31st, and June 1st – September 30th. The water year time step began October 1st and ended September 30th of the following year. Post processing of hydroclimate data to replace missing or erroneous data points was performed as needed with mathematical models using data from the Sanborn Field weather station and USGS gauging station (site #4).

Descriptive statistics were calculated including mean, minimum, maximum, median, and standard deviation of daily hydroclimate data. High resolution (15 minute interval) T_w data were also examined with descriptive statistics, and for the days T_w was above 32 ℃ and 35 ℃ [similar to the work of Sinokrot and Gulliver (2000)]. Additionally, the maximum duration T_w was above 32 ℃ and 35 ℃ was analyzed.

Monk et al. (2008) used one way Analysis of Variance (p>0.05) and Tukey-Kramer multiple comparison test to test for significant differences in hydroclimate measurements between multiple gauging stations. In this study, similar methods were

36

conducted using statistics software (Origin) at a 95% CI (α=0.05). Tukey-Kramer is an effective test for significant difference in means between all sites, like ANOVA, but can elucidate specifically which sites differ. Tukey-Kramer was used for this research because it produces more narrow confidence intervals than other post-hoc multiple comparison tests (Stoline, 1981).

ANOVA is dependent on sample size (n) (Bonett, 2002). As n increases, the observed mean of a sampled population is closer to the "true mean". The true mean is the mean of the population if every individual, or in this case every possible temperature sample, were considered in the calculation. If the observed mean were equal to the true mean, then there would be no doubt that any differences in mean would be "significant", meaning free from the error associated with estimating the true mean with only a small part of the population. However, the observed mean will never equal the true mean when sampling a continuum, no matter how many samples are collected, because a continuum, by definition, is infinite and it's impossible to collect an infinite amount of samples. Therefore, statistical tests like ANOVA were created to be less dependent on sample size to quantitatively test for significant differences in means. As sample size increases, there is a less likely chance that differences in means are due to error associated with estimating the true mean using only a small part of the population. Thus, any differences in observed means are more likely to be significant. There are more costs associated with sampling high resolution data for long time periods compared to low resolution data for short time periods; however, one major benefit is increased n provides an increased confidence that any results derived with the use of statistics are error free, or significant (Peck and Devore, 2012).

Sudden rises in T_w due to summer thunderstorms

As per the work of Nelson and Palmer (2007), temperature time series were examined to quantitatively characterize sudden rises in stormwater temperature (T_w surge) due to summer thunderstorms in stormwater inputs that flow into Hinkson Creek. T_w surges following summer thunderstorms, defined as sudden rises of >1 °C increase in T_w within a 15 minute time period (Anderson et al. 2011), were verified with a TE525WS Rain Gage located <50m from the T_w sensor. Results indicating date and time of surge, pre-surge T_w, peak surge T_w, T_w surge (calculated as the difference between pre-surge and peak surge T_w), and T_w surge duration (defined as the time required for T_w to return to pre-surge T_w) for each sensor were calculated in Excel (Nelson and Palmer, 2007; Rice et al. 2010; Anderson et al. 2011). The summer season (June 1st to August 31st) of stormwater T_w data were analyzed for the summer of 2009. Additionally, in-stream T_w data were analyzed for the 2010, 2011, 2012, and 2013 water years.

The effects of discharge on stream water temperature

The effects of stream discharge on T_w and the T_w / T_a relationship were analyzed by performing statistical analyses above and below median discharge values for each site similar to the work of Webb et al. (2003). Separating mean T_w into different flow classes similar to the methods used by Webb et al. (2003) elucidated T_w at each gauging site in Hinkson Creek relative to flow. The <50% flow class best represented T_w during periods of low flow, or base flow. The >50% flow class best represented stormflows. To investigate T_w during stormflow periods in the current work flow classes >50% were separated into an additional four flow classes (>60, >70, >80, and >90%). The >90%

38

flow class represented peakflows. The 90% flow class was also separated into an additional nine flow classes. The >99% flow class showed T_w when Hinkson Creek was close to or overbank full. Time series mean discharge, T_a, and T_w data were first sorted in ascending order according to discharge value. Then, mean discharge, T_a, and T_w were recorded for each flow class and tested for significant differences (p>0.5).

Stream and air temperature relationships

As mentioned earlier (see introduction), a common method for analyzing T_w and T_a relationships includes development of regression models (Webb et al. 2003; Caissie, 2006; Webb et al. 2008). Therefore, linear regression analyses (equation 1), and nonlinear regression analyses (equation 2) were performed using mean T_w vs. mean T_a data for each site at 15 minute, hourly, daily, weekly, monthly, and seasonal time steps using statistics software (Origin). Results from regression analyses were used to create T_w models.

Because accounting for time lag (Figure 3) with cross-correlation analysis was previously shown to improve results of T_w / T_a regression analysis (Webb et al. 2003), cross-correlation analyses were performed in the current work using the cross correlation function (CCF):

$$R_k = \frac{\sum_{t=1}^{n-k}(x_t-\mu_x)(y_{t+k}-\mu_y)}{s_x s_y} \tag{11}$$

where R_k is the correlation coefficient at lag k, n is the number of observations, t is time, k is the lag, μ_x is mean T_a, μ_y is mean T_w, s_x is computed using the following equation:

$$s_x = \sqrt{\sum_{t=1}^{n}(x - \mu_x)^2} \tag{12}$$

s_y is calculated with the following equation:

$$s_y = \sqrt{\sum_{t=1}^{n}(y - \mu_y)^2} \tag{13}$$

R_k values range from 0 and 1.0. A value of zero is no correlation. A value of 1 is a perfect correlation.

Ultimately, results from the CCF can be used to quantify the optimum amount of time lag between T_a and T_w time series. Cross correlation analyses produced a time series of R_k values for each time lag k. The optimum amount of time lag was the value of k that corresponds with the maximum R_k value in the R_k time series. Once time lag was known, the T_a time series was shifted forward the appropriate amount of time lag. For example, if maximum R_k value in the R_k time series corresponded to $k=1$, then the entire T_a time series was shifted forward one unit of time. Results from cross-correlation analyses were used to improve T_w models.

To further improve T_w models, calibration coefficients were added to the 15 minute linear stream water temperature model. A 15 minute "calibrated linear stream water temperature model" was created in Origin for each gauging site. Sub-daily time series T_w data resembled a sin curve over the course of a day. By adding calibration coefficients to the 15 minute linear T_w models, the amplitude of the sin curve was decreased. Simulated 15 minute stream water temperature estimates were weighted to daily mean T_a for each day of simulation using the following equation:

$$T_w = \alpha(b_0 + b_1 * x) + \beta(\Delta T_a) \tag{14}$$

$$\alpha + \beta = 1 \tag{15}$$

where T_w is stream water temperature, b_1 is the independent variable (e.g. T_a), b_0 is T_w at the y-intercept, x is the slope of the linear relationship between the dependent variable

and the independent variable, ΔT_a is daily mean T_a for the day of simulation, and α and β are calibration coefficients.

The calibrated linear stream water temperature models were forced and calibrated in Excel using observed T_a data from each Hinkson Creek gauging site and linear regression coefficients derived from linear regression analyses (time lag was accounted for). After the model was calibrated at a 15 minute time step, the model outputs were reduced in Excel by averaging 15 minute data to hourly and daily time steps.

The effects of discharge on T_w and T_a relationships

The effects of stream discharge on T_w / T_a relationships were analyzed by performing statistical analyses above and below median discharge values for each site similar to the work of Webb et al. (2003). First, hydroclimate data were separated into 15 different flow classes by sorting time series data sets in ascending order according to discharge value. Then, regression analyses were performed on time series T_w and T_a data for each flow class (Webb et al. 2003). Finally, coefficient of determination values (r^2 values) were compared and contrasted. The r^2 values quantify the total variation in y values attributed to the model relationship (Moriasi et al. 2007).

SWAT modeling

The current SWAT T_w model (SWAT 2012) (equation 4) was manually configured in Microsoft Excel, and forced with T_a data collected from five hydroclimate sites in HCW. Next, the new SWAT T_w model, developed by Ficklin et al. (2012)

(equations 5, 6, 7, and 8) was forced in Microsoft Excel using input data extracted from SWAT 2012.

To acquire the needed forcing data to run the Ficklin et al. (2012) T_w model, a SWAT 2012 project was created using ArcSWAT 2012. The watershed was delineated using the automatic watershed delineation option in ArcSWAT. The needed input files for watershed delineation, land use, soils, and slope are provided above in Table 5. The SSURGO soils input files were edited using the SWAT editor tool found on the SWAT website. The slope classes were defined as a single slope. Weather input data from the five Hinkson Creek hydroclimatic stations and Sanborn Field weather station. When prompted to change "Manning's n" default values, overland flow Manning's n was set to 0.065, and channel flow Manning's n was set to 0.05. Troubleshooting problems encountered while attempting to "Write Input Tables" were addressed by mining online SWAT forums and via email communications with the SWAT development team members Georgie Mitchell, and Nancy Sammons.

Once the SWAT project was successfully parameterized, SWAT model watershed general input data parameters under the pathway "Edit SWAT Input" > "Watershed Data" were edited as follows:

- Potential ET method was "Penman-Monteith"

- Crack flow was set to "Active"

- Channel routing was set to "Muskingum"

- Channel degradation was set to "Active"

- Pesticide routing was left blank.

Hydrologic Response Units (HRU's) files (format .hru) were edited to show land use practices realistic for Hinkson Creek Watershed. Agricultural HRU's were set to a corn-soybean rotation with three fertilization operations (anhydrous ammonia, elemental nitrogen, and elemental phosphorus) and tandem disk tillage. Pasture HRU's were set to a grazing operation. Urban HRU's were set to a fescue growing operation by default, but lawn fertilization and street sweeping operations were scheduled by keying in a schedule into SWAT management operations tab.

SWAT was manually calibrated and validated for flow at a daily time step using discharge data from the five Hinkson Creek gauging sites. Water years 2010, 2011, and 2012 were used for calibration and water year 2013 was used for validation. To enhance the reliability of SWAT model calibration and validation results, SWAT was calibrated at site #5 nearest the watershed outlet as well as the 4 nested subbasins concurrently. Each subbasin was calibrated in order of increasing downstream distance from site #1 in the headwaters to site #5 nearest the watershed outlet. During manual calibration of SWAT several parameters were adjusted including curve number (CN), alpha base flow (ALPHA_BF), SURLAG, and ESCO. The parameters were chosen for adjustment during calibration because they were among the most adjusted parameters for streamflow calibration found in the literature as reported by in a review by Arnold et al. (2012). All CN's (CN2 and CNOP) were increased by 3 simultaneously using the SWAT manual calibration helper tool. The pathway to the SWAT manual calibration helper tool is "SWAT Simulation" > "Manual Calibration Helper". ALPHA_BF was increased by 0.4 in the groundwater input files (.gw). The SURLAG value was set to 1.0 in the basin input files (.bsn). And, ESCO was set to 1.0 using the SWAT manual calibration helper tool.

Model evaluation

Moriasi et al. (2007) suggested the use of three model evaluation criteria to assess

hydrologic model performance including Nash-Sutcliffe efficiency (NSE), ratio of root

mean square error to the standard deviation of observed data (RSR), and percent bias

(PBIAS). In addition to the three model evaluation criteria suggested by Moriasi et al.

(2007), three error indices were used to evaluate model efficiency including mean

absolute error (MAE), mean squared error (MSE) and root mean squared error (RMSE).

Moriasi et al. (2007) suggested general performance ratings for the three aforementioned

model evaluation criteria at a monthly time step (Table 6). To be conservative, the current

research used the same ratings for evaluation of sub-daily and daily model efficiency.

Table 6. Ratings used in this research to quantitatively evaluate sub-daily and daily model efficiency.

Rating	RSR	NSE	PBIAS
Very good	$0.30 < RSR \leq 0.50$	$0.75 < NSE \leq 0.90$	$\pm 5 \leq PBIAS < \pm 10$
Good	$0.50 < RSR \leq 0.60$	$0.65 < NSE \leq 0.75$	$\pm 10 \leq PBIAS < \pm 15$
Satisfactory	$0.60 < RSR \leq 0.70$	$0.50 < NSE \leq 0.65$	$\pm 15 \leq PBIAS < \pm 25$
Unsatisfactory	$RSR > 0.70$	$NSE \leq 0.50$	$PBIAS \geq \pm 25$

Nash-Sutcliffe efficiency tests are used to quantify the variance of observed

versus simulated data relative to a 1:1 best fit line NSE values range between ∞ and one,

where an NSE value of one is a perfect simulation. Any NSE value greater or equal to

zero indicates that the simulated value estimated the constituent of concern better than the

mean observed value. NSE values can be calculated using the following equation:

$$NSE = 1 - \left[\frac{\sum_{i=1}^{n}(Y_i^{obs} - Y_i^{sim})^2}{\sum_{i=1}^{n}(Y_i^{obs} - Y_i^{mean})^2} \right] \qquad (16)$$

where Y_i^{obs} is the *i*th observed datum for the variable being estimated. Y_i^{sim} is the *i*th

simulated datum for the variable being estimated, Y_i^{mean} is the mean of observed data for

the variable being estimated, and *n* is the total number of observations.

Ratio of root mean square error to the standard deviation is an error index

statistic. RSR values of zero equal a perfect simulation. Any RSR value less than 0.50

indicates an acceptable simulation. RSR values can be calculated using the following

equation:

$$RSR = \left[\frac{\sqrt{\sum_{i=1}^{n}(Y_i^{obs} - Y_i^{sim})^2}}{\sqrt{\sum_{i=1}^{n}(Y_i^{obs} - Y_i^{mean})^2}} \right] \qquad (17)$$

where Y_i^{obs} is the *i*th observed datum for the variable being estimated. Y_i^{sim} is the *i*th

simulated datum for the variable being estimated, Y_i^{mean} is the mean of observed data for

the variable being estimated, and *n* is the total number of observations.

Percent bias tests are used to indicate the average tendency of simulated data to be

greater than or less than the observed data. Any negative PBIAS value indicates the

simulated data were greater than the observed data on average. Conversely, any positive

PBIAS value indicates the simulate data were less than the observed data on average. A

PBIAS value of zero is a perfect simulation. PBIAS values can be calculated using the

following equation:

$$PBIAS = \left[\frac{\sum_{i=1}^{n}(Y_i^{obs} - Y_i^{sim}) * 100}{\sum_{i=1}^{n}(Y_i^{obs})} \right] \qquad (18)$$

where Y_i^{obs} is the *i*th observed datum for the variable being estimated. Y_i^{sim} is the *i*th

simulated datum for the variable being estimated, and *n* is the total number of observations.

Mean absolute error (MAE) is estimated to quantify the error in units of observed versus simulated data. MAE values are a measure of the average of the absolute value of the difference between simulated and observed values. MAE values of zero equal a perfect simulation. MAE values can be calculated using the following equation:

$$MAE = \frac{1}{n}\sum_{i=1}^{n}\left|Y_i^{obs} - Y_i^{sim}\right| \tag{19}$$

where Y_i^{obs} is the *i*th observed datum for the variable being estimated. Y_i^{sim} is the *i*th simulated datum for the variable being estimated, and *n* is the total number of observations.

Mean square error is calculated to quantify the error in squared units of observed versus simulated data. MSE values are the average of the squared differences between simulated and observed data. MSE values of zero equal a perfect simulation. NSE values can be calculated using the following equation:

$$MSE = \frac{1}{n}\sum_{i=1}^{n}(Y_i^{obs} - Y_i^{sim})^2 \tag{20}$$

where Y_i^{obs} is the *i*th observed datum for the variable being estimated. Y_i^{sim} is the *i*th simulated datum for the variable being estimated, and *n* is the total number of observations.

Root mean square error is estimated to quantify the error, in squared units of observed versus simulated data. RMSE is the square-root of the average of the squared differences between simulated and observed data. RMSE values of zero equal a perfect simulation. RMSE values can be calculated using the following equation:

$$RMSE = \sqrt{MSE} \tag{21}$$

Finally, graphical representations, and the six aforementioned model evaluation criteria were used to compare the current SWAT T_w model, the Ficklin et al. (2012) T_w model, Hinkson Creek T_w models (linear / nonlinear / calibrated linear), and observed data (2011, 2012 and 2013 water years) collected from five hydroclimate sites in Hinkson Creek.

CHAPTER III

RESULTS

HYDROCLIMATE

Climate

Summary of climate statistics recorded from the five HCW climate stations and the Sanborn Field climate station during the three year study period (WY 2011 – 2013) are shown in Appendix A and descriptive statistics in Table 7. Average annual total precipitation ranged from 803.8 mm at site #5 to 872.1 mm at site #3 with a six site mean of 837.9 mm. Maximum T_a during the study period ranged from 40.8 °C at Sanborn Field to 43.0 °C at site #3 with a mean of 41.9 °C. Mean T_a ranged from 12.3 °C at site #1 to 13.9 °C at Sanborn Field with a six site mean of 13.1 °C. Minimum T_a during the study period ranged from -30.8 °C at site #1 to -19.8 °C at Sanborn Field with a six site mean of -27.2 °C. Mean relative humidity ranged from 65.4% at Sanborn Field to 71.8% at site #1 with a six site mean of 69.3%. Mean wind speed ranged from 0.8 m/s at site #4 to 2.0 m/s at Sanborn Field with a six site mean of 1.3 m/s. Mean daily total solar radiation ranged from 12.9 MJ/m^2 at site #4 to 14.8 MJ/m^2 at site #2 with a six site mean of 13.8 MJ/m^2. There were no significant differences found in daily maximum T_a between sites (p=0.66). There were, however, significant differences found in daily mean T_a (p=0.01) and daily minimum T_a (p<0.01).

Table 7. Summary of daily climate statistics during the study period (WY 2010 – 2013) for six climate stations located in Hinkson Creek Watershed, Missouri, USA. *Precipitation (Precip) data are average annual totals. **Solar radiation data are daily totals. Air Temp = Air Temperature. "St. Dev." is standard deviation.

Climate Data	Daily Statistic	Site #1	Site #2	Site #3	Site #4	Site #5	Sanborn Field
*Precip. (mm)	Annual Total	838.4	826.5	872.1	866.0	803.8	820.4
Air Temp (°C)	Max	31.6	32.2	33.4	32.3	32.3	33.8
	Mean	12.3	12.9	13.5	13.1	13.0	13.9
	Min	-30.8	-30.4	-26.6	-26.7	-29.0	-19.8
	St. Dev.	10.6	10.7	10.7	10.5	10.6	10.6
Relative Humidity (%)	Max	97.7	98.0	98.0	97.1	99.4	98.0
	Mean	71.8	70.3	67.5	70.8	70.0	65.4
	Min	33.6	33.0	32.3	33.5	32.5	32.7
	St. Dev.	11.4	11.3	12.1	10.8	11.0	13.4
Wind Speed (m/s)	Max	5.2	3.8	4.1	3.0	4.1	5.3
	Mean	1.3	1.1	1.2	0.8	1.3	2.0
	Min	0.0	0.0	0.0	0.0	0.0	0.0
	St. Dev.	0.7	0.6	0.6	0.4	0.6	0.7
**Solar Radiation (MJ/m^2)	Max	30.1	31.5	29.2	28.3	29.3	29.3
	Mean	13.8	14.8	13.4	12.9	13.9	14.1
	Min	0.4	0.6	0.8	0.5	0.3	0.5
	St. Dev.	7.8	8.3	7.8	7.3	7.6	7.8

Discharge

A summary of average daily discharge statistics recorded from the five Hinkson Creek (HC) sites during the three year study period (WY 2011 to 2013) is provided in Table 8. Mean discharge ranged from 0.7 m^3/s at site #1 to 2.5 m^3/s at site #5 with a five site mean of 1.3 m^3/s. Maximum discharge ranged from 66.4 m^3/s at site #2 to 137.9 m^3/s at site #5 with a five site mean of 97.6 m^3/s. Median discharge ranged from 0.0 m^3/s at site #1 to 0.4 m^3/s at site #5 with a five site mean of 0.2 m^3/s. Minimum discharge ranged from 0.0 m^3/s at site #1 to 0.1 m^3/s at site #2 with a five site mean of 0.0 m^3/s. There was a significant (p<0.01) difference found in mean discharge between gauging sites.

Drainage area and cumulative percent urban land use accounted for 92.6% of the

explained variance.

Table 8. Summary of average daily discharge (m^3/s) statistics during the study period
(WY 2010 – 2013) for five hydroclimate stations located in Hinkson Creek Watershed,
Missouri, USA. "St. Dev." is standard deviation.

Daily Statistic	Site #1	Site #2	Site #3	Site #4	Site #5
Mean	0.7	0.7	1.0	1.5	2.5
St. Dev.	4.5	4.2	5.3	6.2	10.0
Minimum	0.0	0.1	0.0	0.0	0.0
Median	0.0	0.1	0.1	0.2	0.4
Maximum	82.1	66.4	86.7	114.9	137.9

Stream water temperature

Summary of average daily T_w statistics recorded from the five Hinkson Creek

climate stations during the three year study period (WY 2011 – 2013) are shown in Table

9. Daily mean T_w ranged from 13.7 °C at site #1 to 14.4 °C at site #4 with a five site mean

of 14.2 °C. Daily maximum T_w for the study period ranged from 32.1 °C at site #1 to 36.1

°C at site #3 with a five site mean of 34.4 °C. Daily median T_w ranged from 13.9 °C at

site #1 to 14.6 °C at site #2 with a five site mean of 14.4 °C. Daily minimum T_w for the

study period ranged from 0.4 °C at site #2 to 0.0 °C at site #1 with a five site mean of 0.2

°C.

Daily mean T_w at rural site #1 in the headwaters was lower than all other Hinkson

Creek gauging sites by 0.5 to 0.7 °C (this is within the sensitivity / accuracy of the T_w

sensors). The greatest absolute difference was 0.7 °C between daily mean T_w between site

#1 and #4. Urban site #4 daily mean T_w was higher than all other Hinkson Creek gauging

sites by 0.2 to 0.7 °C. Maximum daily mean T_w was also lower at rural site #1 in the

headwaters compared to all other Hinkson Creek gauging sites by 1.7 to 2.5 °C. Site #4

maximum daily mean T_w was higher than all other Hinkson Creek gauging sites by 0.4 to

2.5 °C. Despite these differences, there were no significant differences found in daily

mean T_w (p=0.51).

Table 9. Summary of average daily stream water temperature (°C) statistics during the
study period (WY 2010 – 2013) for five hydroclimate stations located in Hinkson Creek
Watershed, Missouri, USA. "St. Dev." is standard deviation.

Daily Statistic	Site #1	Site #2	Site #3	Site #4	Site #5
Mean	13.7	14.2	14.2	14.4	14.2
St. Dev.	8.6	9.7	9.5	9.5	9.4
Minimum	0.0	0.4	0.2	0.1	0.1
Median	13.9	14.6	14.6	14.4	14.4
Maximum	32.1	34.7	36.1	33.9	32.9

Stream water temperature data were also analyzed at a 15 minute time step.

Summary of average 15 minute T_w statistics for the entire three year study period, and

each water year (WY 2011 – 2013) are shown in Table 10. Fifteen minute mean T_w

ranged from 13.1 °C at site #1 during WY2013 to 15.7 °C at site #4 during WY 2012

with a five site mean of 14.2 °C for the study period. Fifteen minute maximum T_w ranged

from 27.9 °C at site #1 during WY 2103 to 36.1 °C at site #3 during WY 2011 with a five

site mean of 34.4 °C for the entire study period. Fifteen minute median T_w ranged from

11.9 °C at site #1 during WY2011 to 16.7 °C at site #4 during WY 2012 with a five site

mean of 14.4 °C during the study period. Fifteen minute minimum T_w ranged from 1.0 °C

at site #3 during WY 2013 to 1.2 °C at site #1 with a five site mean of 0.6 °C during the study period.

There were significant differences found in 15 minute mean T_w between gauging sites for the study period (p<0.01), and for each water year investigated (p<0.01). For WY2011, T_w was significantly lower (p=0.01) at site #1 compared to all other Hinkson Creek sites by 0.5 (sites #3 and #4) to 0.6 °C (sites #2 and #5). During WY 2012 mean T_w was significantly lowest at site #1 (14.7 °C) and highest at site #4 (15.7 °C) compared to all other Hinkson Creek sites by 0.6 to 1.0 °C, and 0.3 to 1.0 °C, respectively. During WY 2013 T_w was significantly lower at site #1 compared to all other Hinkson Creek sites (with the exception of site #2) by 0.3 to 0.6 °C. Also, mean T_w was significantly higher at urban site #4 0.3 to 0.6 °C. Fifteen minute maximum T_w was highest at site #3 for every WY of the study period compared to all other Hinkson Creek sites by 1.4 to 4.0 °C. The greatest difference in maximum T_w was between sites #3 and #1. Minimum T_w was higher at site #1 compared to all other Hinkson Creek sites for every WY in this study by 0.4 to 1.0 °C.

Table 10. Summary of average 15 minute stream water temperature (°C) statistics during the study period (WY 2010 – 2013) for five hydroclimate stations located in Hinkson Creek Watershed, Missouri, USA. "Study Period" is a three year average for the study period. "St. Dev." is standard deviation.

	Water Year	Site #1	Site #2	Site #3	Site #4	Site #5
Mean	2011	13.4	14.0	13.9	13.9	14.0
	2012	14.7	15.3	15.4	15.7	15.3
	2013	13.1	13.2	13.4	13.7	13.4
	Study Period	13.7	14.2	14.2	14.4	14.2
St. Dev.	2011	9.5	10.2	10.1	10.0	10.1
	2012	8.1	9.5	9.3	9.2	9.0
	2013	8.3	9.7	9.6	9.2	9.2
	Study Period	8.7	9.8	9.7	9.5	9.4
Minimum	2011	0.3	0.3	0.4	0.4	0.1
	2012	1.2	0.2	1.0	0.6	0.1
	2013	0.0	1.0	1.0	0.1	0.1
	Study Period	0.3	1.0	1.0	0.4	0.1
Median	2011	13.7	14.2	14.1	14.4	14.2
	2012	15.7	16.4	16.4	16.7	16.2
	2013	11.9	12.6	12.8	12.6	12.5
	Study Period	13.9	14.5	14.5	14.6	14.5
Maximum	2011	30.9	33.3	36.1	33.9	32.9
	2012	32.1	34.7	35.9	33.0	32.9
	2013	27.9	30.0	34.2	31.5	31.6
	Study Period	32.1	34.7	36.1	33.9	32.9

15 minute T_w data were also analyzed at a seasonal (winter / spring / summer) time step (Table 11). Mean T_w ranged from 6.3 °C at site #2 during the winter to 24.8 °C at site #4 during the summer. Maximum T_w ranged from 21.6 °C at site #1 during the winter to 36.1 °C at site #3 during the summer. Median T_w ranged from 5.0 °C at site #2 during the winter to 25.3 °C at site #4 during the summer. Minimum T_w ranged from 1.0 °C at site #3 during the winter to 12.3 °C at site #4 in the summer.

There were significant differences ($p < 0.05$) found in 15 minute mean T_w between gauging sites for each season investigated. During the winter seasons, T_w was significantly higher at sites #1 and #4 compared to all other Hinkson Creek sites by 0.3 to 0.5 °C, and 0.4 to 0.6 °C, respectively. During the spring seasons, mean T_w was significantly lower at site #1 compared to all other Hinkson Creek sites by 0.4 to 0.6 °C. During the summer seasons, mean T_w was significantly lower at sites #1 and #5 compared to all other Hinkson Creek sites by 1.3 to 1.7 °C, and 0.2 to 0.4 °C, respectively. During the summer seasons, T_w was significantly higher at site #4 compared to all other Hinkson Creek sites by 0.2 °C to 1.7 °C.

Table 11. Summary of seasonal average stream water temperature (°C) statistics during the study period (WY 2010 – 2013) for five hydroclimate stations located in Hinkson Creek Watershed, Missouri, USA.

Statistic	Season	Site #1	Site #2	Site #3	Site #4	Site #5
Mean	Winter	6.8	6.3	6.5	6.9	6.5
	Spring	11.2	11.6	11.6	11.7	11.8
	Summer	23.1	24.6	24.6	24.8	24.4
St. Dev.	Winter	4.8	6.1	6.1	5.5	5.6
	Spring	7	7.4	7.3	7.3	7.1
	Summer	3.5	3.9	4.2	4	4
Minimum	Winter	0	1	1	0.1	0.1
	Spring	0.3	0.1	0.1	0.4	0.1
	Summer	11.8	12.0	9.8	12.3	12
Median	Winter	5.5	5	5.5	5.8	5.9
	Spring	11.9	12.2	12.2	12.4	12.4
	Summer	23.4	25.0	24.9	25.3	24.8
Maximum	Winter	21.6	26.8	26.5	23.2	22.3
	Spring	27.6	31.9	31	28.7	28.7
	Summer	32.1	34.7	36.1	33.9	32.9

Thermal maximum

The total number of days T_w was >32 °C (thermal maximum) for each Hinkson Creek gauging site are summarized in Table 12. Results showed that the number of days T_w was >32 °C ranged from 1 day at site #1 to 55 days at site #3 with an all site mean of 19 days. The maximum duration T_w were >32 °C ranged from 0.25 hours at site #1 to 9.75 hours at site #4 with an all site mean of 6.55 hours. Stream T_w was >35 °C (critical thermal maximum) at site #3 for 5 days. The maximum duration T_w was >35 °C at site #3 was 2.5 hours. The days T_w was >32 °C were significantly correlated (p=0.04) to maximum T_w for the study period, while the maximum duration T_w was >32 °C was significantly (p<0.01) correlated to mean T_w for the study period.

Table 12. Days and duration stream water temperature was greater than 32 and 35 °C during the study period (WY 2010 – 2013) for five hydroclimate stations located in Hinkson Creek Watershed, Missouri, USA.

Critical Thermal Criteria	Site #1	Site #2	Site #3	Site #4	Site #5
Days T_w >32 °C	1	12	55	20	8
Max duration T_w >32 °C (hours)	0.25	7.25	8.25	9.75	7.25
Days T_w >35 °C	0	0	5	0	0
Max duration T_w >35 °C (hours)	0	0	2.5	0	0

Sudden rises in stream water temperature

Results showed that 23 iButton temperature sensors detected a total of 40 T_w surges in stormwater outfalls at 12 general locations in Hinkson Creek subsequent to urban stormwater inputs during summer 2009 (Table 13). All 12 locations where the T_w surges were detected had >12.9 km^2 urban land use within the drainage subbasins. Mean

T_w surge and surge duration was 4.0 °C and 11.4 hours, respectively. While, maximum

T_w surge and surge duration was 5.6 °C and 24.75 hours, respectively.

Table 13. Summary statistics of T_w surges detected in stormwater outfalls between gauging sites #3 and #5 during summer 2009 (N = 40).

Data	Mean	Stand. Dev.	Minimum	Median	Maximum
Peak T_w (°C)	25.1	2.7	20.5	24.4	33.4
T_w Surge (°C)	4.0	2.3	2.0	3.2	5.6
Surge Duration (h)	11.4	6.2	2.5	11.0	24.75

Stream water temperature data from the five Hinkson Creek gauging sites were also analyzed for T_w surges during summers 2010, 2011, and 2012. When investigated at five minute and 30 minute resolution, five minute data showed more T_w surges of greater magnitude in Hinkson Creek. For example, nine T_w surges were detected at a 30 minute resolution data. Conversely, results showed a total of 15 T_w surges when using five minute resolution T_w data. Furthermore, in one instance, a decrease in T_w was shown with the 30 minute data resolution while the five minute resolution detected a T_w surge of 1.22 °C and 1.25 hours surge duration during the same time period.

Results from the five minute data set are shown in Table 14. Mean peak T_w was 26.5 °C. Maximum peak T_w was 34.2 °C. Mean T_w surge and surge duration was 1.6 °C and 1.8 hours, respectively. While, maximum T_w surge and surge duration was 2.6 °C and 6.3 hours, respectively.

Table 14. Summary statistics of T_w surges sensed between gauging sites #3 and #5 in Hinkson Creek during summers 2010, 2011, and 2012 (N = 15).

Data	Mean	Stand. Dev.	Minimum	Median	Maximum
Peak T_w (°C)	26.5	2.7	22.3	26.8	34.2
T_w Surges (°C)	1.6	0.5	1.1	1.5	2.6
Surge Duration (h)	1.8	1.5	0.3	1.4	6.3

The effects of discharge on stream water temperature

Daily mean discharge, T_a, and T_w data were sorted into 15 different flow classes to investigate the effects of stream discharge on hydroclimate. Statistical analyses provided information pertaining to mean discharge, T_a, and T_w for 15 different flow classes at each gauging site. Please see Methods section (page 38) for more information regarding the methods used (including statistical analyses). Results from statistical analyses quantifiably characterize the relationship in mean discharge, T_a, and T_w between gauging sites as flow class increased and are presented in the following sections.

Discharge increased linearly from site #1 to site #5 below median flow values (<50% flow class), and exponentially above median flow values (>50% flow class). The rate of exponential growth increased as flow class increased because of the relationship between drainage area, urban land use, and discharge at each site. Discharge in the <50% flow class (below median discharge) increased from 0.0 m³/s at site #1 to 0.2 m³/s at site #5 with a five site mean of 0.1 m³/s (Table 15). Discharge in the >50% flow class (above median discharge) increased from 1.3 m³/s at site #1 to 4.6 m³/s at site #5 with a five site mean of 2.5 m³/s. Discharge in the >90% flow class increased from 6.2 m³/s at site #1 to 19.7 m³/s at site #5 with a five site mean of 10.84 m³/s. Discharge in the >99% flow class increased from 30.1 m³/s at site #1 to 89.9 m³/s at site #5 with a five site mean of 48.64

57

m^3/s. For a complete detailed description of mean discharge at each gauging site for each

flow class considered in this research see Table 15.

Table 15. Daily mean stream discharge (m^3/s) for fifteen different flow classes and five
hydroclimate stations located in Hinkson Creek Watershed, Missouri, USA.

Flow Class	Stream Discharge (m^3/s)				
(%)	Site #1	Site #2	Site #3	Site #4	Site #5
<50	0.0	0.1	0.1	0.1	0.2
>50	1.3	1.5	2.0	3.1	4.6
>60	1.6	1.8	2.5	3.8	5.7
>70	2.1	2.3	3.3	5.0	7.4
>80	3.2	3.4	4.8	7.2	10.7
>90	6.2	6.6	9.0	12.7	19.7
>91	6.8	7.3	9.8	13.9	21.6
>92	7.5	8.1	10.9	15.2	23.9
>93	8.6	9.2	12.2	16.8	26.8
>94	9.9	10.6	13.9	18.9	30.5
>95	11.7	12.3	16.0	21.7	35.4
>96	14.2	14.8	19.1	25.4	42.1
>97	17.5	17.0	23.1	30.6	51.6
>98	22.4	21.6	29.4	38.6	66.3
>99	30.1	29.2	40.3	53.7	89.9

Results showed there was no significant ($p > 0.05$) effect of discharge on mean T_a

as flow class increased. Mean T_a in the <50% flow class (below median discharge)

ranged from 13.4 °C at site #1 to 14.8 °C at site #3 with a five site mean of 14.1 °C. Mean

T_a in the >50% flow class (above median discharge) increased from 11.1 °C at site #1 to

12.3 °C at site #3 with a five site mean of 11.8 °C. Mean T_a in the >90% flow class

increased from 11.1 °C at site #1 to 12.0 °C at site #3 with a five site mean of 11.6 °C.

Mean T_a in the >99% flow class increased from 12.4 °C at site #1 to 13.1 °C at site #3

with a five site mean of 12.9 °C. For a complete detailed description of mean T_a at each

gauging site for each flow class considered in this research see Table 16.

Table 16. Daily mean air temperature (°C) for fifteen different flow classes and five
hydroclimate stations located in Hinkson Creek Watershed, Missouri, USA.

Flow Class	Air Temperature (°C)				
(%)	Site #1	Site #2	Site #3	Site #4	Site #5
<50	13.4	14.1	14.8	14.2	14.2
>50	11.1	11.7	12.3	11.9	11.9
>60	11.3	11.9	12.4	12.1	12.2
>70	11.1	11.7	12.2	11.9	11.9
>80	11.1	11.6	12.1	11.8	11.9
>90	11.1	11.6	12.0	11.7	11.8
>91	11.0	11.5	11.9	11.7	11.7
>92	11.1	11.6	12.0	11.7	11.8
>93	11.2	11.7	12.1	11.9	12.0
>94	11.5	12.0	12.4	12.1	12.2
>95	11.6	12.1	12.5	12.3	12.3
>96	11.6	12.2	12.5	12.3	12.4
>97	11.8	12.3	12.7	12.4	12.5
>98	12.3	12.8	13.2	13.0	13.1
>99	12.4	12.9	13.1	13.0	13.1

While there were no apparent trends pertaining to mean T_a between sites as flow

class increased, stream water temperature increased at the downstream gauging sites #4

and #5 relative to the upstream gauging sites as flow class increased. The effect of

discharge was not found to be significant ($p>0.05$) for any flow class considered, but a

significant ($p=0.04$) effect of urban land use on T_w was observed for flow classes >90%.

Results showing mean T_w for each gauging site and flow class considered in this research

see Table 17. Mean T_w in the <50% flow class (below median discharge) ranged from

14.4 °C at site #1 to 15.1 °C at site #4 with a five site mean of 14.8 °C. Mean T_w in the

>50% flow class (above median discharge) increased from 13.0 °C at site #1 to 13.7 °C at

site #4 with a five site mean of 13.4 °C. Mean T_w in the >90% flow class increased from

11.7 °C at site #1 to 12.4 °C at site #4 with a five site mean of 12.1 °C . Mean T_w in the

>99% flow class increased from 13.2 °C at site #1 to 14.0 °C at site #3 with a five site

mean of 13.6 °C.

Table 17. Daily mean stream water temperature (°C) for fifteen different flow classes and five hydroclimate stations located in Hinkson Creek Watershed, Missouri, USA.

Flow Class	Stream Temperature (°C)				
(%)	Site #1	Site #2	Site #3	Site #4	Site #5
<50	14.4	15.0	15.0	15.1	14.5
>50	13.0	13.5	13.5	13.7	13.5
>60	12.9	13.4	13.4	13.6	13.5
>70	12.5	12.9	13.0	13.2	13.1
>80	12.1	12.5	12.5	12.8	12.7
>90	11.7	12.0	12.1	12.4	12.4
>91	11.7	12.0	12.0	12.3	12.3
>92	11.6	11.9	11.9	12.2	12.2
>93	11.7	11.9	12.0	12.3	12.3
>94	11.8	12.1	12.1	12.5	12.5
>95	11.9	12.2	12.2	12.6	12.6
>96	11.9	12.1	12.2	12.6	12.6
>97	12.2	12.4	12.5	12.9	12.9
>98	12.6	12.8	12.9	13.3	13.3
>99	13.2	13.4	13.5	14.0	14.0

STREAM AND AIR TEMPERATURE RELATIONSHIPS

Linear and nonlinear regression analyses (performed in Origin) using mean T_w vs.

mean T_a data from each site (sites #1 to #5) and at each time step (15 minute, hourly,

daily, weekly, monthly, and seasonal) yielded r^2 values; linear coefficients a (slope), and b (y-intercept) for linear regression T_w models (equation 1); and nonlinear coefficients α (estimated maximum T_w), β (T_a at the inflection point of the function), and γ (measure of the steepest slope) for nonlinear regression models (equation 2). Linear and nonlinear T_w models were created using the results of the regression analyses. Results from linear and nonlinear regression analyses are shown in Tables 18 to 20.

Linear and nonlinear T_w models showed significant ($p<0.01$) increased levels of explained variance as time scale increased from 15 minute to seasonal averages. Linear regression analyses resulted in five site mean r^2 values ranging from 0.80 for a 15 minute time step to 0.99 at a seasonal time step (Table 16). Nonlinear regression analyses resulted in five site mean r^2 values ranging from 0.81 for a 15 minute time step to 1.00 at a seasonal time step.

Information regarding the effects of time scale on linear and nonlinear coefficients may also be important for improving our understanding of the relationship between T_w and T_a. Linear coefficients a and b were affected by time scale. Coefficients a decreased with time scale, while coefficients b increased with time scale. Five site mean "coefficient a" ranged from 1.96 at a seasonal time step to 4.67 at a 15 minute time step. Five site mean "coefficient b" ranged from 0.72 at a 15 minute time step to 0.93 at a seasonal time step.

Nonlinear coefficients α, and β were not apparently affected by time scale (Table 17). But, coefficient γ increased from sub-daily to monthly time scale. Five site mean "coefficient α" ranged from 29.99 at a 15 minute time step to 32.71 at a daily time step. Five site mean "coefficient β" ranged from 14.39 at a seasonal time step to 16.10 at a

61

daily time step. Five site mean "coefficient γ" ranged from 0.12 at an hourly (with time lag) time step to 0.16 at a monthly time step.

The effects of time lag were investigated using cross correlation analyses and statistical software (Origin). The reader is directed to the Methods section page 35 for information on using cross-correlation analysis to quantify time lag. Time lag between T_w and T_a data was found at sub-daily time steps for linear and nonlinear regression results. Cross correlation analyses using the cross correlation function (CCF) (equations 11, 12, 13) showed time lag ranged from 1.5 hours at site #2 (CCF=0.96) to 4.25 hours at site #5 (CCF=0.95) when calculated using 15 minute data. When CCF were calculated using hourly data, time lag ranged from two hours at site #2 (CCF=0.96) to four hours at site #5 (CCF=0.95). Accounting for time lag increased levels of explained variance for sub-daily T_w models (Tables 16 and 17). But, the level of explained variance was still poor compared to the daily and post daily T_w models. This was especially true for the 15 minute linear T_w models.

To improve the 15 minute linear T_w model results, calibration parameters (α and β) were added to the linear T_w models (equations 14 and 15). 15 minute mean T_w was more dependent on daily mean T_a for the day interest, than 15 minute mean T_a as calibration parameter β was increased. Greater values for β resulted in decreased diel (i.e. 24hr) range of 15 minute mean T_w. Please see Methods section page 36 for information on the "calibrated linear stream water temperature models". Results showing final calibration parameter values of the 15 minute linear T_w models are in Table 21. Calibration parameter α ranged from 0.3 at site #4 to 0.45 at site #2. Calibration parameter β ranged from 0.55 at site #2 to 0.7 at site #4.

Table 18. Coefficients of determination (r^2) from linear and nonlinear regression analyses are shown for each time step considered (15 minute, hourly, daily, weekly, monthly, and seasonal) for each of five gauging sites in Hinkson Creek Watershed, U.S.A. The term "time lag" denotes analyses that accounted for the lagged response of T_a relative to T_w. Lag was determined using cross-correlation analysis.

Time step	Model	Site #1	Site #2	Site #3	Site #4	Site #5
15 minute	Linear	0.760	0.832	0.810	0.813	0.776
	Nonlinear	0.779	0.847	0.821	0.828	0.790
15 minute	Linear	0.797	0.843	0.832	0.839	0.799
(time lag)	Nonlinear	0.818	0.858	0.845	0.853	0.814
Hourly	Linear	0.772	0.838	0.858	0.791	0.784
	Nonlinear	0.790	0.853	0.869	0.800	0.792
Hourly	Linear	0.804	0.849	0.860	0.823	0.808
(time lag)	Nonlinear	0.821	0.865	0.872	0.831	0.816
Daily	Linear	0.900	0.911	0.921	0.905	0.896
	Nonlinear	0.919	0.927	0.933	0.917	0.908
Weekly	Linear	0.968	0.968	0.971	0.969	0.966
	Nonlinear	0.977	0.975	0.976	0.973	0.970
Monthly	Linear	0.990	0.989	0.991	0.990	0.989
	Nonlinear	0.993	0.991	0.991	0.989	0.989
Seasonal	Linear	0.994	0.993	0.994	0.992	0.993
	Nonlinear	0.995	0.995	0.996	0.994	0.995

Table 19. Coefficients *a* (slope) and *b* (y-intercept) from linear regression analyses are shown for each time step considered (15 minute, hourly, daily, weekly, monthly, and seasonal) for each of five study sites in Hinkson Creek Watershed, U.S.A. The term "time lag" denotes analyses that accounted for the lagged response of T_a relative to T_w. Lag was determined using cross-correlation analysis.

Time step	Coefficient	Site #1	Site #2	Site #3	Site #4	Site #5
15 minute	*b*	5.621	4.101	3.869	4.840	4.902
	a	0.654	0.774	0.732	0.747	0.705
15 minute	*b*	5.432	4.038	3.743	4.680	4.763
(time lag)	*a*	0.670	0.779	0.742	0.759	0.716
Hourly	*b*	5.550	4.443	3.876	4.864	4.878
	a	0.664	0.766	0.770	0.727	0.703
Hourly	*b*	5.297	4.377	3.863	4.668	4.737
(time lag)	*a*	0.676	0.771	0.771	0.742	0.713
Daily	*b*	4.067	3.276	2.838	3.325	3.360
	a	0.781	0.854	0.844	0.841	0.815
Weekly	*b*	3.199	2.397	2.015	2.391	2.376
	a	0.849	0.920	0.902	0.910	0.888
Monthly	*b*	2.893	2.036	1.689	2.045	2.009
	a	0.873	0.946	0.926	0.936	0.915
Seasonal	*b*	2.715	1.746	1.503	1.929	1.897
	a	0.887	0.968	0.939	0.944	0.924

Table 20. Coefficients α (estimated maximum T_w) and β (T_a at the inflection point of the function) γ (measure of the steepest slope) from nonlinear regression analyses are shown for each time step considered (15 minute, hourly, daily, weekly, monthly, and seasonal) for each of five study sites in Hinkson Creek Watershed, U.S.A. The term "time lag" denotes analyses that accounted for the lagged response of T_a relative to T_w. Lag was determined using cross-correlation analysis.

Time step	Coefficient	Site #1	Site #2	Site #3	Site #4	Site #5
15 minute	α	28.187	31.878	30.489	30.418	28.980
	β	13.185	15.577	15.758	14.162	13.776
	γ	0.122	0.130	0.126	0.133	0.130
15 minute (time lag)	α	29.173	31.906	30.759	31.398	29.173
	β	13.931	15.576	15.891	14.848	13.921
	γ	0.121	0.132	0.128	0.130	0.132
Hourly	α	27.957	32.503	32.429	30.426	30.805
	β	12.838	15.686	16.300	14.392	15.164
	γ	0.127	0.126	0.125	0.124	0.117
Hourly (time lag)	α	29.355	32.469	31.813	31.470	31.092
	β	14.072	15.651	15.877	15.128	15.360
	γ	0.121	0.127	0.129	0.122	0.119
Daily	α	31.429	32.924	32.533	33.668	33.014
	β	15.342	15.869	16.307	16.460	16.524
	γ	0.130	0.138	0.137	0.129	0.128
Weekly	α	29.886	31.474	31.024	31.917	31.156
	β	14.134	14.793	15.190	15.185	15.147
	γ	0.148	0.155	0.154	0.147	0.148
Monthly	α	29.361	30.661	30.262	31.274	30.429
	β	13.774	14.294	14.698	14.768	14.664
	γ	0.154	0.164	0.161	0.155	0.157
Seasonal	α	30.715	31.905	31.495	30.593	29.900
	β	14.256	14.623	15.088	14.002	13.977
	γ	0.130	0.139	0.136	0.142	0.142

Table 21. Calibration parameters for the calibrated
15 minute linear T_w model.

Gauging Site	α	β
Site #1	0.38	0.62
Site #2	0.45	0.55
Site #3	0.41	0.59
Site #4	0.30	0.70
Site #5	0.32	0.68

The effects of discharge on T_w and T_a relationships

Daily mean discharge, T_a, and T_w data were sorted into 15 different flow classes

to investigate the effects of stream discharge on the T_w and T_a relationship. Please see

Methods section (page 41) for more information regarding the methods used (including

statistical analyses). Linear regression analyses were performed using daily mean T_w and

T_a data for each flow class to better elucidate the effects of discharge on the T_w and T_a

relationship at a daily time step. Results from linear regression analyses for 15 different

flow classes showed that the r^2 values decreased significantly (p<0.01) as flow class

increased (Table 22). This information may be important for water resource managers

that are using T_w models to estimate stream water temperature during stormflow periods.

The r^2 values in the <50% flow class (below median discharge) ranged from 0.91 at site

#1 to 0.94 at site #3 with a five site mean of 0.92. The r^2 values in the >50% flow class

(above median discharge) ranged from 0.86 at site #1 to 0.89 at site #3 with a five site

mean of 0.88. The r^2 values in the >90% flow class ranged from 0.68 at site #4 to 0.72 at

site #2 with a five site mean of 0.70. The r^2 values in the >99% flow class ranged from

0.57 at site #4 to 0.73 at site #1 with a five site mean of 0.68.

Results from linear regression analyses for 15 different flow classes showed linear "coefficient b" decreased, while linear "coefficient a" increased as flow class increased (Table 23). When daily T_w / T_a relationships were analyzed at 15 different flow classes, results showed five site mean "coefficient a" ranged from 0.10 at the >98% flow class to 3.86 at >60% flow class. Five site mean "coefficient b" ranged from 0.72 at >93% flow class to 0.94 at the >99% flow class. For a complete detailed description of linear regression results for each flow class considered see Tables 22 and 23.

Table 22. Coefficient of determination (r^2) values from linear regression results for fifteen different flow classes using daily average stream and air temperature data collected from five hydroclimatic stations located in Hinkson Creek Watershed, Missouri, USA.

Flow Class (%)	Site #1	Site #2	Site #3	Site #4	Site #5	Five site Mean
<50	0.910	0.934	0.942	0.921	0.912	0.924
>50	0.856	0.885	0.889	0.879	0.871	0.876
>60	0.836	0.880	0.873	0.866	0.856	0.862
>70	0.841	0.872	0.850	0.827	0.820	0.842
>80	0.822	0.832	0.799	0.800	0.788	0.808
>90	0.714	0.719	0.701	0.680	0.682	0.699
>91	0.692	0.696	0.696	0.682	0.661	0.685
>92	0.679	0.703	0.702	0.686	0.653	0.685
>93	0.687	0.711	0.668	0.687	0.619	0.674
>94	0.682	0.688	0.634	0.644	0.602	0.650
>95	0.668	0.673	0.660	0.645	0.620	0.653
>96	0.697	0.686	0.668	0.659	0.576	0.657
>97	0.672	0.655	0.627	0.634	0.472	0.612
>98	0.689	0.669	0.638	0.686	0.638	0.664
>99	0.730	0.728	0.638	0.570	0.709	0.675

Table 23. Flow empirical analysis *a* and *b* coefficients for fifteen different flow classes at a daily time step using data collected from five hydroclimate stations located in Hinkson Creek Watershed, Missouri, USA.

Flow Class (%)	Coefficient	Site #1	Site #2	Site #3	Site #4	Site #5
<50	*b*	4.421	2.267	1.897	2.855	2.557
	a	0.773	0.908	0.901	0.881	0.853
>50	*b*	4.155	3.749	3.262	3.771	4.044
	a	0.761	0.821	0.802	0.801	0.790
>60	*b*	4.125	3.784	3.549	3.844	3.978
	a	0.740	0.815	0.771	0.787	0.780
>70	*b*	4.056	3.482	3.577	3.577	4.135
	a	0.757	0.824	0.752	0.790	0.744
>80	*b*	3.970	2.962	3.403	3.396	3.657
	a	0.751	0.823	0.725	0.770	0.760
>90	*b*	3.480	3.077	3.046	3.672	3.866
	a	0.740	0.738	0.727	0.712	0.708
>91	*b*	3.343	3.271	2.908	3.521	3.887
	a	0.744	0.720	0.723	0.714	0.697
>92	*b*	3.350	3.349	3.050	3.387	3.947
	a	0.739	0.708	0.725	0.722	0.680
>93	*b*	3.131	3.152	3.045	3.004	3.964
	a	0.753	0.731	0.716	0.733	0.673
>94	*b*	2.713	2.467	2.671	2.525	3.950
	a	0.770	0.773	0.738	0.775	0.670
>95	*b*	2.455	1.576	1.556	2.345	3.470
	a	0.783	0.826	0.804	0.781	0.712
>96	*b*	1.053	1.238	0.593	1.614	3.392
	a	0.860	0.837	0.859	0.822	0.724
>97	*b*	0.201	0.101	0.929	0.676	5.080
	a	0.933	0.892	0.824	0.872	0.624
>98	*b*	0.817	1.123	0.863	0.864	3.152
	a	0.995	0.997	0.933	0.979	0.761
>99	*b*	1.217	5.748	1.656	2.006	5.629
	a	1.069	1.272	0.848	0.858	0.665

SWAT MODELING

SWAT calibration

The SWAT model was successfully calibrated at a daily time step using observed stream discharge data from site #5 and the four nested subbasins during the 2010 to 2012 water years (results are summarized in Table 24). Model evaluation results from site #5 nearest the watershed outlet showed a Nash-Sutcliffe efficiency (NSE) value of 0.56, percent bias (PBIAS) value of 24.15%, and a ratio of root mean square error to the standard deviation of observed data (RSR) value of 0.66. Simulated mean stream discharge was 2.6 m^3/s, which was 0.8 m^3/s less than observed mean discharge during the calibration period. Simulated maximum stream discharge was 125.9 m^3/s, observed maximum stream discharge was 217.7 m^3/s.

Model evaluation results for the other four gauging sites showed NSE values ranging from 0.50 at site #1 to 0.66 at site #4. PBIAS values ranged from -8.53% at site #2 to 14.71% at site #3. RSR values ranged from 0.58 at site #4 to 0.71 at site #1. MAE ranged from 0.76 m^3/s at site #1 to 1.58 m^3/s at site #4. MSE ranged from 7.12 m^3/s at site #1 to 23.84 m^3/s at site #4. RMSE ranged from 2.67 m^3/s at site #1 to 4.88 m^3/s at site #4. See Table 24 for more information on SWAT calibration results.

Table 24. Simulated and observed stream discharge calibration results showing daily descriptive statistics and six model evaluation criterion for five gauging sites in Hinkson Creek, USA. Observed data are shown in parentheses for comparison with simulated data.

Statistic	Site #1	Site #2	Site #3	Site #4	Site #5
Mean (m^3/s)	0.9 (0.8)	1.2 (1.1)	1.4 (1.59)	2.3 (2.3)	2.6 (3.4)
Max (m^3/s)	36.9 (60.3)	57.8 (69.2)	70.2 (117.7)	115.7 (145.0)	125.9 (217.7)
Median (m^3/s)	0.2 (0.0)	0.3 (0.1)	0.3 (0.2)	0.5 (0.3)	0.5 (0.5)
Min (m^3/s)	0.0 (0.0)	0.0 (0.0)	0.0 (0.0)	0.0 (0.0)	0.0 (0.0)
NSE	0.50	0.51	0.60	0.66	0.56
PBIAS (%)	-4.19	-8.53	14.71	0.43	24.15
RSR	0.71	0.70	0.63	0.58	0.66
MAE (m^3/s)	0.76	1.06	1.21	1.58	2.40
MSE (m^3/s)	7.12	10.80	18.69	23.84	60.47
RMSE (m^3/s)	2.67	3.29	4.32	4.88	7.78

NSE is Nash-Sutcliffe efficiency, PBIAS is percent bias, RSR is ratio of root mean square error to the standard deviation of observed data, MAE is mean absolute error, MSE is mean square error, RMSE is root mean square error.

SWAT validation

SWAT was successfully validated at a daily time step using observed stream discharge data from site #5 and the four nested gauging sites during the 2013 water year (results are summarized in Table 25). Model evaluation results from site #5 nearest the watershed outlet showed a NSE value of 0.48, PBIAS value of 45.00%, and a RSR value of 0.72. Observed mean stream discharge during the calibration period was 4.3 m^3/s while simulated stream discharge was 2.3 m^3/s. Observed maximum stream discharge was 137.9 m^3/s, simulated maximum stream discharge was 83.8 m^3/s.

Model evaluation results during the validation period for the other four gauging sites showed NSE values ranging from 0.49 at site #1 to 0.67 at site #4. PBIAS values ranged from 3.9% at site #1 to 21.97% at site #3. RSR values ranged from 0.71 at site #1 to 0.57 at site #4. MAE ranged from 0.96 m^3/s at site #1 to 1.66 m^3/s at site #4. MSE

ranged from 12.73 m^3/s at site #1 to 33.62 m^3/s at site #3. RMSE ranged from 3.57 m^3/s

at site #1 to 5.80 m^3/s at site #3. See Table 25 for more information on SWAT validation

results.

Table 25. SWAT simulated and observed stream discharge validation results showing
daily descriptive statistics and six model evaluation criterion for five gauging sites in
Hinkson Creek, USA. Observed data are shown in parentheses.

Statistic	Site #1	Site #2	Site #3	Site #4	Site #5
Mean (m^3/s)	0.9 (.9)	1.2 (1.2)	1.3 (1.7)	2.1 (2.2)	2.3 (4.3)
Max (m^3/s)	24.4 (57.5)	35.4 (66.4)	42.1 (86.7)	75.0 (114.9)	83.8 (137.9)
Median (m^3/s)	0.1 (0.0)	0.1 (0.1)	0.1 (0.1)	0.2 (0.1)	0.2 (0.4)
Min (m^3/s)	0.0 (0.0)	0.0 (0.1)	0.0 (0.0)	0.0 (0.0)	0.0 (0.2)
NSE	0.49	0.49	0.52	0.67	0.48
PBIAS	3.9	5.79	21.97	4.54	45.00
RSR	0.71	0.71	0.69	0.57	0.72
MAE (m^3/s)	0.96	1.31	1.50	1.66	3.25
MSE (m^3/s)	12.73	22.50	33.62	29.59	127.07
RMSE (m^3/s)	3.57	4.74	5.80	5.44	11.27

NSE is Nash-Sutcliffe efficiency, PBIAS is percent bias, RSR is ratio of root mean square error to the
standard deviation of observed data, MAE is mean absolute error, MSE is mean square error, RMSE is root
mean square error.

STREAM TEMPERATURE MODEL COMPARISON

Simulation results from the linear (equation 1), nonlinear (equation 2), and

calibrated linear (equation 15), T_w models were tested using six model evaluation criteria

to compare the effectiveness of each of the T_w models at daily and sub-daily (15 minute

and hourly) time steps. The original SWAT T_w model (equation 4), and Ficklin et al.

(2012) T_w model (equations 5, 6, 7, and 8) were also tested at a daily time step for T_w

model comparison. Evaluation results for the calibration period (WY 2011 and 2012) and

validation period (WY 2013) are shown in Tables 26, 27, and 28. Five site mean T_w

model evaluation results are shown to summarize the data. More detailed tables showing

T_w model evaluation results for each of the five gauging sites are provided in Appendix B.

15 minute stream temperature models

Results showed model evaluation tests including NSE, RSR, MAE, MSE, and RMSE all significantly (p<0.01) favored the 15 minute calibrated linear T_w model over the 15 minute linear and nonlinear T_w models (with the exception of PBIAS values). Model evaluation results were not significantly (p>0.05) different for the 15 minute nonlinear T_w models and the 15 minute linear T_w models (Table 26).

NSE values can range from ∞ to 1.0 (a value of 1.0 is a perfect simulation). Multiple evaluation results revealed five site mean NSE values ranging from 0.83 for the 15 minute linear T_w model to 0.91 for the 15 minute calibrated linear T_w model during the calibration period. Five site mean NSE values ranged from 0.83 for the 15 minute linear T_w model to 0.89 for the 15 minute calibrated linear T_w model during the validation period.

PBIAS results can range from -100% to 100% (a value of 0.00 is a perfect simulation). Five site mean PBIAS values ranged from 0.02% for the 15 minute linear T_w model to 2.37% for the 15 minute calibrated linear T_w model during the calibration period. Five site mean PBIAS values ranged from 0.38% for the 15 minute nonlinear T_w model to 4.50% for the 15 minute calibrated linear T_w model during the validation period.

RSR values can range from 0.0 to 1.0 (a value of 0.0 is a perfect simulation). Five site mean RSR values ranged from 0.29 for the 15 minute calibrated linear T_w model to 0.41 for the 15 minute linear T_w model during the calibration period. Five site mean RSR

values ranged from 0.33 for the 15 minute calibrated linear T_w model to 0.42 for the 15 minute linear T_w model during the validation period.

MAE, MSE, and RMSE values are a measure of model error that can range from 0.0 to ∞ °C (a value of 0.0 °C is a perfect simulation). Five site mean MAE, MSE, and RMSE values ranged from 1.66, 6.18, and 2.46 °C, respectively, for the 15 minute calibrated linear T_w model to 3.00, 14.82, and 3.85 °C, respectively, for the 15 minute linear T_w model during the calibration period. Five site mean MAE, MSE, and RMSE values ranged from 2.26, 8.88, and 2.98 °C, respectively, for the 15 minute calibrated linear T_w model to 2.97, 14.69, and 3.83 °C, respectively, for the 15 minute linear T_w model during the validation period.

Table 26. Five site mean summary of 15 minute linear, nonlinear, and calibrated linear stream water temperature model evaluation results during calibration and validation periods for five gauging sites in Hinkson Creek Watershed, USA.

Five Site Mean 15 Minute Stream Water Temperature Model Evaluation Results			
Statistic	Linear	Nonlinear	Calibrated Linear
Calibration			
NSE	0.83	0.84	0.91
PBIAS (%)	0.02	0.62	2.37
RSR	0.41	0.4	0.29
MAE (°C)	3	2.97	1.66
MSE (°C)	14.82	14.44	6.18
RMSE (°C)	3.85	3.8	2.46
Validation			
NSE	0.83	0.84	0.89
PBIAS (%)	0.69	0.38	4.5
RSR	0.42	0.4	0.33
MAE (°C)	2.97	2.81	2.26
MSE (°C)	14.69	13.66	8.88
RMSE (°C)	3.83	3.69	2.98

NSE is Nash-Sutcliffe efficiency, PBIAS is percent bias, RSR is ratio of root mean square error to the standard deviation of observed data, MAE is mean absolute error, MSE is mean square error, RMSE is root mean square error.

Hourly stream temperature models

Results showed model evaluation tests including NSE, RSR, MAE, MSE, and RMSE all significantly ($p<0.01$) favored the hourly calibrated linear T_w model over the hourly linear and hourly nonlinear T_w models (with the exception of PBIAS values). Model evaluation results were not significantly ($p>0.05$) different for the hourly nonlinear T_w models and the hourly linear T_w models.

Results from hourly linear, hourly nonlinear, and hourly calibrated linear T_w models are summarized in Table 27. Results showed five site mean NSE values ranged from 0.84 for the hourly linear T_w model to 0.91 for the hourly calibrated linear T_w model

during the calibration period. Five site mean NSE values ranged from 0.83 for the hourly linear T_w model to 0.90 for the hourly calibrated linear T_w model during the validation period.

Five site mean PBIAS values ranged from 0.52% for the hourly linear T_w model to 2.92% for the hourly calibrated linear T_w model during the calibration period. Five site mean PBIAS values ranged from 1.27% for the hourly linear T_w model to 4.28% for the hourly calibrated linear T_w model during the validation period.

Five site mean RSR values ranged from 0.29 for the hourly calibrated linear T_w model to 0.40 for the hourly linear T_w model during the calibration period. Five site mean RSR values ranged from 0.32 for the hourly calibrated linear T_w model to 0.41 for the hourly linear T_w model during the validation period.

Five site mean MAE, MSE, and RMSE values ranged from 2.07, 7.73, and 2.78 °C, respectively, for the hourly calibrated linear T_w model to 2.97, 14.64, and 3.82 °C, respectively, for the hourly linear T_w model during the calibration period. Five site mean MAE, MSE, and RMSE values ranged from 2.21, 8.42, and 2.90 °C, respectively, for the hourly calibrated linear T_w model to 2.93, 14.48, and 3.80 °C, respectively, for the hourly linear T_w model during the validation period.

Table 27. Five site mean summary of hourly linear, nonlinear, and calibrated linear stream water temperature model evaluation results during calibration and validation periods for five gauging sites in Hinkson Creek Watershed, USA.

Five Site Mean Hourly Stream Water Temperature Model Evaluation Results			
Statistic	Linear	Nonlinear	Calibrated Linear
Calibration			
NSE	0.84	0.84	0.91
PBIAS (%)	0.52	0.14	2.92
RSR	0.40	0.40	0.29
MAE (°C)	2.97	2.97	2.07
MSE (°C)	14.64	14.39	7.73
RMSE (°C)	3.82	3.79	2.78
Validation			
NSE	0.83	0.84	0.90
PBIAS (%)	1.27	1.18	4.28
RSR	0.41	0.40	0.32
MAE (°C)	2.93	2.81	2.21
MSE (°C)	14.48	13.60	8.42
RMSE (°C)	3.80	3.68	2.90

NSE is Nash-Sutcliffe efficiency, PBIAS is percent bias, RSR is ratio of root mean square error to the standard deviation of observed data, MAE is mean absolute error, MSE is mean square error, RMSE is root mean square error.

Daily stream temperature models

Results showed model evaluation tests including NSE, RSR, MAE, MSE, and RMSE favored the Ficklin et al. (2012) T_w model over the original SWAT T_w model, but the differences were not significant ($p < 0.05$). Overall, every T_w model tested performed well, with NSE values > 0.88 and RMSE values < 3.17 °C. However, results from ANOVA analyses showed the daily nonlinear T_w model performed significantly better than the original SWAT T_w model for every model evaluation test considered including NSE ($p = 0.04$), PBIAS ($p < 0.01$), RSR ($p < 0.01$), MAE ($p < 0.01$), MSE ($p < 0.01$), and RMSE ($p < 0.01$) during the validation period (WY 2013). The calibrated linear T_w model

showed significantly (p<0.01) lower error (MAE, MSE, and RMSE) compared to the original SWAT T_w during the validation period. Results from daily linear, daily nonlinear, daily calibrated linear, the original SWAT model, and the Ficklin et al. (2012) T_w models are summarized in Table 28.

Results showed the mean NSE values for all five sites ranged from 0.90 for the original SWAT T_w model to 0.94 for the daily nonlinear T_w model during the calibration period. The mean NSE values for all five sites ranged from 0.88 for the original SWAT T_w model to 0.91 for the daily nonlinear T_w model during the validation period.

The mean PBIAS values for all five sites ranged from -4.64% for the original SWAT T_w model to 3.02% for the Ficklin et al. (2012) T_w model during the calibration period. The mean PBIAS values for all five sites ranged from -4.99% for original SWAT T_w model to 5.6% for the Ficklin et al. (2012) T_w model during the validation period.

The mean RSR values for all five sites ranged from 0.24 for the daily calibrated linear T_w model to 0.32 for the original SWAT T_w model during the calibration period. The mean RSR values for all five sites ranged from 0.29 for the daily nonlinear T_w model to 0.35 for the original SWAT T_w model during the validation period.

The original SWAT T_w model showed the greatest amount of error with the mean MAE, MSE, and RMSE values for all five sites of from 2.28, 9.07, and 3.01 °C, respectively, during the calibration period, and, 2.45, 10.10, and 3.17, respectively, during the validation period. The calibrated linear T_w model showed the least amount of error during the calibration period with the mean MAE, MSE, and RMSE values for all five sites ranging from 1.94, 6.76, and 2.60 °C, respectively. The nonlinear T_w model

showed the least amount of error during the validation period with the mean MAE, MSE,

and RMSE values for all five sites ranging from 1.99, 7.07, and 2.65 °C, respectively.

Table 28. Summary of the mean model evaluation results from all five sites for the daily linear, nonlinear, calibrated linear, original SWAT, and Ficklin et al. (2012) stream water temperature model evaluation results during calibration and validation periods for five gauging sites in Hinkson Creek Watershed, U.S.A.

Daily Stream Water Temperature Model Evaluation Results					
Statistic	Linear	Nonlinear	Calibrated Linear	Original SWAT	Ficklin et al. (2012)
Calibration					
NSE	0.92	0.92	0.94	0.90	0.91
PBIAS (%)	-0.97	-0.64	2.90	-4.64	3.02
RSR	0.29	0.28	0.24	0.32	0.30
MAE (°C)	2.01	1.99	1.94	2.28	2.06
MSE (°C)	7.29	6.77	6.76	9.07	7.61
RMSE (°C)	2.70	2.60	2.60	3.01	2.76
Validation					
NSE	0.90	0.91	0.91	0.88	0.89
PBIAS (%)	-0.07	-0.14	4.29	-4.99	5.60
RSR	0.32	0.29	0.30	0.35	0.32
MAE (°C)	2.18	1.99	2.10	2.45	2.21
MSE (°C)	8.25	7.07	7.61	10.10	8.65
RMSE (°C)	2.87	2.65	2.75	3.17	2.93

NSE is Nash-Sutcliffe efficiency, PBIAS is percent bias, RSR is ratio of root mean square error to the standard deviation of observed data, MAE is mean absolute error, MSE is mean square error, RMSE is root mean square error.

CHAPTER IV

DISSCUSSION

HYDROCLIMATE

Climate

Climate during the three year study period (WY 2011 – 2013) recorded at Sanborn Field climate station located on University of Missouri campus is shown in Appendix A. Climate during the study period was generally dryer than average. Drought conditions were observed during summer of WY 2012. Average annual total precipitation of 837.9 mm recorded during the three year study period was approximately 244 mm less than the aforementioned 30 year historic annual average precipitation of 1082 mm. Average annual mean T_a of 13.1 °C was approximately 1.0 °C lower than the historic annual average of 14 °C. Average annual total daily solar radiation was of 13.8 MJ/m^2 was 0.7 MJ/m^2 lower than the 14 year record of 14.5 MJ/m^2 measured at Sanborn Field climate station.

One-way ANOVA revealed significant (p=0.01) differences in daily mean T_a. Tukey-Kramer post hoc multiple comparison tests showed mean T_a was significantly (p=0.01) 1.2 °C higher at site #3 compared to site #1 (Figure 6). Considering site #3 climate station is located in the urban area of HCW (2.5 km east of the center of the City of Columbia) while site #1 climate station is located in the rural area of HCW (11.2 km northeast of the center of the City of Columbia), these results supply evidence of an urban heat island effect. Daily mean T_a was greater at site #3 compared to site #1 by 1.6 °C. Studies by Akyuz et al. (2004) and Hubbart et al. (2014) also reported a "distinct urban

influence" on T_a in Columbia, Missouri. Akyuz et al. (2004) reported monthly maximum

T_a was 1.5 °C to 3.5 °C greater in urban sites compared to rural sites. Hubbart et al.

(2014) showed an urban heat island effect on local climate during 1995 to 2013 where

significant differences (p<0.01) in mean air temperature and relative humidity ranged

from 13.47 °C and 12.89 °C, and 69.11% and 72.51% in urban and rural sites,

respectively.
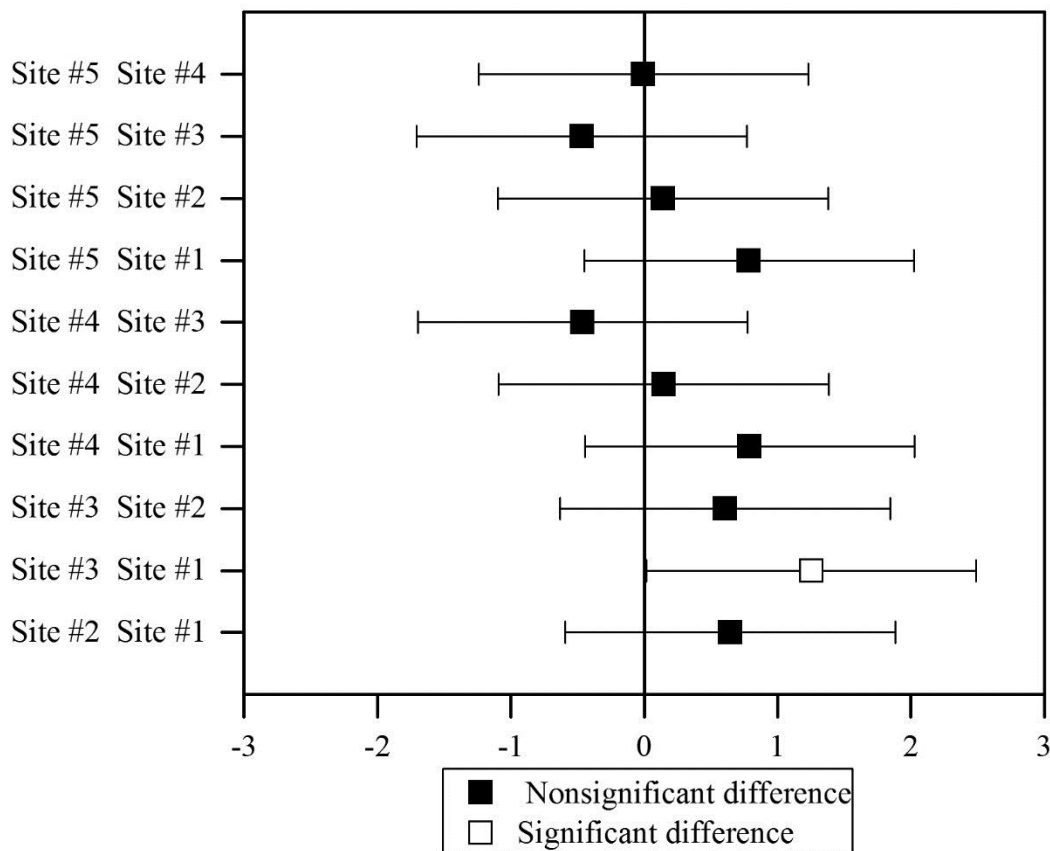
Figure 6. Tukey-Kramer multiple comparison results showing significant differences in daily mean air temperature in Hinkson Creek Watershed, Missouri, USA. The x-axis shows confidence interval values. The y-axis shows all possible pairs of sample means being compared. The bars show the confidence interval for each pair of sample means being compared. A significant difference is shown when a confidence interval does not contain the value of zero.

Discharge

　　　Dryer than average climate conditions during throughout the study period affected average discharge as well. Problems associated with decreased discharge during times of high temperature (summer months) are exacerbated with increased stream water evaporation rates and can impact aquatic ecosystem health (Bond et al. 2008). As water levels recede from riparian and littoral (shallow well lit portion of a stream) zones lateral connectivity between riparian zone and the stream is reduced leading to reduced habitat area (Boulton, 2003). Non motile fauna and flora in the littoral zone are left stranded to desiccate. Normally productive photosynthetic macrophytes in the littoral zone can no longer provide needed DO to microorganisms, macroinvertebrates, herptiles, and fish (Furey et al. 2006).

　　　Precipitation and flow graphs in Figure 7 show precipitation and discharge data recorded at five gauging sites during the three year study period (WY 2011 – 2013). Mean discharge at site #4 during the three year study period was 0.18 m^3/s less than the aforementioned 23 year historic annual average discharge of 1.78 m^3/s recorded at U.S. Geological Survey gauging station (#06910230). Mean discharge was lowest at site #1 and greatest at site #5 as expected because site #1 is in the headwaters and site #5 is near the watershed outlet. Maximum discharge was greatest as site #5 (137.9 m^3/s) as expected because drainage area was greatest at site #5 nearest the watershed outlet.

　　　Results of One way ANOVA indicated significant ($p<0.01$) differences in daily mean discharge between the five HC gauging stations. Tukey-Kramer multiple comparison test showed mean discharge was significantly higher at site #5 compared to all other HC sites (Figure 8). Site #4 daily mean discharge was significantly higher than

gauging sites #1 and #2. It's reasonable to expect that sites #4 and #5 would have significantly higher discharge considering drainage area increases from site #1 to site #5. In fact, sites #4 and #5 drain 78 and 89% of HCW, respectively. There was a linear relationship found between observed mean discharge and drainage area upstream of the gauging site ($r^2=0.842$). There was also a linear relationship between discharge and percent urban land use upstream of the gauging site ($r^2=0.946$). Urban land use area (associated with impervious surfaces) increases exponentially from site #1 to #5 (Figure 9). At site #5, Hinkson Creek drains approximately 60% of the City of Columbia which contains 27.74 km^2 of impervious surface (Zhou et al. 2012). Impervious surfaces degrade the quality and increase the quantity of stormwater runoff (Brabec et al. 2002) by decreasing soil infiltration rates. Many stormwater drains in Columbia direct stormwater runoff into Hinkson Creek. Thus, area of the watershed drained and urban land use affected discharge in Hinkson Creek (Table 2).
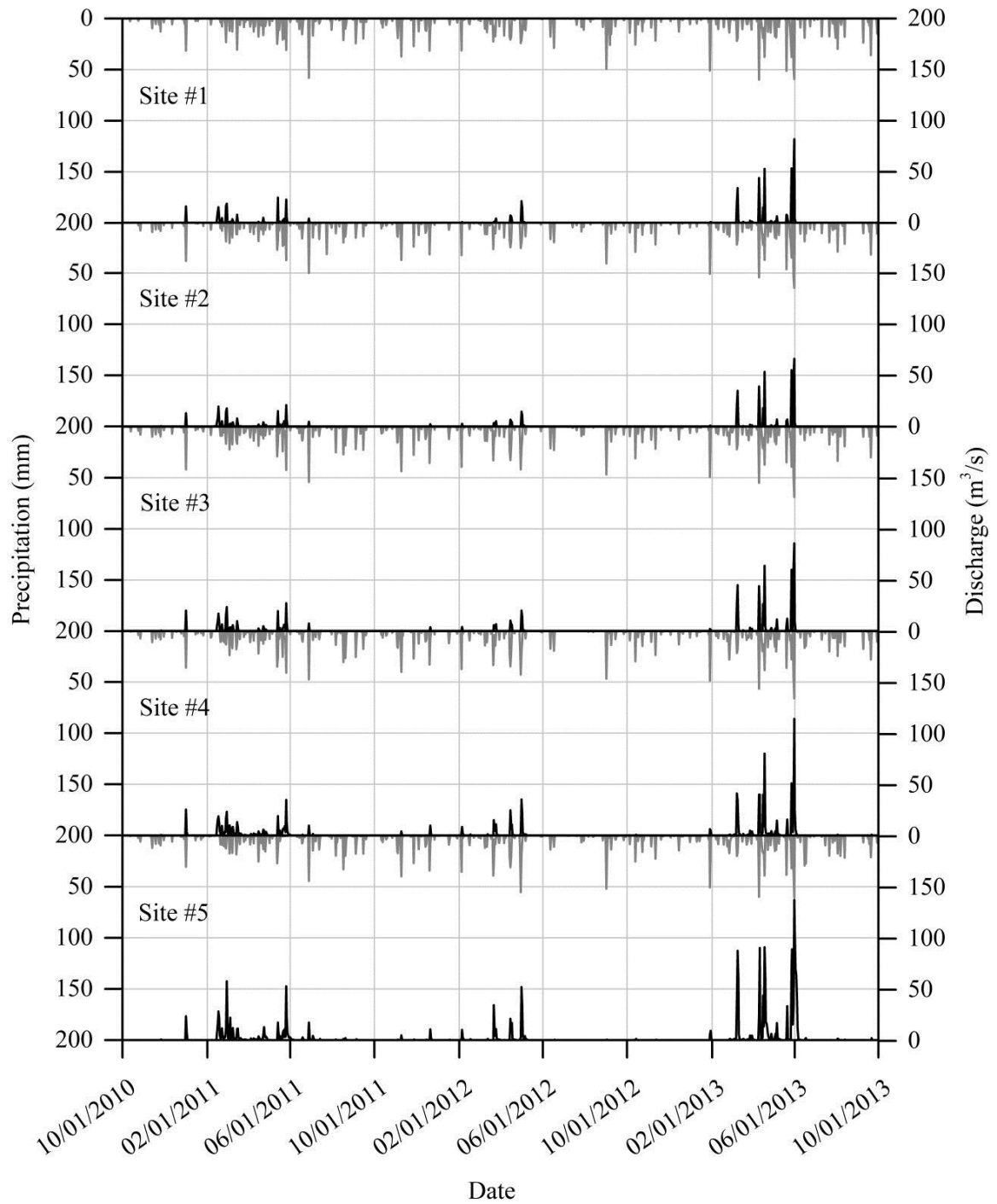
Figure 7. Time series precipitation and discharge are shown for the study period (WY 2010 – 2013) recorded at five climate stations (site #1 on top – site #5 on bottom) located in Hinkson Creek Watershed, Missouri, USA.
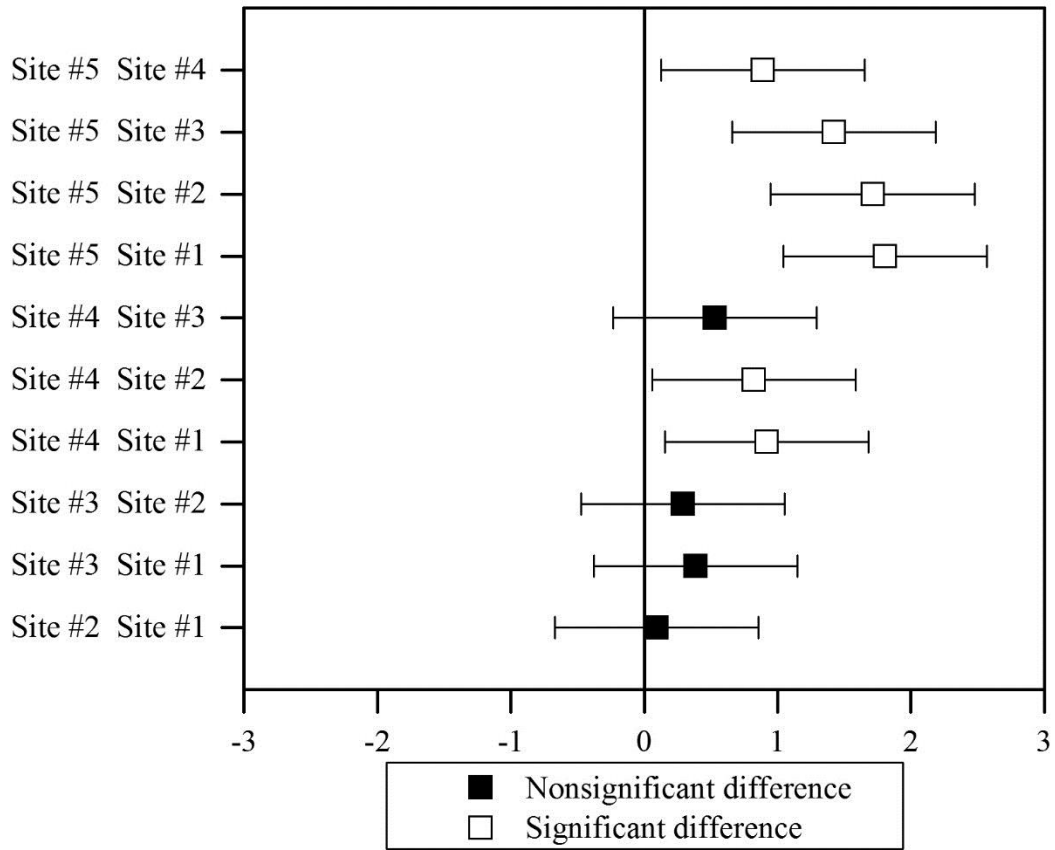
Figure 8. Tukey-Kramer multiple comparison results showing significant differences in daily mean discharge in Hinkson Creek Watershed, Missouri, USA. The x-axis shows confidence interval values. The y-axis shows all possible pairs of sample means being compared. The bars show the confidence interval for each pair of sample means being compared. A significant difference is shown when a confidence interval does not contain the value of zero.
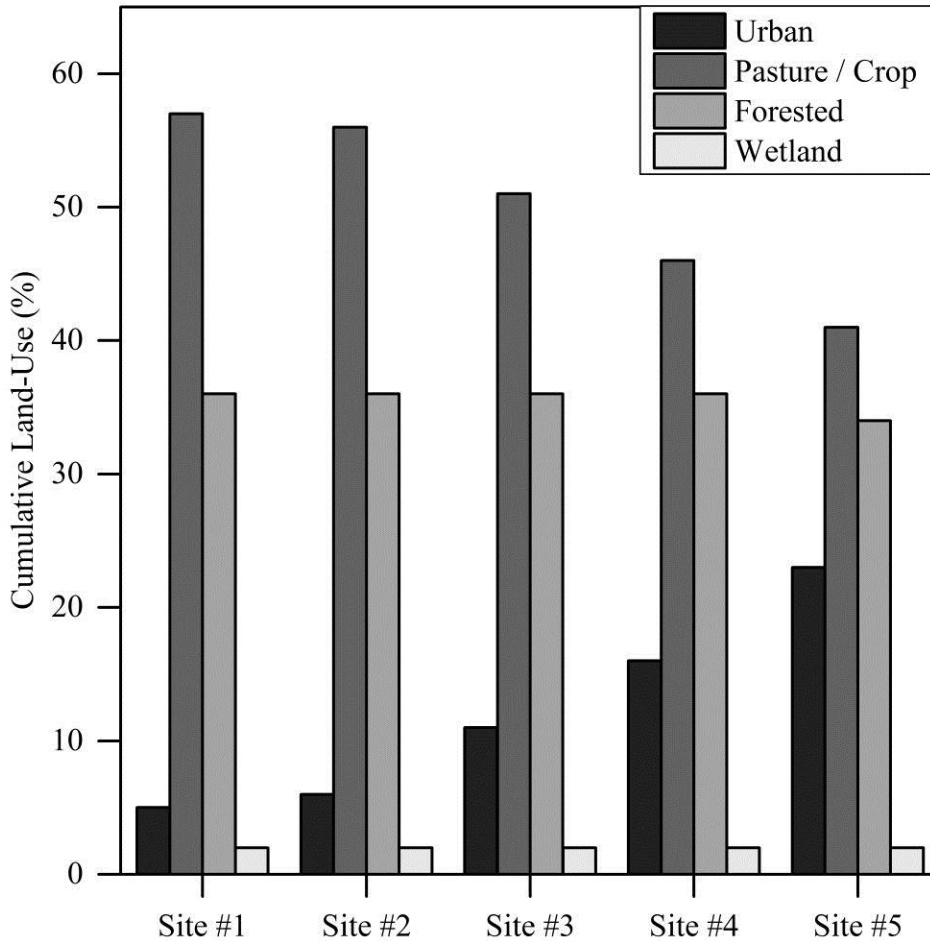
Figure 9. Cumulative land use percent showing percent urban, pasture / crop, forested, and wetland land uses for five subbasins located in Hinkson Creek Watershed, Boone County, Missouri. Site number increases with downstream distance from the headwaters. Site #1 is located in the headwaters, and site #5 is located near the watershed outlet.

Stream water temperature

While the differences between monitoring sites found in daily mean T_w were not significant (p=0.51) (Figure 10), there were significant (p<0.01) differences found in 15 minute mean T_w between gauging sites during the study period, for each water year (WY 2011, 2012, 2013), and for each season (winter, spring, summer).

The differences in T_w were presumably attributable to differences in natural processes (e.g. meteorological conditions, and stream discharge, hydrogeomorphological variability) at each site and anthropogenic impacts from the drainage area upstream and upland of each gauging site. Maximum, mean, and minimum T_a data were lower at site #1 compared to all other sites. The differences in T_a were, in part, due to an urban heat island effect. Site #1 has 1 to 18% less urban land use than the other sites.

Topographic differences, including stream width and stream length, between monitoring sites could also explain the differences in daily mean T_w since at the time of this study site #1 had the narrowest stream width (12.2 m) while site #4 had the widest channel (18.4 m). Narrow stream channels in headwater subbasins like site #1 can have lower T_w due to increased sheltering of stream heating from incoming solar radiation by overhanging riparian vegetation and stream banks (Webb, 2008). Wider stream channels are often less shaded and wind sheltered by riparian vegetation (Caissie, 2006). Consequently, more solar radiation and advected energy can reach the stream surface.

Stream water temperature has also been shown to increase with linear stream distance and with percent urban land use (Caissie, 2006). The stream is exposed to meteorological conditions (including solar radiation) as the stream flows from its source in the headwaters to the watershed outlet. When T_w variability was investigated for each season during the study period results showed mean T_w increased with downstream distance during the spring, but the same trend was not observed in the winter or summer seasons. Spring is the wet season in the central U.S. As a result, discharge is usually higher. As discharge increases, residence time decreases, and the stream is well mixed. There was a general trend for increased T_w with stream distance during the spring. In this

86

research the linear relationship between daily mean T_w and stream distance was weak (r^2=0.30) and not significant (p=0.20) for the entire study period. Thus, stream distance did not account for 70% of the explained variance in mean T_w for the study period Multiple regression analysis showed stream distance and urban land use combined increased the explained variance to 0.78, but the relationship was not significant (p=0.11). When mean T_w during the spring was regressed against stream distance, however, explained variance in mean T_w significantly (p=0.04) increased by 42% (r^2=0.72). Multiple regression analysis showed stream distance and urban land use combined increased the explained variance in mean T_w during the spring to 98%! (r^2=0.98). This was also shown to be a significant relationship (p<0.01).
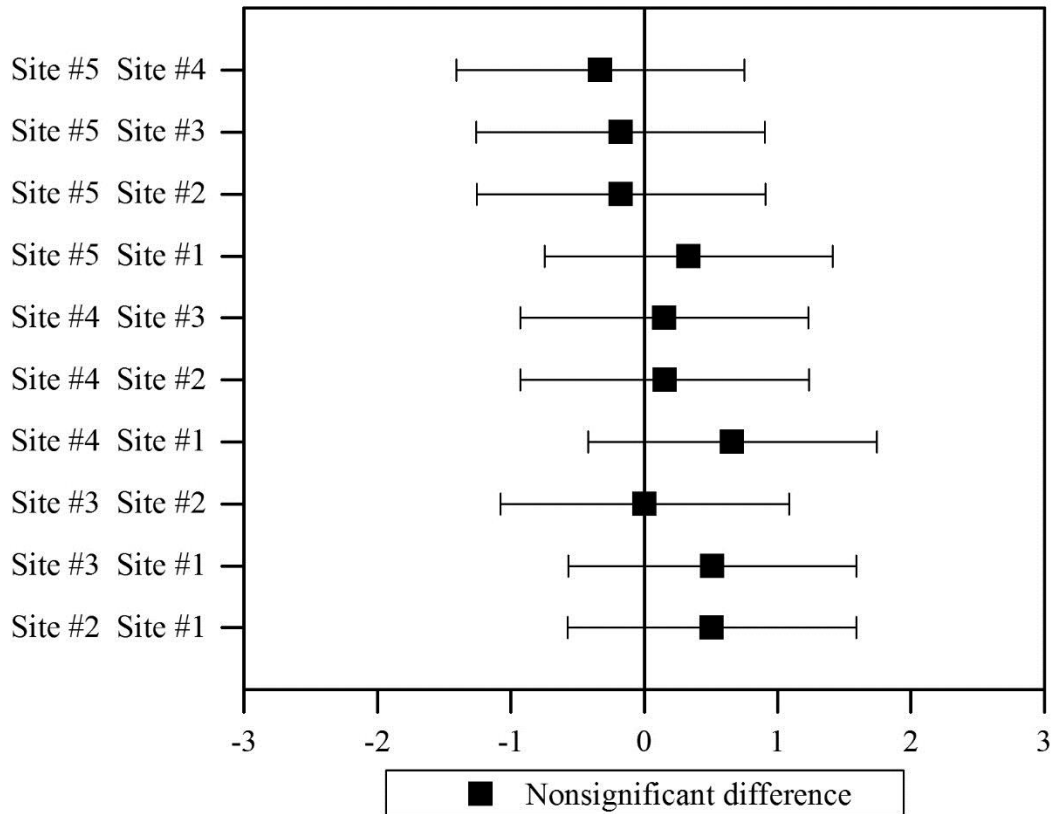
Figure 10. Tukey-Kramer multiple comparison results showing no significant differences in daily mean stream water temperature in Hinkson Creek, Missouri, USA. The x-axis shows confidence interval values. The y-axis shows all possible pairs of sample means being compared. The bars show the confidence interval for each pair of sample means being compared. A significant difference is shown when a confidence interval does not contain the value of zero.

Thermal maximum

The stacked plot in Figure 11 shows when T_w exceeded the 32 °C thermal maximum threshold and the 35 °C critical thermal maximum threshold. The number of day's T_w was above the 32 °C thermal maximum peaked at site #3 for 55 days and decreased with stream distance. Maximum T_w was above the 35 °C critical thermal maximum at site #3 for 5 days. In comparison to the study by Sinokrot and Gulliver (2000) in Platte River, Nebraska, the maximum number of day's T_w was above 32 °C,

and 35 °C was 46 days fewer, and 21 days fewer, respectively, in Hinkson Creek. The

Platte River in Nebraska has a reputation for being "a mile wide and an inch deep".

Increased stream width most likely contributed to the difference in the number of days T_w

was greater than 32 °C, and 35 °C during the study when discharge was low and solar

radiation rates were high.
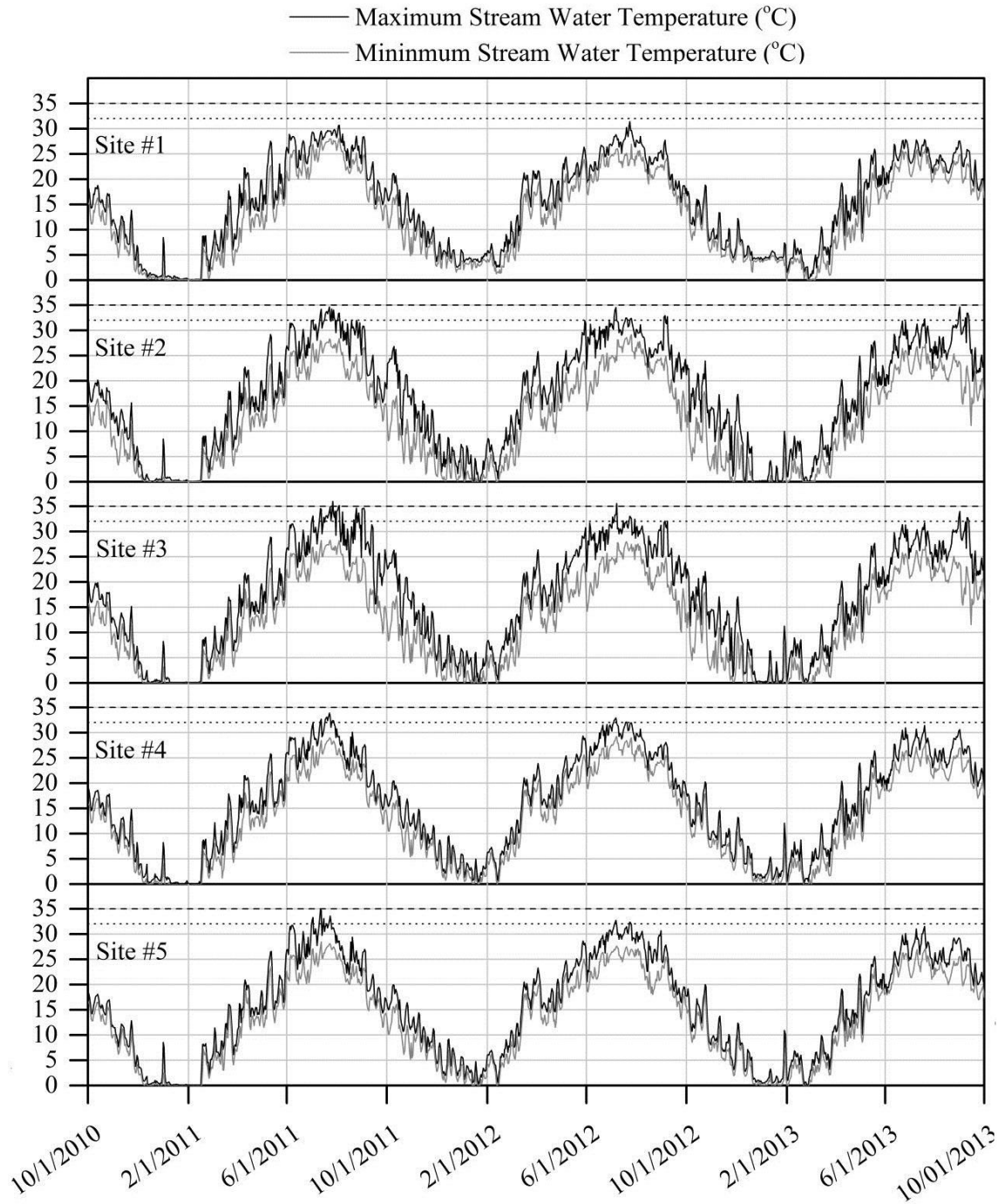
Figure 11. Time series daily maximum and minimum stream water temperatures are shown for the study period (WY 2010 – 2013) recorded at five climate stations (site #1 on top – site #5 on bottom) located in Hinkson Creek Watershed, Missouri, USA. The dotted line signifies the 32 °C thermal maximum threshold. The dashed line signifies the 35 °C critical thermal maximum threshold.

During the summer of 2012, T_w peaked at 36.1 °C and exceeded the critical

thermal maximum threshold of 35 °C for 2.5 hours at site #3, in part, due to reduced

streamflow. Reduced cloud cover increased direct beam solar radiation at the stream

surface. The stream reach at site #3 is lined with limestone bedrock. When limestone

bedrock is heated by incoming solar radiation, the bedrock reemits long wave radiation

that can lead to stream water heating (Webb et al. 2008). Residence time increased as

discharge decreased at site #3. Stream water is exposed to local contributions to stream

heating as residence time increases (Erickson and Stefan, 2000). Additionally, lower

volumes of stream water associated with reduced rainfall respond faster to temperature

changes considering heat capacity of water is dependent on the volume of water

(Erickson and Stefan, 2000).

Considering anthropogenic impacts including deforestation, flow alteration, and

increased impervious surfaces have been shown to affect T_w regimes (Caissie, 2006;

Webb et al. 2008), anthropogenic impacts may have contributed to the high T_w recorded

at site #3. Percent urban land use in site #3 was 11%. Urban land use associated with

impervious surfaces could have contributed to the observed urban heat island effect

where maximum, mean and minimum T_a were greatest at urban site #3 (Hubbart et al.

2014).

Sudden rises in stream water temperature

To investigate urban land use effects on stream heating, Thermochron iButtons

(temperature sensors) were deployed during summer 2009 (June 1st to August 31st).

Twenty-three iButton temperature sensors detected T_w surges during summer 2009 from

the urbanized reaches of Hinkson Creek. The T_w surges were observed following summertime precipitation events when heat from the impervious surfaces was transferred to stormwater runoff and transported into Hinkson Creek. It was assumed that impervious surfaces were hottest in the summer during the early afternoon when seasonal and diel solar radiation rates were highest for the year.

A recent study by Hester and Baumen (2012) also showed T_w surges at a stormwater outfall at Stroubles Creek located in Blacksburg, Virginia USA during summer of 2009, corresponding to the time when the iButton sensors were deployed in Hinkson Creek. The T_w surges recorded by iButton sensors in Hinkson Creek showed mean T_w surge and mean T_w surge duration >1.2 °C and >9.4 hours, respectively, compared to the study by Hester and Baumen (2012). Maximum T_w surge and maximum T_w surge duration >5.6 °C and >24.75 hours, respectively. The differences in magnitude and duration of T_w surges were likely due to difference in location of the T_w sensors, and the amount of water present (i.e. discharge) at the location of the sensor.

T_w surges were also observed when data were analyzed from the in-stream T_w sensors at each of the five gauging site in Hinkson Creek during summers of 2010, 2011, and 2012. Examples of T_w surges found in this study are provided in Figures 12, 13, and 14. Figure 12 shows how relatively small T_w surges (approximately 1 °C increase in T_w within 15 minutes) persisted from suburban site #3 to downstream gauging sites #4 and #5. The T_w surge began at site #3 as discharge increased following a precipitation event at 6:00 a.m. on July 20th, 2010 (Figure 12). Figure 13 shows how plumes of heated stormwater with a peak discharge of approximately 40 m[3]/s can increase T_w by as much as 4 °C for up to 5 hours as the flood wave moves downstream from the City of

Columbia. The T_w surge at site #5 at 18:00 p.m. on July 3rd, 2011 was not detected upstream at gauging site #4. Therefore the T_w surge must have come from stormwater runoff that entered the stream downstream of site #4. Flat Branch Creek, a 1st order tributary of Hinkson Creek, intersects with Hinkson Creek between sites #4 and #5 approximately 1.3 linear km downstream of site #4. The headwaters of Flat Branch Creek originate in the downtown area of the City of Columbia and drain the majority of the high density urban land use from the City of Columbia. Rain transported heated stormwater runoff into Hinkson Creek between sites #4 and #5. This finding was important because it showed how the nested-scaled experimental watershed study design traced the source of a nonpoint source thermal pollutant.

Figure 14 shows how small summer precipitation events during summertime can transport heat into Hinkson Creek leading to T_w surges, even in the middle of the night. For example, at 23:00 p.m. on July 29th, 2012 (during the summer of drought) discharge was low in Hinkson Creek at site #3 (<0.1m^3/s). A small precipitation event that occurred at approximately 00:15 a.m. transported heat from the urban subbasin #3 into Hinkson Creek. At that time, there were two T_w surges detected at site #3 with a mean T_w surge of approximately 1.5 °C. Had the precipitation event been larger and occurred when impervious surfaces were hottest for the day (e.g. around 18:00 hours) like the event observed in Figure 13, the magnitude and duration of the T_w surge observed in Figure 14 could have been larger.
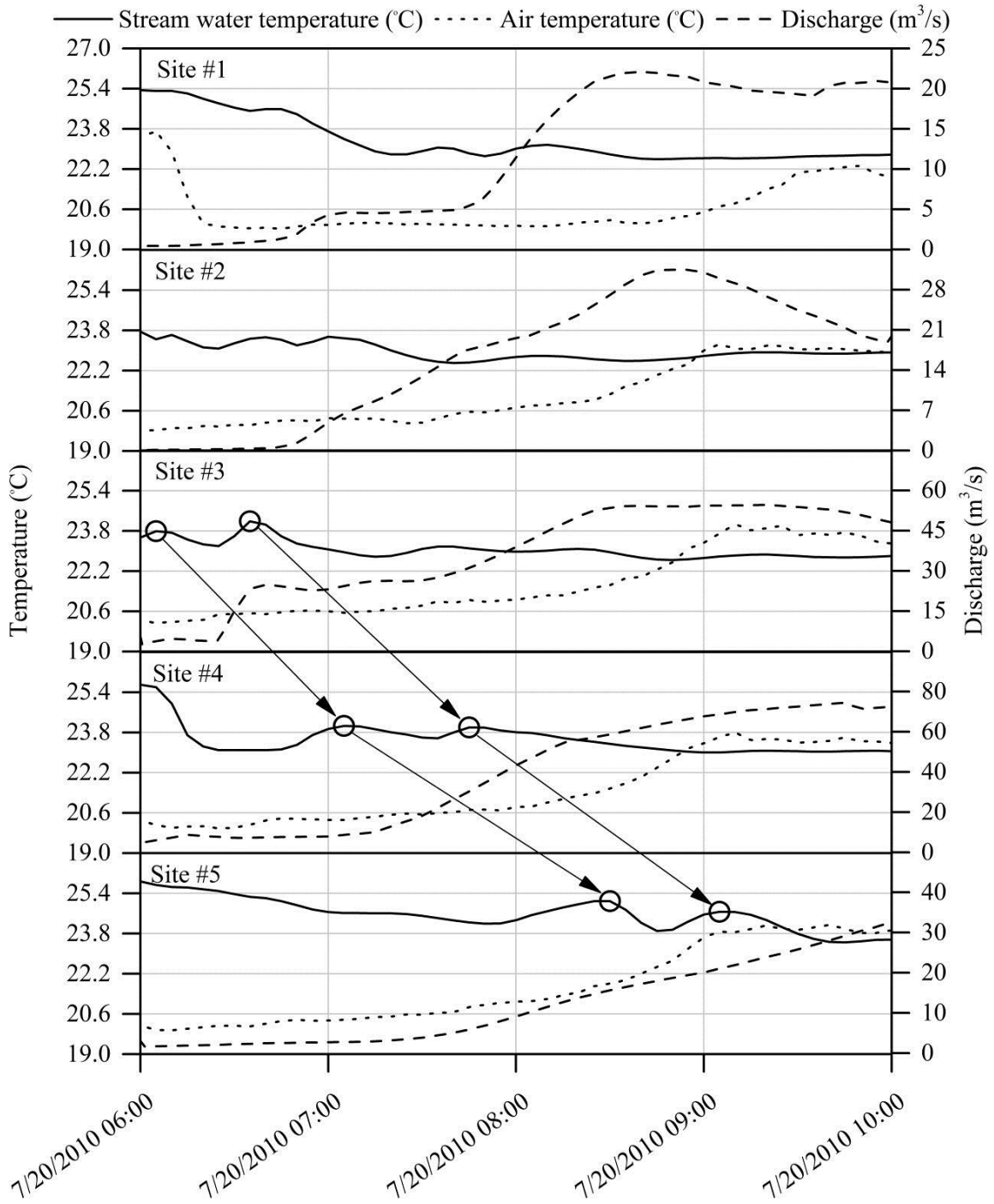
Figure 12. Stream water temperature surges following a summer thunderstorm sensed at gauging sites #3, #4, and #5 in Hinkson Creek near sunset during summer 2010. The black circles mark the peak T_w surges and the arrows track the T_w surges downstream from site #3 to sites #4 and #5. This figure shows how T_w surges persisted at downstream gauging sites and how T_w surge duration was longer at sites #4 and #5.
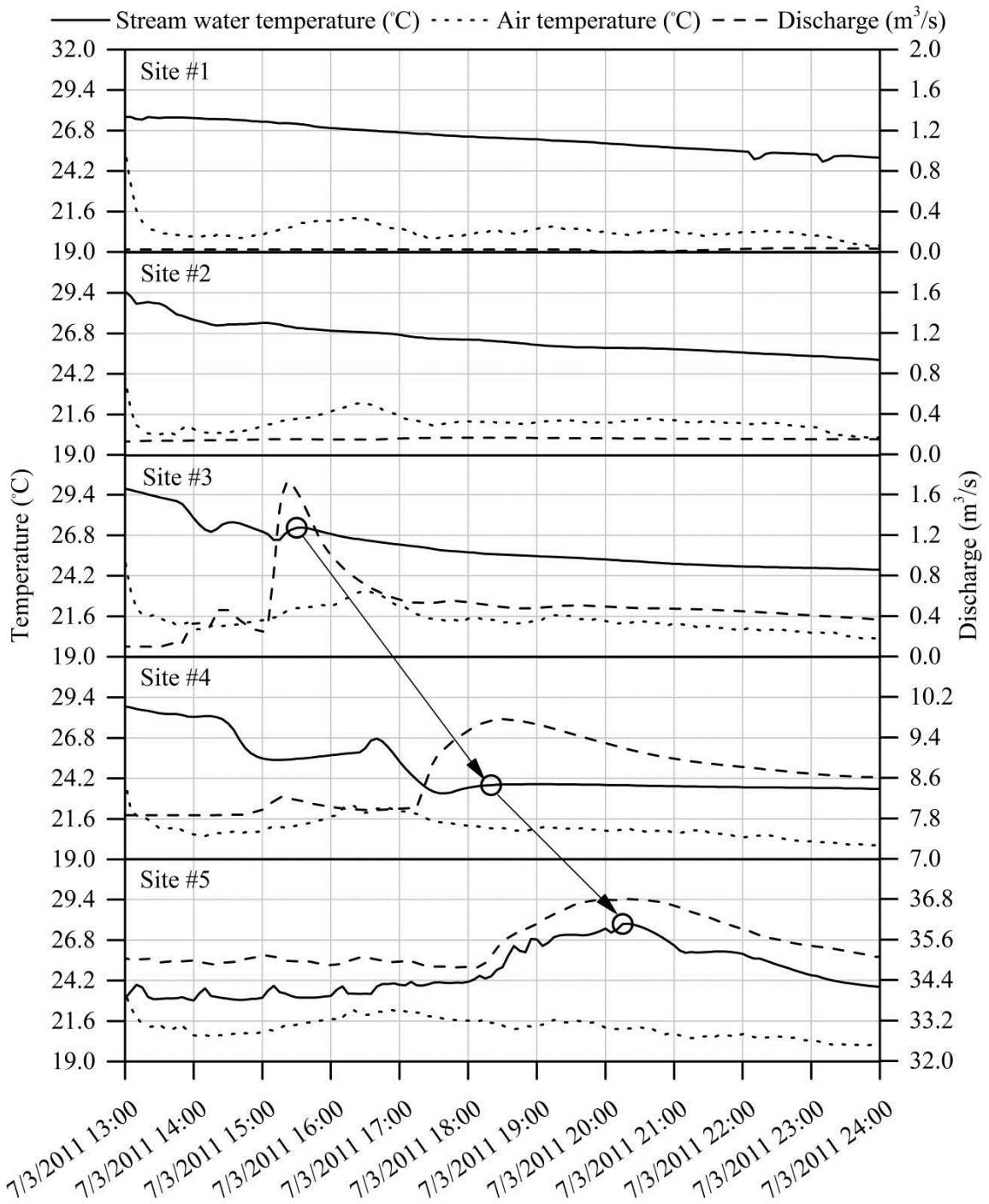
Figure 13. Plume of heated stormwater after a summer thunderstorm sensed at site #5 in Hinkson Creek during summer 2011. The black circles mark the peak T_w after the increase in discharge and the arrows track the event downstream from site #3 to sites #4 and #5. The plume of heated stormwater was observed at site #5, but not upstream at site #4. Thus, the origin of the heated stormwater was downstream of site #4 and upstream of site #5.
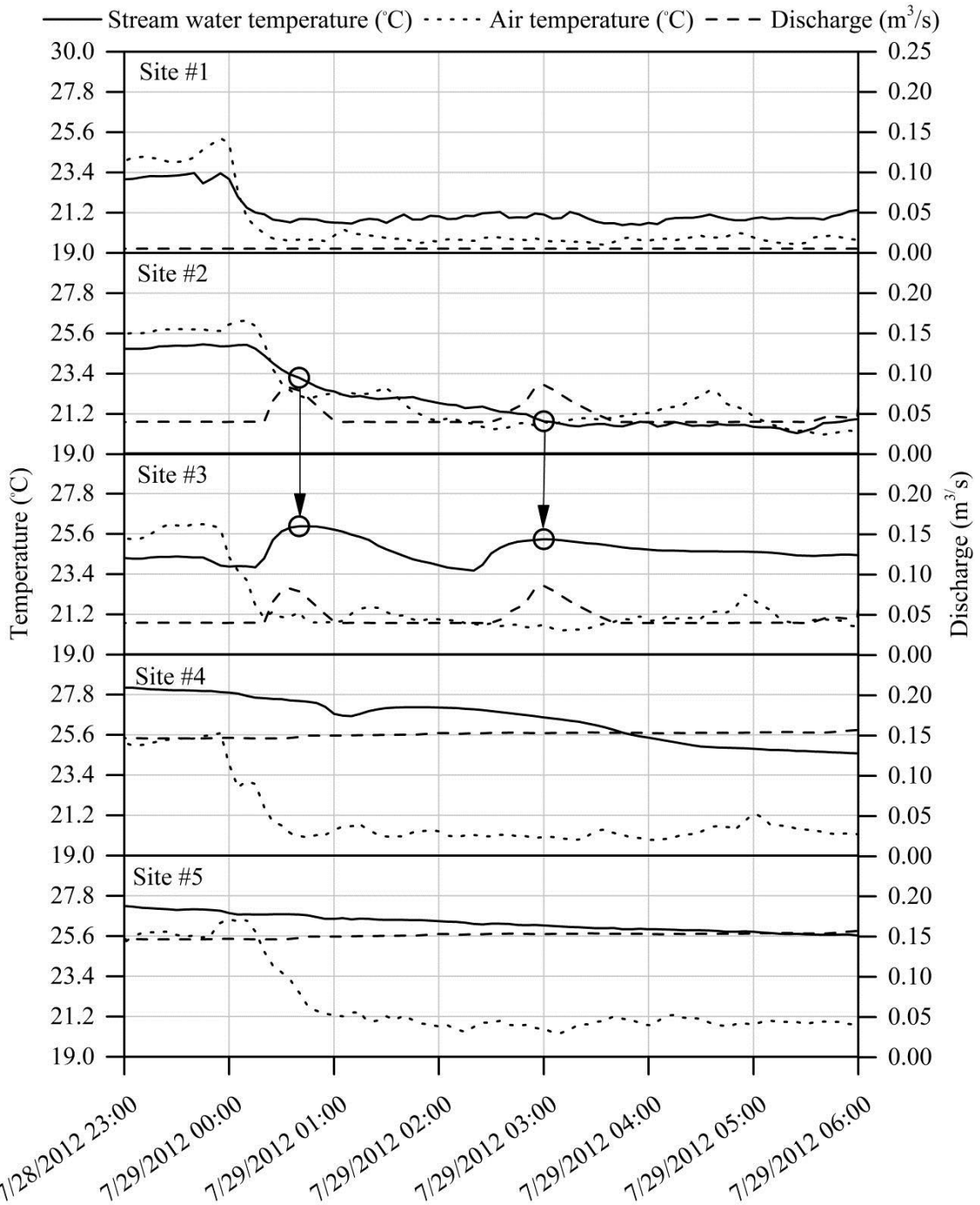
Figure 14. Two stream water temperature surges following a summer thunderstorm sensed at site #3 in Hinkson Creek during summer 2012. The black circles mark the peak T_w following the increase in discharge at site #3 and the arrows track the event downstream from site #2 to site #3. This figure shows how the T_w surges were observed at site #3, but not observed upstream showing the origin of the heated stormwater was downstream of site #2 and upstream of site #3.

Nelson and Palmer (2007), Rice et al. (2011), and Anderson et al. (2011) also reported evidence concerning the effects of urban land use and land cover on increased T_w. Nelson and Palmer (2007) showed minimum and maximum T_w surges of >1.0 °C and >4.8 °C, respectively, in comparison to the in-stream temperature surges observed during the summers of 2010, 2011, and 2012 in this study. Rice et al. (2011) showed minimum and maximum T_w surges of >0.3 °C and >1.1 °C, respectively, when compared to this study. The relationship between amount of impervious surface coverage (ISC) and magnitude of mean T_w surges would explain why Nelson and Palmer and Rice et al. (2011) found T_w surges of greater magnitude and duration. Rice et al. (2011) found that ISC within smaller spatial scales (i.e. 25 meter buffer of the urban stream) correlated with T_w surge events when buffers of 1% ISC showed mean T_w surge amplitude of 1.9 °C and buffers of 75% ISC showed mean T_w surge amplitude of 3.27 °C. The comparison of this work to other work was important because results showed that any additional ISC within a 25 meter buffer of Hinkson Creek could increase the magnitude and duration of T_w surges.

The effects of discharge on stream water temperature

Separating mean T_w into different flow classes (similar to the methods used by Webb et al. 2003) supplied relationships of T_w at each gauging site in Hinkson Creek to increasing flow. Flow classes <50% best predicted T_w during periods of low flow, or base flow. While, the >50% flow class best represented stormflows. To investigate T_w during stormflow periods the >50% flow class was separated into an additional four flow classes. The >90% flow class was assumed to best represent peakflow times when the

stream was turbid and presumably well mixed, so it's assumed there was less variability of T_w with depth and lateral distance. The 90% flow class was also separated into an additional nine flow classes. The >99% flow class was assumed to best represent T_w when Hinkson Creek was close to or overbank full. It was important to analyze T_w at different flow classes to examine the effects of urban stormwater on T_w in Hinkson Creek. Results showing mean stream discharge, mean T_a, and mean T_w for 15 different flow classes are shown in Figures 15 to 17. The increase in stream discharge was nonlinear for every flow class considered from site # 1 to site #5 (Figure 15). When T_a was investigated at each flow class, urban site # 3 was always the highest for T_a, and site #1 was always the lowest for T_a. Figure 16 shows how T_a at rural sites #1 and #2 was always lower than urban sites #3, #4, and #5. Conversely, T_w at urban sites #4 and #5 increased with each flow class relative to the other Hinkson Creek gauging sites as shown in Figure 17. The change in T_w between gauging sites as flow class increased was less correlated to a change in T_a between sites as flow class increased. Conversely, correlations between discharge and mean T_w increased as flow class increased, but ANOVA analyses did not show a significant relationship at the 95% confidence level (p=0.07). This information shows that the difference in T_w between sites was not caused by a change in T_a, and not solely caused by increased. The increase in T_w at sites #4 and #5 was likely caused by urban land use.

Mean T_w at sites #2, #3, and #4 was significantly (p>0.5) higher than sites #1 and #5 when discharge was lower for the <50% flow class. When discharge is low T_w can be more variable with depth, laterally (from bank to bank), and longitudinally (with stream distance) compared to when discharge is high and the stream is well mixed (Webb et al.

2008). As discharge increased, results from the >50% flow class showed mean T_w at sites #4 and #5 were significantly (p>0.5) higher than sites #1, #2, #3 (see Figure 21). Stream water temperature at sites #4 and #5 continued to increase relative to sites #1, #2, and #3 as flow class increased from the >50% flow class to the >90% flow class (Figure 17). This information was important because it provided evidence that urban land use effected T_w.

There was a significant (p=0.01) longitudinal increase in T_w in Hinkson Creek with stream distance as the stream flowed from the headwaters at site #1 to site #5. Increased travel time coupled with increased exposure to meteorological conditions and friction between the streambed and the banks were assumed to have contributed to higher T_w at sites #4 and #5 relative to the other sites. Stream travel time from the headwaters was calculated as approximately 4.8 hours at site #4 and 6.2 hours at site #5. A study by Webb and Zhang (1997, 1999) that reported heat fluxes measured at 17 different sites in the United Kingdom showed friction between the stream bed and banks contributed 15.8% of stream heating. While the increase in T_w at sites #4 and #5 was presumably, at least in part, due to natural impacts of exposure to meteorological conditions and friction, the primary cause was believed to be due to urban stormwater runoff considering the sudden increases in T_w at urban gauging sites and the relative significant (p<0.01) differences in mean T_w at urban sites relative rural sites. As previously stated, multiple regression analyses showed significant (p=0.05) correlations between stream distance and urban land use as flow class increased accounting for 90% of the explained variance in mean T_w.

Urban site #5 showed the greatest increase in T_w with increased flow relative to all the other Hinkson Creek sites. For the <50% flow class, T_w was 0.6 C lower at site #5 compared to site #4, and from the >90% flow class and beyond T_w between sites #4 and #5 were nearly equal with differences in $T_w < 0.1$ °C. These data provided additional significant (p=0.02) evidence that heated stormwater runoff flowed into Hinkson Creek between sites #4 and #5 during the study period. A review by Webb et al. (2008) also indicated that increased impervious surfaces can increase T_w when stormwater runoff transports heat energy from impervious surfaces to a stream.

The difference in T_w between sites #2 and #3 was negligible (0.1 °C), but urban site #4 showed an increase in T_w with increased flow relative to the upstream suburban / rural Hinkson Creek sites. The difference in mean T_w between sites #4 and #3 was 0.5 °C at the >99% flow class (n=265) as shown in Figure 17. Site #4 drained 15.7 km^2 more urban land cover, associated with impervious surfaces, compared to site #3.
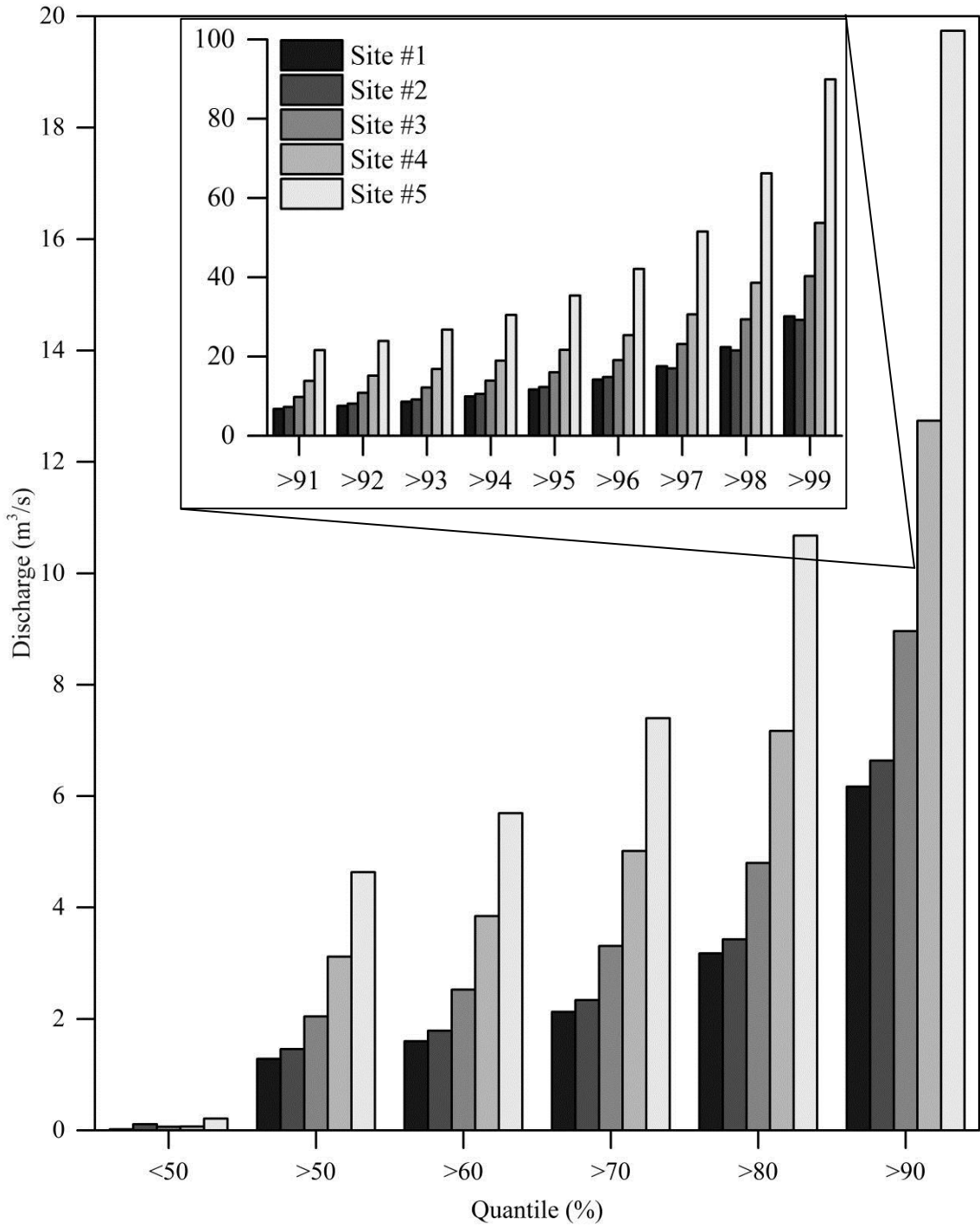
Figure 15. Mean discharge above and below median values are shown for each study site examined during the study period in Hinkson Creek Watershed, U.S.A. Additionally, four other flow classes are shown. A nested plot expands the >90% quantile for a total of 15 flow classes.
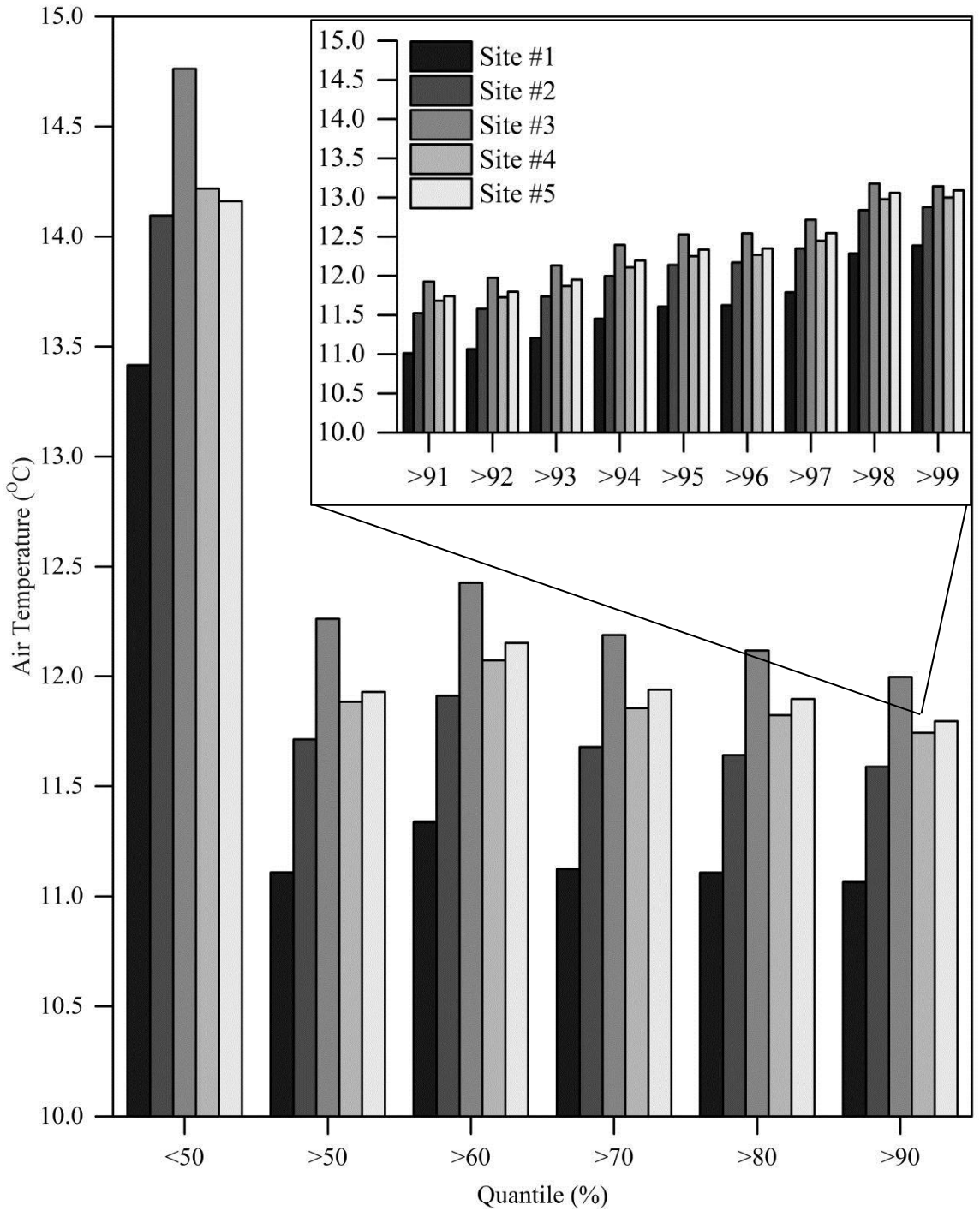
Figure 16. Mean air temperatures above and below median values are shown for each study site examined during the study period in Hinkson Creek Watershed, U.S.A. Additionally, four other flow classes are shown. A nested plot expands the >90% quantile for a total of 15 flow classes.
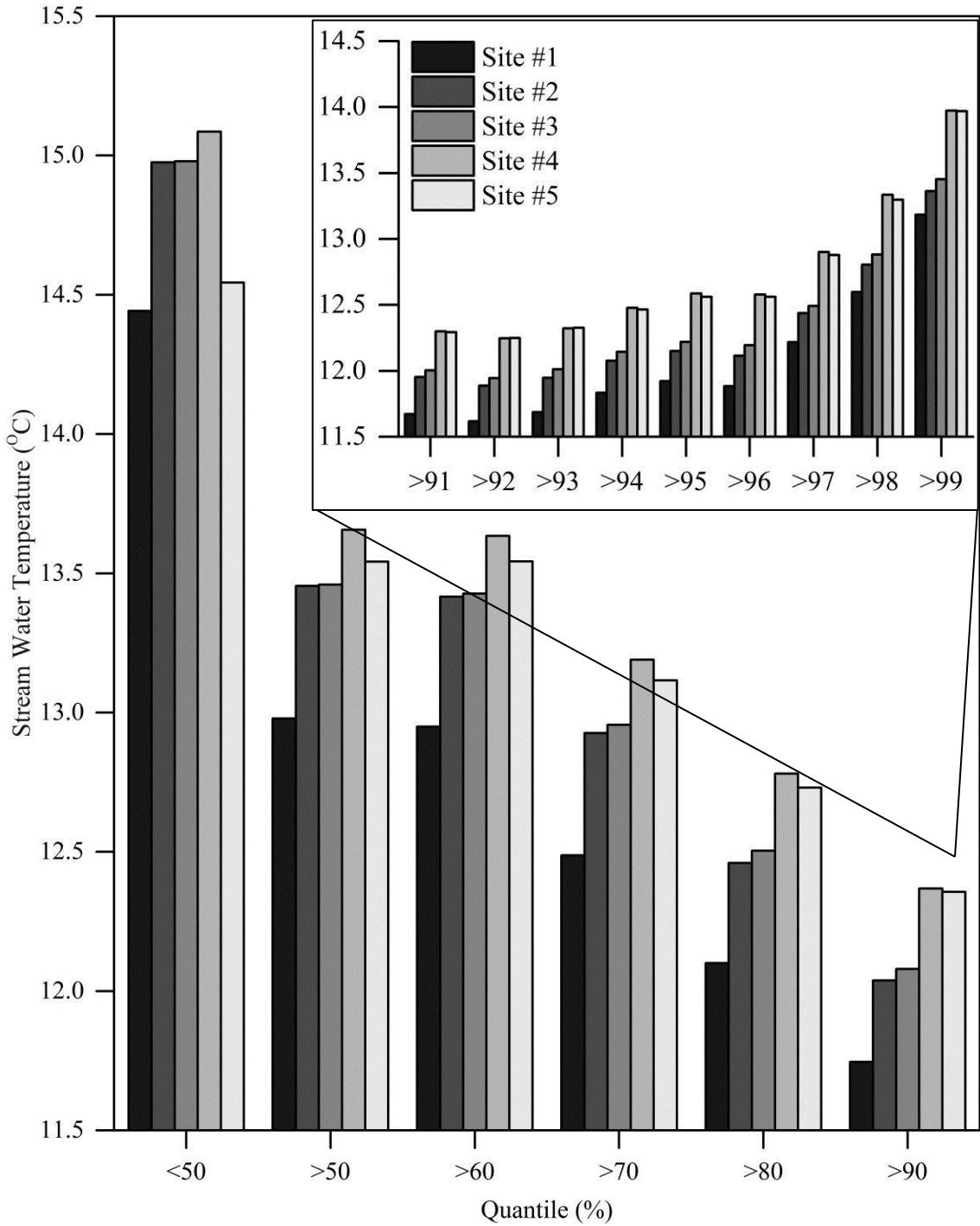
Figure 17. Mean stream water temperatures above and below median values are shown for each study site examined during the study period in Hinkson Creek Watershed, U.S.A. Additionally, four other flow classes are shown. A nested plot expands the >90% quantile for a total of 15 flow classes.

STREAM AND AIR TEMPERATURE RELATIONSHIPS

Linear and nonlinear T_w models (see Methods) were created to simulate mean T_w using observed mean T_a data. T_w models are useful tools for water resource managers because the models provide a cost effective way to predict T_w changes due to land use or other anthropogenic impacts (e.g. global warming due to human induced climate change). The equations can be forced in computer programs (e.g. Excel) using readily available T_a data from nearby weather stations and the appropriate corresponding coefficients. For example, if the model user needed to know daily mean T_w at site #1, then they could run the daily linear T_w model in Excel. To force the T_w model in Excel, the model user would have to first, create a new workbook. Then, manually input daily mean T_a for the day of interest into a column, and corresponding row (e.g. cell "A1"). Next, the linear T_w model for site #1 would need to be manually input into an adjacent column, and corresponding row (e.g. cell "B1") using linear coefficients *a* and *b* derived from linear regression analyses that correspond to the appropriate T_w model. Table 19 shows linear coefficients *a*, and *b* were 0.781, and 4.067, respectively, for the daily linear T_w model. So, the format of the function typed into the adjacent cell (e.g. cell "B1") would be "=(0.781*A1)+4.067". If daily mean T_a was 21.0 °C at site #1, then simulated daily mean T_w would be 20.5 °C.

Results from linear and nonlinear regression analyses are shown in Figures 18 to 21. Accounting for time lag at sub-daily time steps increased r^2 values for linear and nonlinear models by 0.2 to 3.7%, and 0.3 to 3.9%, respectively (Figure 18). Results showed site #1 had a weaker T_w and T_a relationship compared to the other gauging sites (Figure 19). Differences in r^2 values between site #1 and the other four gauging sites

ranged from 8.6 to 1.1%. Site #1 also showed a lag of 4.25 hours. Figure 11 shows how

T_w at site #1 was often higher in the winter (above freezing) and lower in the summer

(below 32 °C) unlike the other sites during WY's 2012 and 2013. Reviews by Caissie

(2006) and Webb et al. (2008) indicated that groundwater influence can lead to increases

in T_w in the winter and decreases in T_w in the summer. The weak T_w / T_a relationship at

site #1 could also be explained by pooling and decreased stream width. Similar results

were presented by Erickson and Stefan (2000) when groundwater inflows, stream shading

and wind sheltering affected T_w / T_a relationship. Groundwater inflows were shown to

increase the y-intercept and decreased the slope of linear T_w / T_a relationships and stream

shading affected the T_w / T_a relationship assuming T_w and T_a are dependent on solar

radiation input at the stream surface (Erickson and Stefan, 2000). In addition, wind

sheltering was found to decrease advective heat transfer at the stream-atmosphere

interface thereby buffering T_w from meteorological conditions (Erickson and Stefan,

2000). Therefore, linear and nonlinear T_w regression models dependent on T_a may not

simulate T_w well in headwater sub basins where groundwater inflows, stream shading and

wind sheltering can affect T_w.
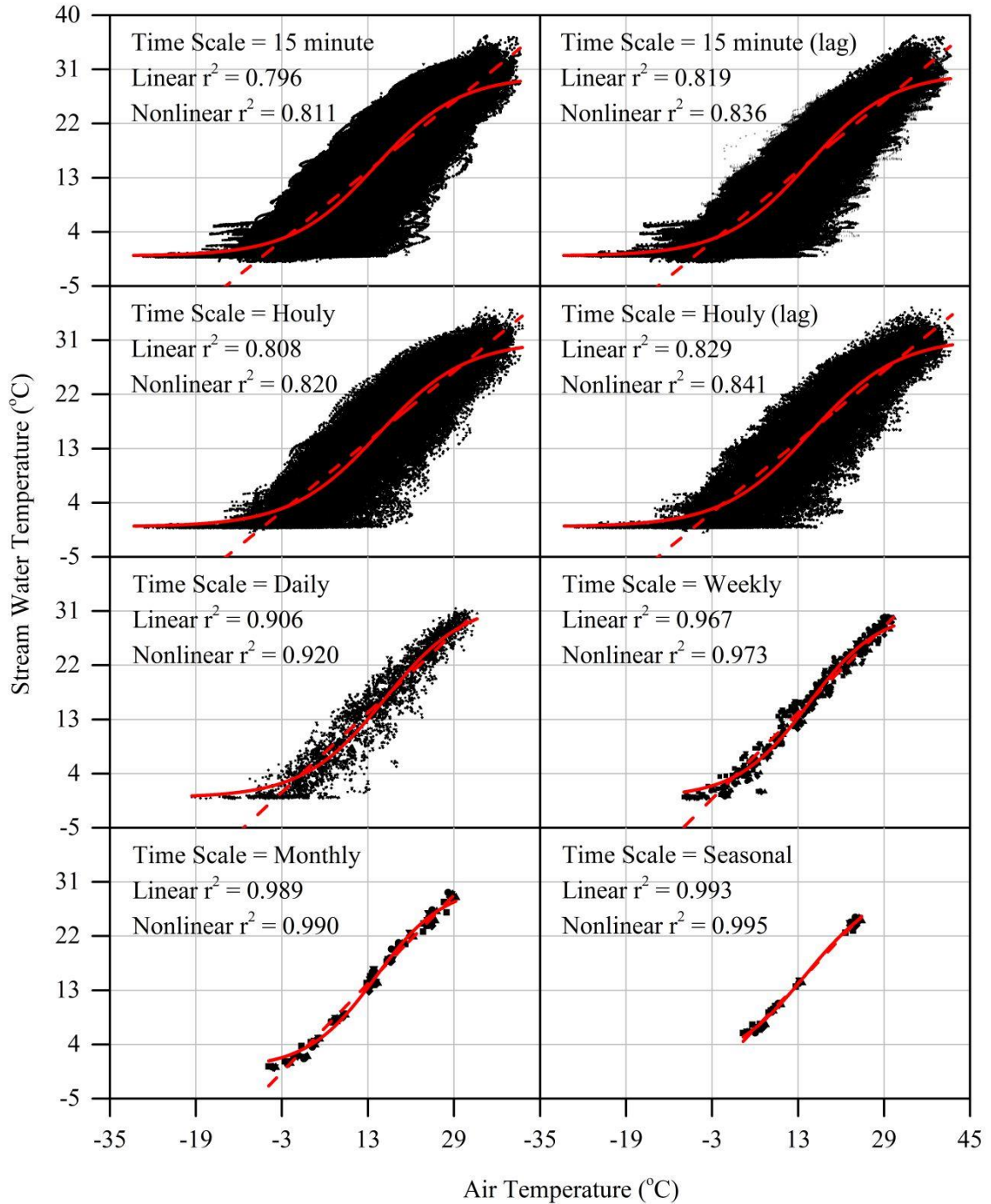
Figure 18. Five site mean coefficients of determination (r^2) from linear (dashed line) and nonlinear (solid curve) regression analyses are shown for each time step considered (15 minute, hourly, daily, weekly, monthly, and seasonal) and for five gauging sites examined during the study period located in Hinkson Creek Watershed, U.S.A.
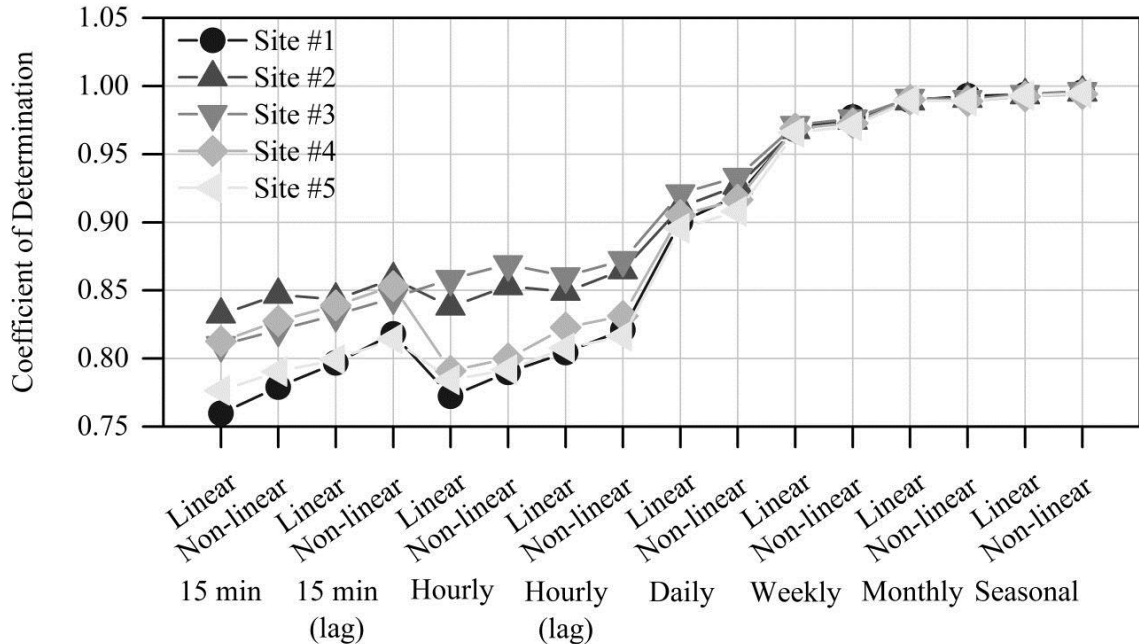
Figure 19. Coefficients of determination from linear and nonlinear regression analyses are shown for each time step considered (15 minute, hourly, daily, weekly, monthly, and seasonal) and for each study site examined during the study period located in Hinkson Creek Watershed U.S.A.

Studies showed T_w / T_a relationships are often affected by increased discharge (Webb et al. 2003) and urban land use (Rice et al. 2011). In this study there was a trend for T_w / T_a relationships to decrease (i.e. time lag increased and r^2 values decreased) from site #2 to site #5 as discharge and urban land use increased. Webb et al. (2003) showed that r^2 values were higher when flow was above median flow values. Increased discharge decreases stream interaction with the atmosphere because surface area to volume ratios decrease as discharge increases below bank-full. Large volumes of water can buffer the relationship between T_w and T_a considering the high specific heat capacity of water (Webb et al. 2003; Stefan and Preud'homme, 1993). Rice et al. (2011) showed that r^2 values decreased as impervious surface land coverage increased by 0.28 for daily linear T_w models and 0.37 for weekly and monthly linear T_w models. The decreases in r^2 values

were attributed to the long term increase in mean T_w and short term temperature surge events where stream water temperature increased by 1 °C within 15 minutes and ground water interaction in a gaining urban stream (Boone Creek) in North Carolina.

Results from the current study showed linear and nonlinear regression r^2 values were significantly (p=0.01) affected by the time scale considered. As time step increased from 15 minute to seasonal averages, r^2 values increased from 0.760 to 0.995. As time series T_a and T_w data were reduced, the variation or "noise" in the data was attenuated by the averaging. The r^2 values quantify the total variation in y values attributed to the model relationship (Moriasi et al. 2007). Obviously, any data reduction by averaging increases r^2 values. Similar results were found in a study by Erickson and Stefan (2000) who showed that stream water temperature was more accurately estimated at timescales greater than one day (e.g. weekly, monthly, and seasonal), in part because there was more "noise" or detail in high resolution T_w data. Therefore, there was an important cost (decrease in detail) and benefit (increase in model accuracy) observed as time scale increased. This information is may be important to land managers that need to predict T_w at less than weekly time steps.

Time scale also significantly affected (p<0.01) linear regression coefficients, but not nonlinear coefficients. The range of the data sets decreased when averaged; meaning, the maximums decrease and the minimums increase. Air temperature had a greater diel and seasonal range than T_w mainly because of the specific heat capacity of water. Thus, T_a was affected more by averaging causing a slight counterclockwise rotation of the best fit line (Erickson and Stefan, 2000). This explains why, for linear regression analyses, the slope of the best fit lines (linear coefficient *a*) increased and the y-intercept (linear

coefficient b) decreased as the data were reduced from 15 minute to seasonal averages (Figure 20). While nonlinear regression coefficients were not affected by data reduction, results showed a positive relationship between alpha / beta coefficients, and an inverse relationship between gamma coefficients and alpha / beta coefficients (Figure 21). Erickson and Stefan (2000) showed similar results for the effect of time scale on linear regression analyses between T_w and T_a. This information helped improve our understanding of the effects of time scale on T_w regression models.
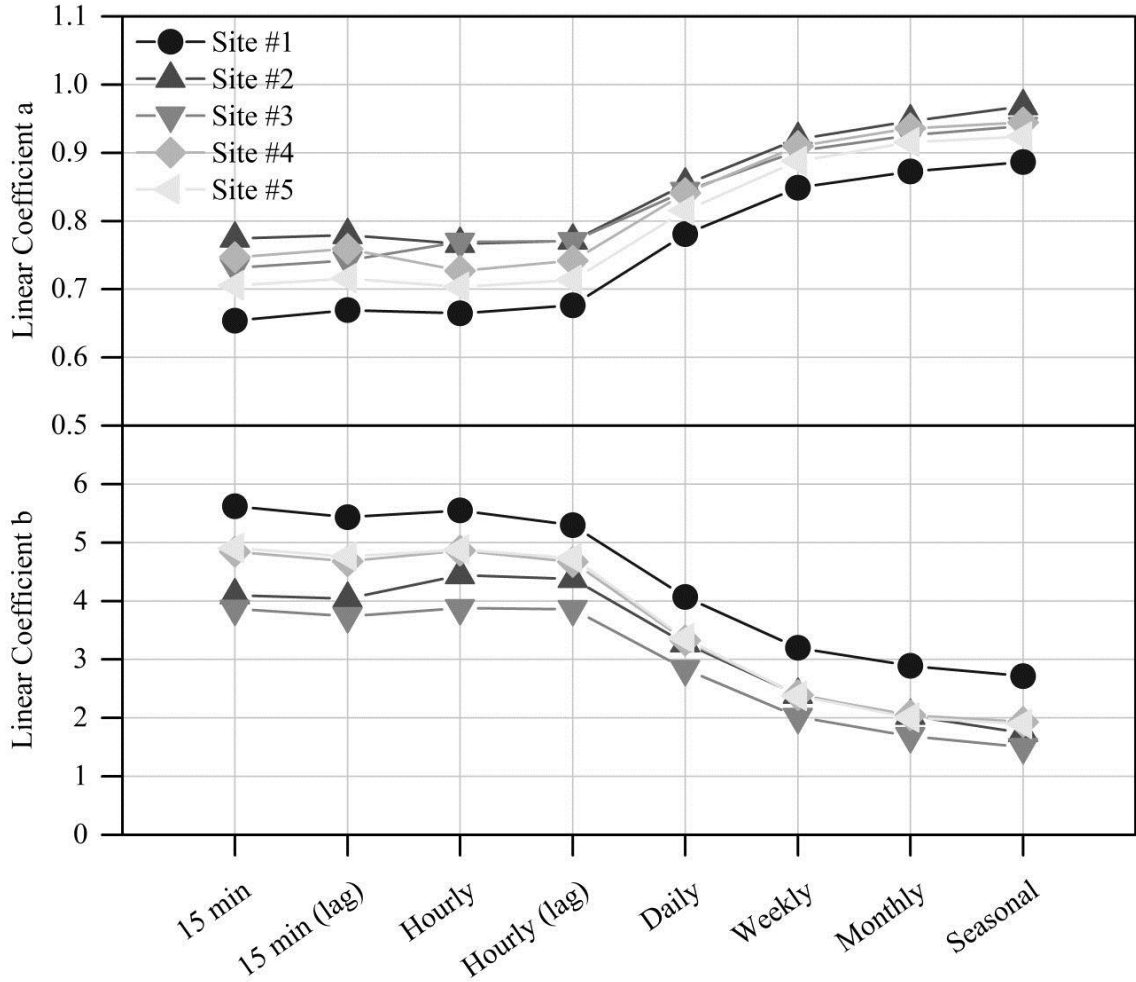
Figure 20. Results from linear regression analyses are shown for comparison of each time step considered (15 minute, hourly, daily, weekly, monthly, and seasonal). Linear coefficients *b* (top) and *a* (bottom) are displayed for each study site during the study period located in Hinkson Creek Watershed, U.S.A.
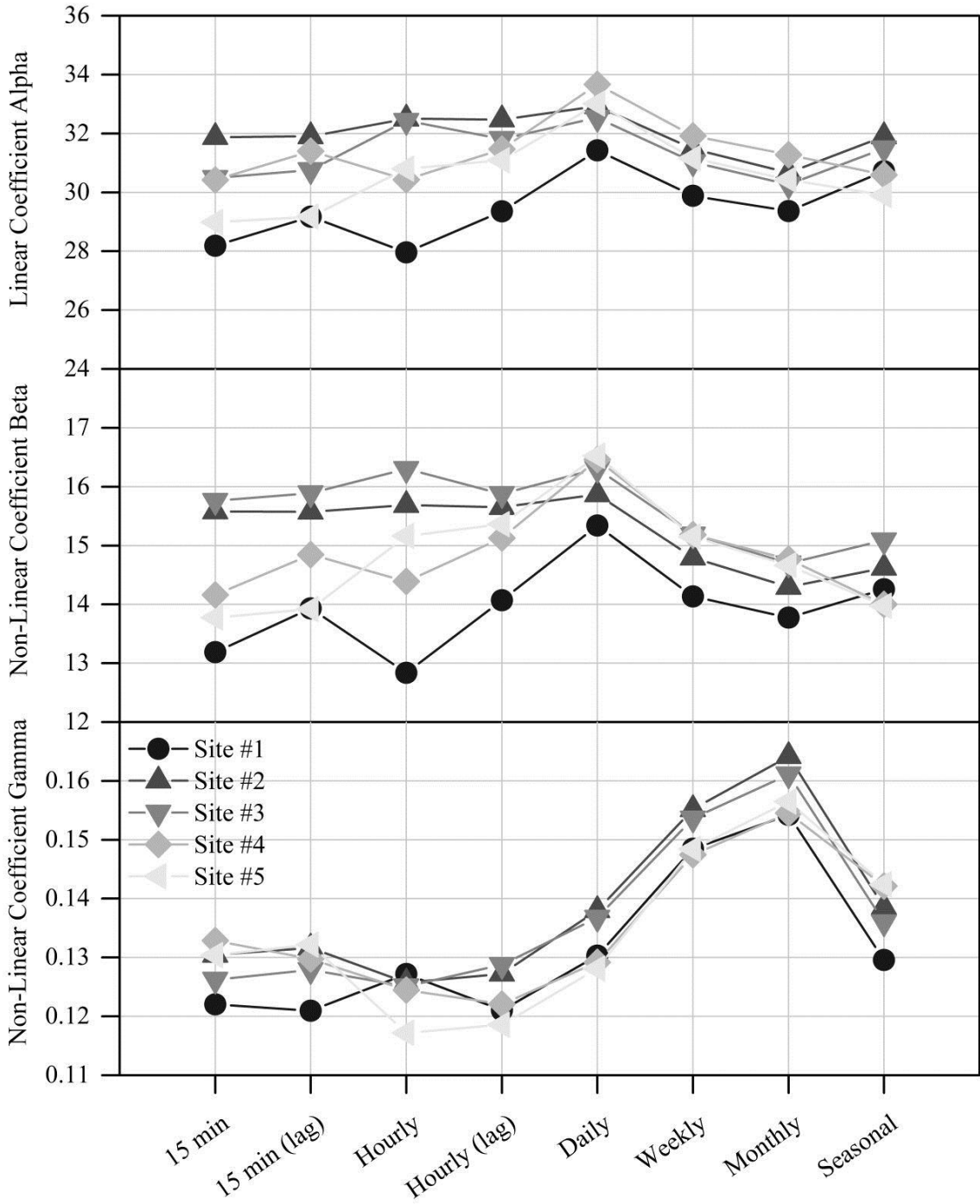
Figure 21. Results from nonlinear regression analyses are shown for each time step considered (15 minute, hourly, daily, weekly, monthly, and seasonal). Nonlinear coefficients alpha (top), beta (middle), and gamma (bottom) are displayed for each study site during the study period located in Hinkson Creek Watershed, U.S.A.

The effects of discharge on T_w and T_a relationships

Results from T_w and T_a linear regression analyses at a daily time step for 15 different flow classes are shown in Figure 22. Results for this study showed as flow class increased r^2 values significantly (p<0.01) decreased. The differences in r^2 values between the <50% flow class and the >50% flow class ranged from 4.9 to 5.4%. The most dramatic change in r^2 values between flow classes was found between the >80% flow class and the >90% flow class. Then, the difference in r^2 values ranged from 9.8 to 11.98%. The decrease in r^2 values slightly decreased the slope of the best fit line. As the slope of the best fit line decreased, y-intercepts increased. Webb et al. (2003) found similar results. Webb et al. (2003) showed for four study catchments in England the r^2 values were significantly higher between the <50% flow class and the >50% flow class ranged from 1.7 to 9.8%. An earlier study by Smith and Lavis (1975) showed daily maximum and minimum air temperature relationships with T_w were affected by discharge in two small upland catchments (approximately 1 km^2 drainage area with elevations ranging from 610 to 470 m) in Upper Waredale, England.

When discharge was below median values, r^2 values were greatest at site #3 (r^2=0.942), and there was no general trend in the change in r^2 values with downstream distance from the headwaters. But, r^2 values generally decreased with stream distance for every flow class above 70%. The observed decreases in r^2 values were explained by accompanied increases in stream discharge (p<0.01), and by urban land use percent in the sub-basin (p=0.03). There were not only significant decreases in T_w / T_a relationships with each increase in flow class, but also with downstream distance from the headwaters when flow rates were above median discharge (p<0.01). Urban land use also increased

with distance from the headwaters. Figure 22 shows the largest difference in r^2 values in the >96% and >97% flow classes when r^2 values were up to 0.20 less at urban site #5 compared to the other gauging sites. The decreased r^2 values found at site #5 was not correlated with increased discharge (p>0.5), but cumulative urban land use percent (p=0.02).

Stream water temperature regimes are controlled by meteorological conditions (e.g. solar radiation, and T_a), particularly during low flow periods. This fact is apparent in this study given T_w and T_w / T_a relationships were higher for the <50% flow class. But, hydrologic factors (e.g. volume of water, source of water) dominate during high flow periods as shown in this study when T_w / T_a relationships were in the >50% flow class. As discharge increases, streams are more thermally stable and less responsive to changes in meteorological conditions, in part, because of the high specific heat capacity of water buffers the streams response to changes in the surrounding environment as discharge increases (Stefan and Preud'homme, 1993). Additionally, residence times decrease as flow rates increase. Decreased residence times decrease stream interaction with the atmosphere (Erickson and Stefan, 2000). Thus, T_w is more dependent on the temperature of inflows as discharge increases (Ward, 1985). Empirical T_w models incapable of accounting for the temperature of inflows will lack the capability to accurately model T_w during high flow periods as shown in this study when daily T_w / T_a relationships r^2 values fell below 0.80 for flow classes >80%.
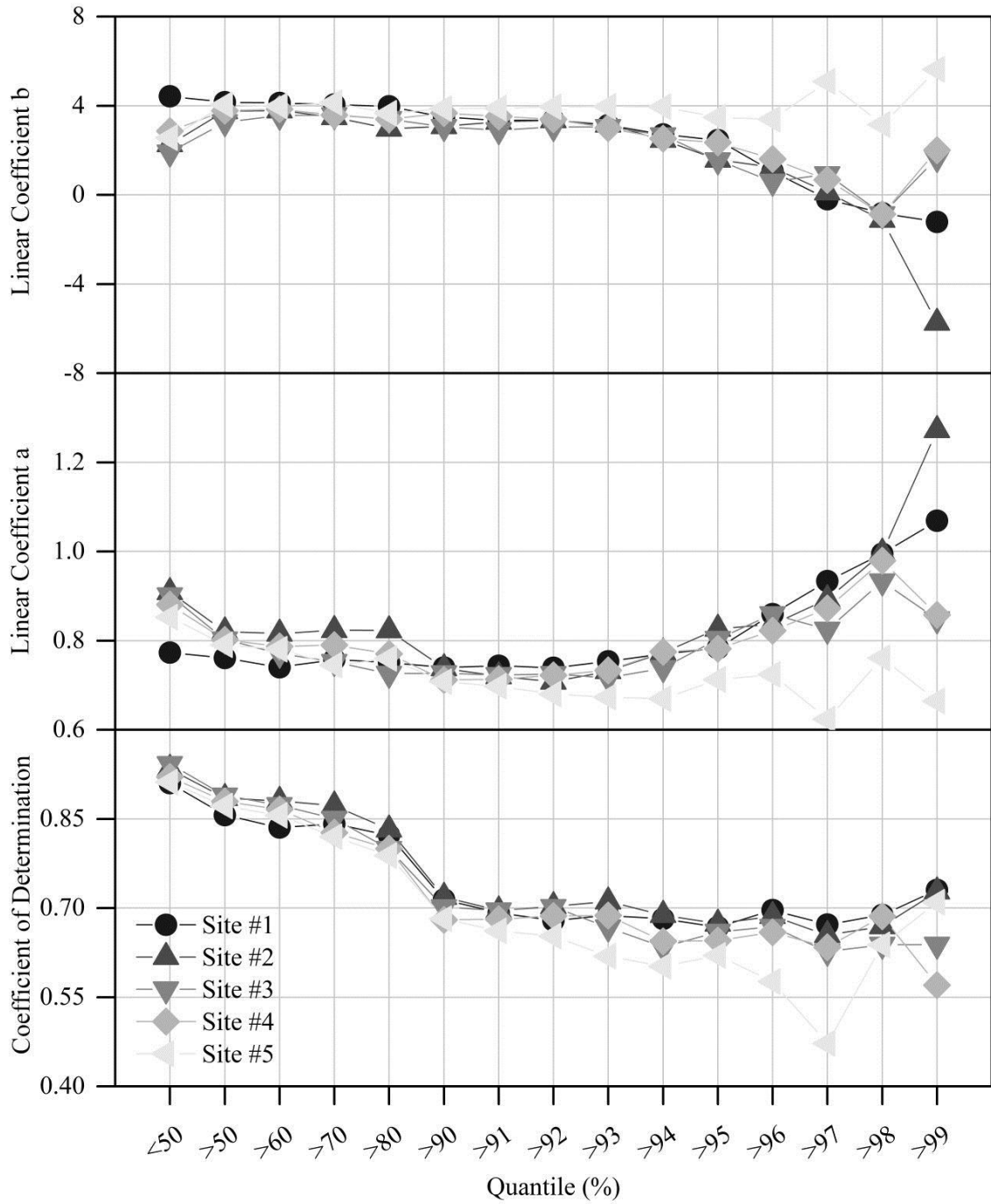
Figure 22. Coefficients of determination from linear regression analyses are shown for 15 different flow classes (quantiles) and for each study site examined during the study period.

SWAT MODELING

SWAT calibration

Arnold et al. (2012) noted that SWAT model calibration should include 1) wet, average, and dry years of observed data, 2) numerous model evaluation criteria, 3) calibrating all variables estimated, and 4) verification that other key model outputs are realistic. To satisfy the four objectives for model calibration proposed by Arnold et al. (2012) this research used three WY's (2010 to 2012) for calibration ranging from wet (WY 2010) to dry (WY 2012), six model evaluation criteria (including NSE, PBIAS, and RSR), and "SWAT check" were used to test if manual calibration yielded realistic results. Observed streamflow data collected during the 2010, 2011, and 2012 water years from all five gauging sites were used for calibration concurrently to improve stream flow simulations at each gauging site as per the work of Qi and Grunwald (2005). SWAT check is a tool embedded in SWAT that tests model output for potential problems (White et al. 2010).

Results from SWAT model calibration are shown in Figure 23. Peak flows were underestimated during the calibration period. For example, maximum simulated discharge was 72.7 m^3/s less than observed discharge at site #5. But, the NSE, PBIAS and RSR values were all above the guidelines published by Moriasi et al. (2007) for satisfactory model evaluation at a monthly time step. Usually, model simulations are less accurate for shorter time scales, therefore, daily model evaluation criteria should be less strict compared to monthly model evaluation criteria (Moriasi et al. (2007). NSE, PBIAS, and RSR values were all in the "Satisfactory" range. Considering standards for model

evaluation at a monthly time step should be stricter than a daily time step the model was deemed well calibrated to site #5 near the watershed outlet.

Results showed NSE and RSR values were just above and below the threshold of "Satisfactory" for sites #1 and #2. But, the model was still deemed sufficiently calibrated for this research using the guidelines proposed by Moriasi et al. (2007) considering the effects of time scale on SWAT model output for streamflow. Model evaluation results showed NSE, PBIAS, and RSR values were all well within the "Satisfactory" range for site #3, and ranged from "Good" to "Very Good" at site #4.

SWAT validation

The SWAT model was validated using observed streamflow data collected during the 2013 water year from all five gauging sites in Hinkson Creek Watershed. Model evaluation results for streamflow during the validation period were not significantly different (p>0.05) from the calibration period. Model performance should be better during calibration compared validation because parameters are optimized by making adjustments during calibration, but not during validation, therefore, the validation results were better than expected. Validation results ranged from slightly "Unsatisfactory" (e.g. NSE=0.49) to "Very Good" (e.g. PBIAS=3.9%). While many of the model evaluation results were just below "Satisfactory" according the criteria published by Moriasi et al. (2007) at a monthly time step, there were at least one model evaluation criterion close enough to the "Satisfactory" threshold for a monthly time step to deem the model capable of simulating acceptable results during WY 2013 at a daily time step. Additionally, considering the model evaluation guidelines used were designed for monthly streamflow

estimations, the model was deemed well validated for the intended use of this work (i.e. to provide the model forcing's required to work the Ficklin et al. (2012) T_w model).
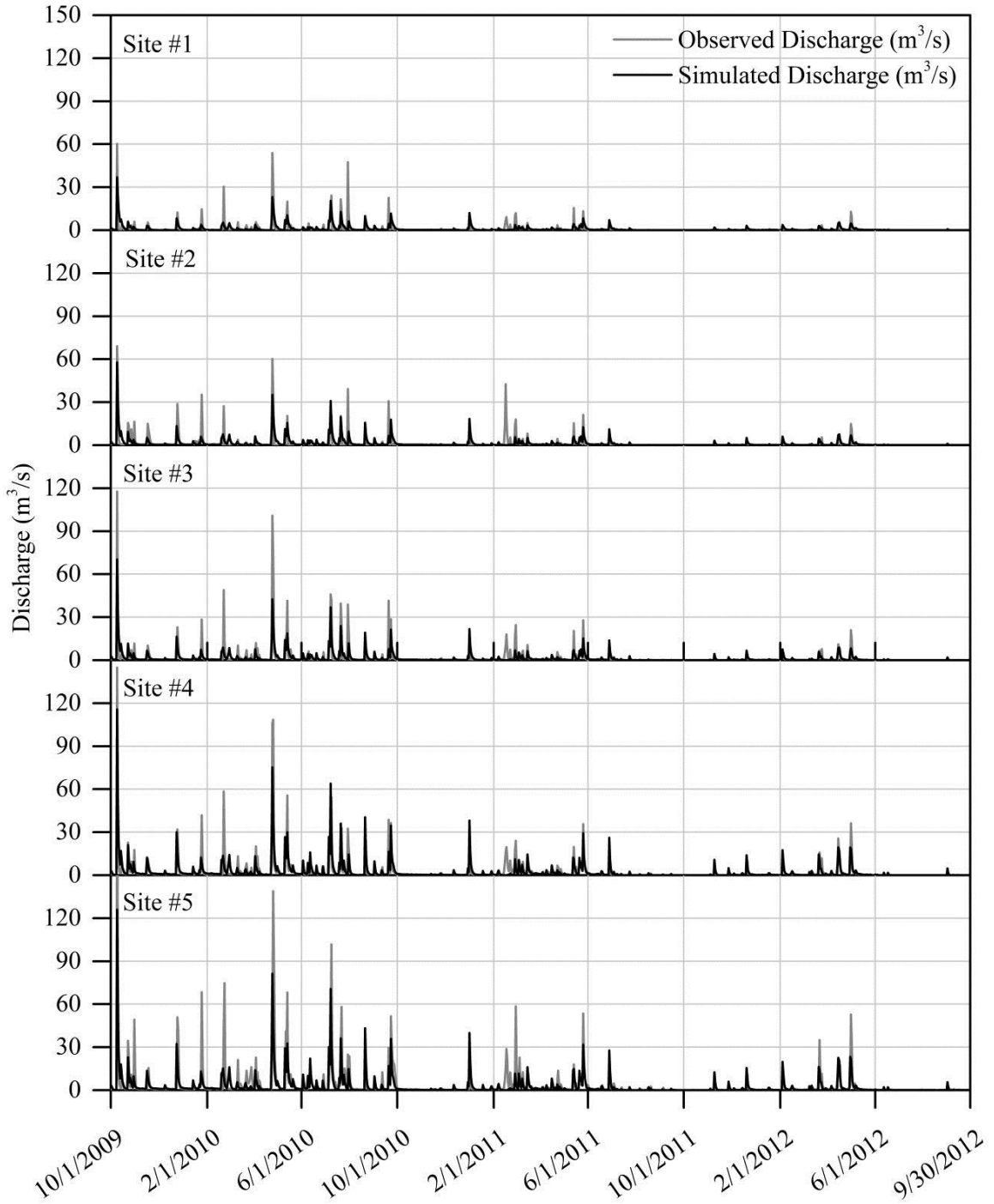
Figure 23. Time series SWAT simulated and observed discharge data collected during the calibration period (water years 2010 – 2012) recorded at five gauging sites located in Hinkson Creek Watershed, U.S.A.

118
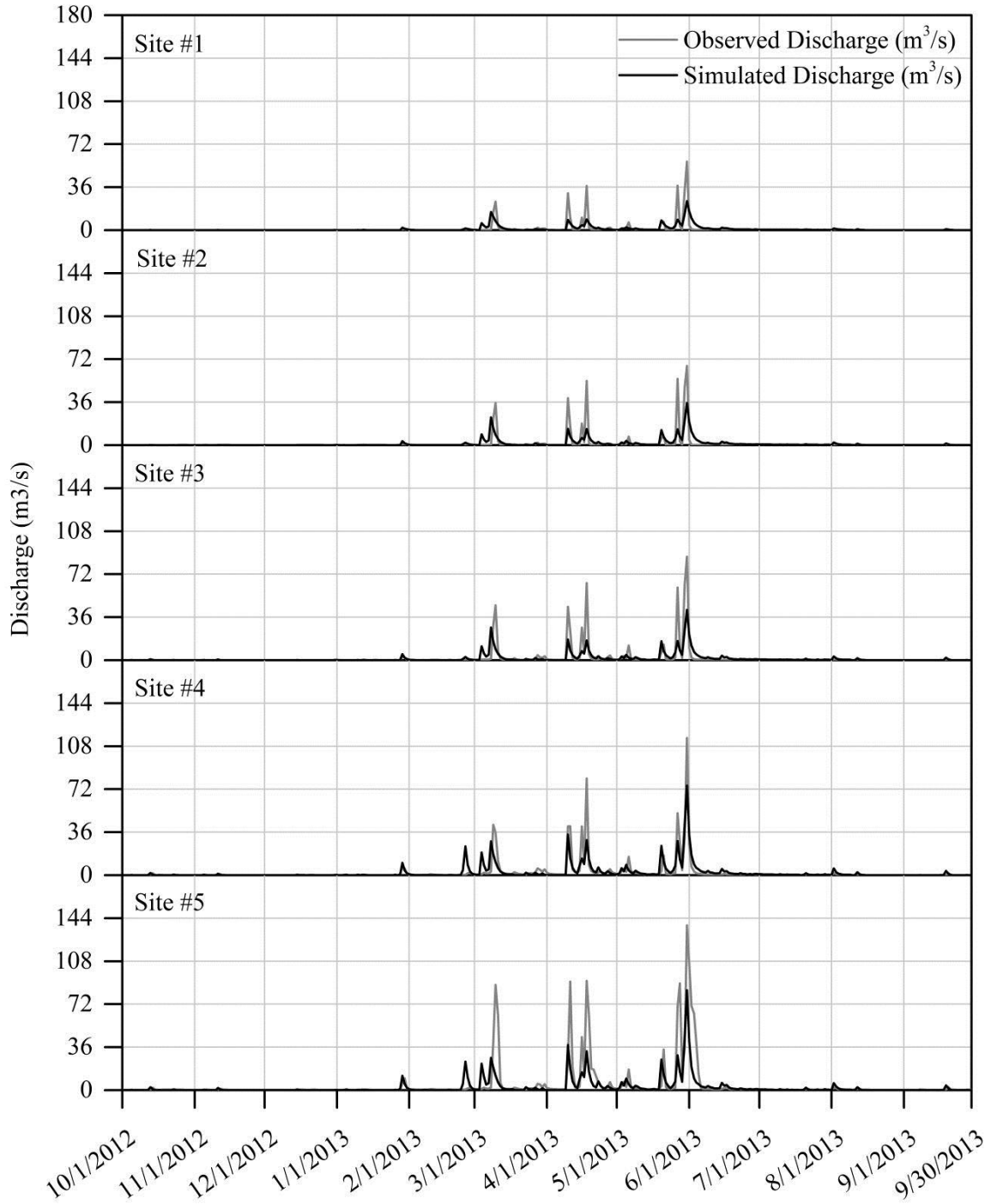
Figure 24. Time series SWAT simulated and observed discharge data collected during the validation period (water year 2013) recorded at five gauging sites located in Hinkson Creek Watershed, U.S.A.
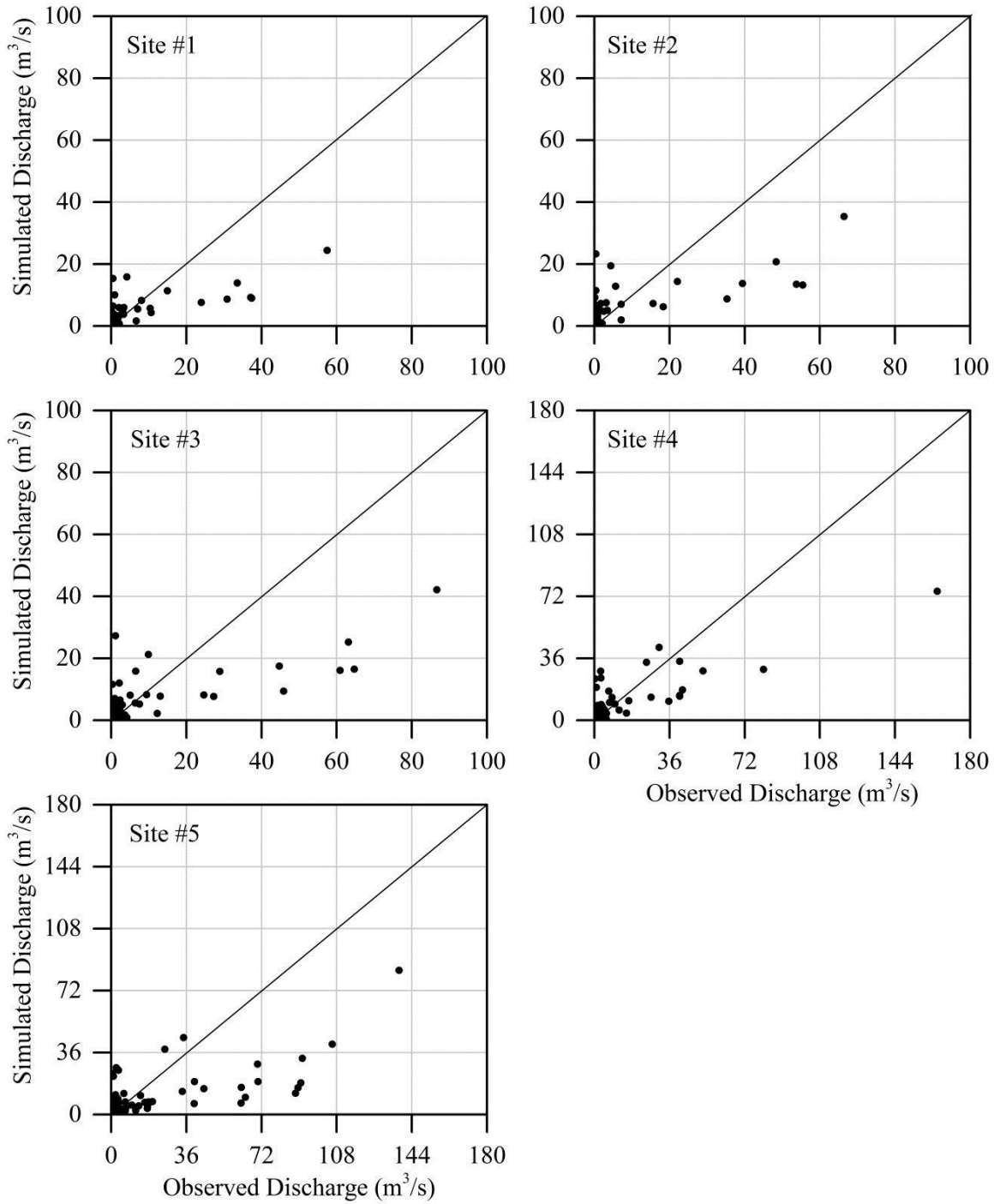
Figure 25. Validation results showing observed discharge versus SWAT simulated discharge data collected during the validation period (water year 2013) recorded at five gauging sites located in Hinkson Creek Watershed, U.S.A.

STREAM TEMPERATURE MODEL COMPARISON

15 minute stream temperature models

The effectiveness of 15 minute regression T_w models were tested using model evaluation criteria. Studies that validated the T_w regression models efficacy at 15 minute time steps were not found in four different literature reviews on T_w written by Smith (1972), Ward (1985), Caissie (2006), and Webb et al. (2008), or after searching online databases of peer-reviewed primary literature. Therefore, model evaluation results could not be compared to other research at the same time scale. Regardless, this work showed that 15 minute linear regression models improved by calibration coefficients α and β performed as well and, at times, better than the hourly and even daily T_w linear and nonlinear regression models tested with RMSE values approximately ≤ 2 °C. Results from this research show that linear and nonlinear models do not produce accurate simulations of T_w at sub-daily time scales, but adding the calibration coefficients α and β to the linear T_w models increased model accuracy significantly (p<0.01) thereby making the model useful at sub-daily time steps.

Results from the three types of T_w regression models tested including 15 minute linear, nonlinear, and calibrated linear T_w models are shown in Appendix C (Figures C1 to C4). Results showed all site mean NSE values from the 15 minute calibrated linear T_w model were 8.0 to 9.2% lower compared to the nonlinear and linear T_w models during the calibration period and 5.8 to 7.0% lower during the validation period. Additionally, all site mean PBIAS values from the 15 minute calibrated linear T_w model were 1.17 to 2.39% higher compared to the linear and nonlinear T_w models during the calibration period and 4.88 to 5.19% higher during the validation period. Finally, all site mean RSR

values from the 15 minute calibrated linear T_w model were 31.9 to 34.29% lower relative to the linear and nonlinear T_w models during the calibration period and 19.18 to 24.00% lower during the validation period. Thus, NSE and RSR values showed that the calibrated linear stream water temperature models tested performed better than the linear and nonlinear models tested, but PBIAS values were stronger for linear and nonlinear models. Therefore, simply adding calibration coefficients α and β to the linear T_w models improved T_w model performance ratings significantly ($p<0.01$).

Linear and nonlinear T_w model output tracked T_a well, which improved T_w estimates at daily and greater time scales, but not at sub-daily time scales. Observed T_w did not track T_a as well at sub-daily time steps as shown in Figure 26. The T_a time series were visibly more "noisy" compared to the T_w data. The difference in noise was, in part, due to the higher heat capacity of water compared to air (Erickson and Stefan, 2000). The linear and nonlinear T_w models simulated T_w nearly equal to the noisy T_a between 5 °C and 20 °C. Conversely, calibrated linear T_w model outputs were visibly less noisy and thus closer to observed T_w (Figure 26). The calibrated linear T_w models decreased the noise associated with the T_w time series by weighting diel T_w periods to daily mean T_a for the day of interest effectively dampening the T_w time series. This explains why the calibrated linear T_w models predicted T_w more accurately than linear and nonlinear models. Adding calibration made 15 minute T_w regression models more robust.
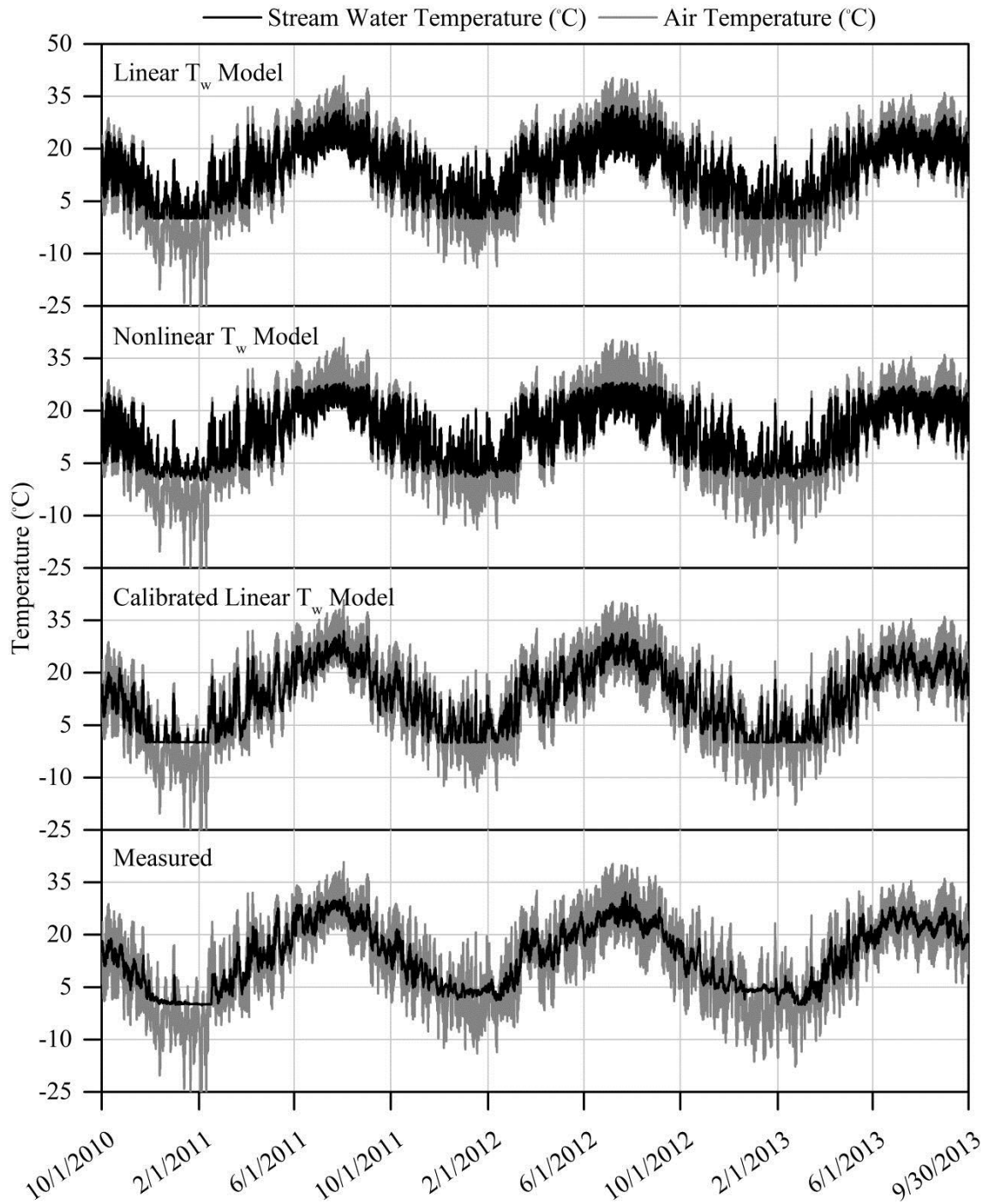
Figure 26. Results from calibrated linear regression model simulations showing 15 minute time series stream water temperature from five gauging sites in Hinkson Creek for the three year study period. Measured air temperature data are shown as a reference.

Hourly stream temperature models

Previous studies successfully predicted T_w at hourly time steps using statistical models (e.g. dispersion, linear and nonlinear regression models) (Caissie, 2006). Hourly T_w regression models are less often found in the literature relative to daily and post daily T_w regression models. Linear and nonlinear regression T_w models work better at daily and greater time scales because reducing the data by averaging attenuates diel variability thereby simplifying the time series. Even less often have the studies tested the accuracy of their regression models with multiple model evaluation criteria. For example, Webb et al. (2003) used linear and nonlinear regression models to predict T_w using T_a data and showed that r^2 values ranged from 0.80 to 0.89 between T_w and T_a, but did not validate the regression models with observed T_w data. Validation results that quantify the accuracy of sub-daily T_w models are important information for end users that need to know the error associated with a specific T_w model. For example, >3 °C RMSE may not be acceptable for fisheries management decisions that rely on accurate T_w estimations.

Rivers-Moore and Lorentz (2004) predicted hourly T_w using a statistical model dependent on T_a. Results showed r^2 values between observed and simulated T_w ranged from 0.73 to 0.88 which was similar to the results from linear and nonlinear T_w models tested in the current work, but the calibrated linear T_w models tested in this work showed higher r^2 values ranging from 3.0% to 19.0% compared to the study by Rivers-Moore and Lorentz (2004). In the current research, r^2 values ranged from 0.81 to 0.87 for the linear T_w models, 0.81 to 0.87 for the nonlinear T_w models, and 0.91 to 0.92 for the calibrated linear T_w models. Calibration coefficients added to the linear T_w models improved r^2 values by 5.4 to 9.6% and decreased model error (RMSE) by approximately 1 °C.

124

Results from hourly stream water temperature models from this research are shown in Appendix C (Figures C5 to C8). Results showed all site mean NSE values from the hourly calibrated linear T_w model compared to the nonlinear and linear T_w models were significantly (p<0.01) 8.0% higher during the calibration period and 6.9 to 8.1% higher during the validation period. Additionally, all site mean PBIAS values from the hourly calibrated linear T_w model were significantly (p=0.01) 3.06 to 3.44% higher during the calibration period and 5.46 to 5.55% higher compared to the linear and nonlinear T_w models during the validation period. All site mean RSR values from the 15 minute calibrated linear T_w model were significantly (p<0.01) 31.8% lower during the calibration period and 22.2 to 24.7% lower compared to the linear and nonlinear T_w models during the validation period. Similar to the results from 15 minute T_w model evaluation, NSE and RSR values showed that the calibrated linear stream water temperature model performed better than the linear and nonlinear models, but PBIAS values were stronger for linear and nonlinear models.

Figure C5 shows measured time series T_w and T_a at an hourly time step. Hourly mean T_w and T_a data showed diel fluctuations in time series temperature. Similar to the 15 minute data, the amplitudes of the diel periods of T_a data were visibly greater than T_w, and thus, the T_a time series appeared more "noisy" (Figures C1 and C5). And, the linear and nonlinear T_w models simulated noisy T_w (Figures C6 and C7). Calibrated linear T_w model outputs were less noisy and predicted T_w more accurately the linear and nonlinear models (Figure C8). Thus, adding calibration coefficients α and β to the linear T_w models improved T_w model performance ratings significantly (p<0.01). This information may be important to land managers that require hourly estimates of T_w.

Daily stream temperature models

Results from daily stream water temperature models are provided in Appendix C (Figures C9 to C13). Results showed nonlinear T_w models performed significantly ($p<0.1$) better than the original SWAT T_w model. There were not significant differences ($p>0.05$) between the original SWAT T_w model and the Ficklin et al. (2012) T_w model. Thus, the nonlinear T_w models are a better choice for land managers that need to estimate or predict T_w at a daily time step in the region for various applications (e.g. fisheries management, ecological modeling, etc.). Additionally, the SWAT model may benefit from considering using a nonlinear T_w model instead of the linear T_w model.

Graphical representations of observed versus simulated T_w are shown in Figure 26. Stream water temperature below 0 °C was not observed because ice that covers a stream limits surface heat exchange between the stream and the atmosphere (Mohseni and Stefan, 1999). The linear, nonlinear, and original SWAT model tended to overestimate T_w in the lower ranges (0 to 5 °C). Conversely, the calibrated linear and Ficklin et al. (2012) T_w model tended to underestimate T_w in the lower ranges (0 to 5 °C). Accurate predictions of T_w in the 0 to 5 °C temperature range are important considering ice covers for extended periods of time can cause fish kills.

All models showed high amounts of variance below 20 °C (Figure 27). High flow rates affect T_w when T_a is between 0 to 20 °C (Mohseni and Stefan, 1999). Thus, one limitation to the linear and nonlinear T_w models is that the models do not account for hydrology and therefore may not estimate T_w accurately when Ta is between 0 to 20 °C (e.g. during the spring season). The Ficklin et al. (2012) T_w model accounts for hydrology, but the variance was not significantly ($p>0.05$) lower compared to the linear

and nonlinear T_w models. There was less variability in T_w results in the higher temperature range (>20 °C). Higher temperature ranges are associated with low flow periods (Mohseni and Stefan, 1999). During low flow periods, T_w is usually more dependent on T_a than hydrology.

The Ficklin et al. (2012) T_w model performed slightly better than the existing SWAT T_w model, but the differences were not significant (p>0.05). Percent differences for all site mean NSE, PBIAS, RSR, MAE, MSE, and RMSE values were 1.10, -42.30, -6.45, -10.14, -17.51, -8.67% during the calibration period and 1.13, 11.52, -8.96, -10.30, -15.47, -7.87% during the validation period, respectively. Like the original SWAT T_w model, the Ficklin et al. (2012) T_w model accounts for T_a. Additionally, the Ficklin et al. (2012) T_w model can be calibrated and accounts for hydrology, including the volume of and temperature of inflows from snowmelt, groundwater, surface water runoff, and soil water lateral flow making the model a more robust option for land management. Thus, the Ficklin et al. (2012) T_w model performed equally as well as the original SWAT T_w model in the central U.S. in the current research, however, the original SWAT T_w model did not perform well in the study by Ficklin et al. (2012).

Ficklin et al. (2012) showed that the original SWAT T_w model did not perform well in the mountainous and coastal regions of the western U.S. with a seven site mean NSE, PBIAS, and mean error (ME) of -0.27, -42.14%, and 3.21 °C, respectively, during the calibration period and -0.26, -41.16%, and 3.02°C, respectively during the validation period. Conversely, the process based T_w model published by Ficklin et al. (2012) performed well with seven site mean NSE, PBIAS, and mean error (ME) of 0.81, -8.91%, and -0.70 °C, respectively, during the calibration period and 0.82, 7.74%, and -.058 °C,

respectively during the validation period. The results of the Ficklin et al. (2012) publication and this research combined show the original SWAT T_w model does not perform satisfactory in all regions, but the Ficklin et al. (2012) T_w model has performed well (NSE values >0.70) in the mountainous and coastal regions of the western U.S. and in the central United States. The Ficklin et al. (2012) T_w model performed better in different regions because it accounts for watershed hydrology (snowmelt, soil water lateral flow, overland flow, and groundwater flow) and meteorological conditions (T_a), whereas the original SWAT T_w model is not process based and only accounts for T_a (Ficklin et al. 2012). Both T_w models; however, showed greater error than the accuracy of modern T_w sensors (± 0.1 °C), and thus, it would be best if directly measured T_w data could be input into SWAT weather input files. This information may be important to the SWAT model development team.

The Ficklin et al. (2012) T_w model was the only model that did not generally underestimate T_w in the higher temperature range in the current research (Figure 27). For example, the original SWAT model and the nonlinear T_w model did not simulate T_w >30 °C during the study period. Accurate predictions of T_w during summer months are important because of the risks associated with elevated T_w and aquatic ecosystem health.
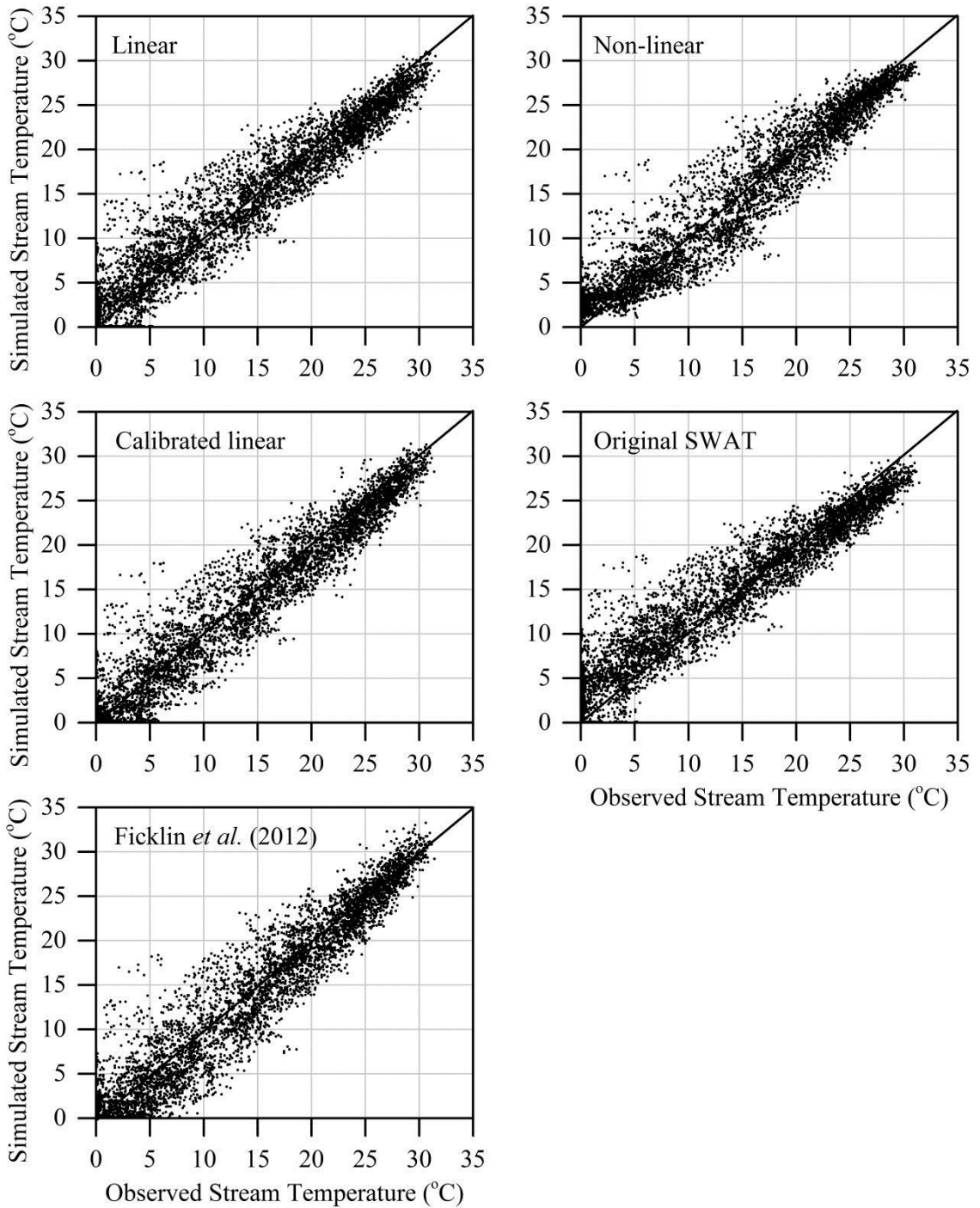
Figure 27. Results showing observed stream water temperature versus simulated stream water temperature data for each of the models tested at a daily time step collected during the study period (water years 2011, 2012, 2013) located in Hinkson Creek Watershed, U.S.A.

STREAM WATER TEMPERATURE MEASURING AND MODELING RECOMMENDATIONS

Choosing the appropriate T_w model is dependent on the objectives of the research and time scale of the required T_w estimations or predictions (Rivers-Moore and Lorentz, 2004). Deterministic T_w models generally result in the most accurate estimates of T_w. But, it's more cost effective to measure T_w directly, than to measure all the meteorological and hydrologic variables needed to calculate the energy balance (Caissie, 2006). Measuring T_w directly whenever possible is best because of the error associated with modeling. But, this may not always be possible due to of costs associated with instruments (sensors, data loggers, etc.) and labor (installation, maintenance, etc.). A best estimate of T_w using regression models dependent on T_a from nearby weather stations may be a more viable option. There is also a cost and benefit to consider involving time scale when deciding on what T_w model to use. Daily and post daily models did not show any detail of diel fluctuations in T_w, but T_w regression model accuracy increased with time scale. This study showed that T_w regression models can be calibrated to accurately predict T_w at sub-daily time scales. Linear and nonlinear regression T_w models without the calibration parameters did not perform as well. If sub-daily T_w data are needed in a situation where T_w cannot be directly measured, then the linear T_w model cannot be calibrated to observed data. Simulating T_w using regression models at sub-daily time scales may not be practical because of the error associated with modeling T_w using regression models at sub-daily time scales.

The SWAT model would benefit from implementing the Ficklin et al. (2012) T_w model because the Ficklin et al. (2012) T_w model has shown to work well in different regions while the linear T_w model in SWAT 2012 has not. The Ficklin et al. (2012) T_w

model performed better than the original SWAT T_w model in the mountainous and coastal regions of the western U.S. (Ficklin et al. 2012), and equally as well as the SWAT T_w model in this study. Another option would be to implement the nonlinear T_w model because results from this research showed that the nonlinear T_w model performed significantly better than the linear T_w model used in the current version of SWAT. It would be best, however, if the end user could input measured T_w data into SWAT. Allowing the end user to input measured T_w data into SWAT could improve estimates of in-stream water quality and biological processes simulated by SWAT. Additionally, changes should be made to SWAT that would simplify SWAT model auto-calibration to make the model a more practical choice for land managers.

Further research is needed to improve mechanistic understanding of the relationships between natural and anthropogenic processes that control T_w (Webb et al. 2008), and ultimately the relationship between T_w and T_a (Caissie, 2006). Ongoing interdisciplinary research is needed to investigate the natural and anthropogenic impacts on interacting physical, chemical, and biological processes, particularly in urbanizing watersheds. Considering most of the increase in human population in the next 35 years will occur in urban areas of the developing world, the effects of urbanization on all aspects of environmental water quality is of great concern (Myer et al. 2005). Nonpoint source thermal pollution is of particular concern due to the central role of T_w in overall aquatic ecosystem health (Rice et al. 2011). Tracing the casual source of thermal pollution is complicated, in part, due to the numerous independent and interacting natural and anthropogenic impacts involved. Long term monitoring is needed to study the effects of urbanization on water quality and the effectiveness of watershed restoration efforts.

The long term in-stream measurement of T_w in urban stream systems is also complicated, in part, because in-stream T_w sensors can be displaced, entrained in sediment, damaged, or lost after large runoff events. Additionally, fluctuations in stage complicate measuring T_w because sensors can come out of water as water levels recede during dry seasons, or be deep below the surface as stage increases during wet seasons. Monitoring of T_w is expensive because of costs associated with purchasing and maintaining instruments (sensors, data loggers, etc.) and labor (installation, maintenance, etc.) (Caissie, 2006; Benyahya et al. 2007), and funding may be limited depending on the state of the economy.

Because of the problems associated with in-stream measurement of T_w, the advent of remotely sensing T_w variability using thermal infrared imagery (TIR) is promising (Webb et al. 2008). TIR data could be collected at multiple spatial scales via satellite, aircraft and ground-based platforms. Comparison of the TIR images overtime could assist in monitoring the effects of anthropogenic impacts on T_w as well as the effectiveness of restoration efforts. For example, satellite TIR images overtime could help monitor the effects of human induced global warming on T_w regimes in high order rivers (e.g. The Amazon River, The Mississippi River, The Congo River). Smaller scale projects targeted at the effects of urbanization on T_w variability in low-order streams like Hinkson Creek could be performed by mounting a camera capable of collecting TIR images to a bridge wing wall over an urban stream to monitor the frequency, magnitude, and duration of T_w surges following summer precipitation events as well as the effectiveness of restoration efforts.

CHAPTER V

CONCLUSION AND SYNTHESIS

Hinkson Creek is a 3rd order stream that drains a multiuse urbanizing watershed in the central United States. The creek was instrumented in fall 2008 with a nested-scale experimental watershed study design (n=5 gauging stations). The current work took advantage of three water years of 15 minute T_w, T_a, and discharge data collected from 2009 to 2012 water years to investigate T_w variability and test and develop T_w / T_a models. Investigation of long term high resolution data in low order urban streams was needed mainly because of the paucity of observed data in "flashy" multi-land use urbanizing catchments (Anderson et al. 2011; Nelson and Palmer, 2007). Investigation of T_w in urban streams was deemed important because increasing urban land use will continue to affect T_w, which is an important water quality variable because of its effects on nearly all aspects of physical and chemical properties of water, and biological processes in aquatic ecosystems (Anderson et al. 2011).

To investigate T_w variability, hydroclimate data including T_w, T_a, and stream discharge from the 2011, 2012, and 2013 water years were reduced to 15 minute, hourly, daily, weekly, monthly, seasonal, and water year time steps for further analysis. The number of days and maximum duration T_w was above 32 °C and 35 °C during the study period were recorded. ANOVA and Tukey-Kramer multiple comparison test were used to test for significant differences ($p<0.05$) in hydroclimate measurements between multiple gauging stations. Observed T_w data were analyzed for T_w surges. T_w data were separated into 15 different flow classes to test for the effects of discharge on T_w and the T_w / T_a

relationship. Linear and nonlinear regression analyses were performed using mean T_w vs. mean T_a data for each site at 15 minute, hourly, daily, weekly, monthly, and seasonal time steps. Calibration confidents α and β were added to the 15 minute and hourly linear regression T_w models to improve T_w model performance at sub-daily time steps. Additionally, the original SWAT linear T_w model and the process based T_w model created by Ficklin et al. (2012) were tested against observed T_w data from five gauging sites.

Significant differences in T_a, T_w, and discharge were found between five stream study sites. Fifteen sudden increases in T_w following summer thunderstorms (T_w surges) with a maximum peak T_w, T_w surge, and surge duration of 34.2 °C, 2.6 °C, and 6.3 hours, respectively, were observed during summers of 2010, 2011, and 2012. The T_w / T_a relationships were compared between five study stream sites. The effects of discharge and land use in the T_w / T_a relationship were quantitatively characterized. The T_w model utilized in the SWAT 2012, and the new T_w model developed by Ficklin et al. (2012) were tested with observed hydroclimate data from multiple sites of the study stream. The Ficklin et al. T_w model produced better predictions than the original SWAT T_w model in seven coastal and mountainous regions of the western United States, however, the models were not tested in the central United States where hydrogeological and land use interactions are different.

FINDINGS ON HYDROCLIMATE IN HINKSON CREEK WATERSHED

Climate during the study period included two wetter than average years (2009 and 2010), and two years of drought (2011 and 2012). Site # 1, located at the intersection of

Rogers's road and Hinkson Creek in Columbia, Missouri, was ephemeral during the summer of 2012 due to reduced rainfall. But, Hinkson Creek was perennial from site #2, located at the intersection of Mexico Gravel Road and Hinkson Creek in Columbia, Missouri, to the watershed outlet. Drought conditions during the summer of 2012 provided a worst case scenario for the effects of low discharge on T_w in a low-order urban stream of the central U.S.

The first objective of this study was to test for significant differences in T_w in the study stream sites. ANOVA analyses showed significant differences in T_w in the stream study sites, therefore the null hypothesis (i.e. no difference in T_w between study sites) was rejected.

FINDINGS ON HIGH STREAM WATER TEMPERATURE IN HINKSON CREEK

It was assumed when impervious surfaces heated up in the summertime, heat energy from impervious surfaces is transferred to stormwater runoff by conduction following precipitation events (Herb et al. 2008). Then, the heated stormwater is transported to streams causing sudden increases in T_w that exceeded 5 °C. Stream water temperature did not return to pre-surge temperature for >6 hours following the surges in T_w. Anthropogenic impacts were suspect when results showed significant evidence of an "urban heat island effect" on T_a at urban site #3 in Hinkson Creek Watershed in the current work. Buffered stream water temperature regime observed at site #1 was due to effects of pooling considering the high specific heat capacity of water (4.184 J/g °C). The observed urban heat island effect may have contributed to elevated T_w observed at

135

gauging site #3 and downstream at site #4. Stream water temperature exceeded "Critical Thermal Maximum" for 5 days for a maximum duration of 2.5 hours at urban site #3.

The effects of discharge on T_w were investigated to explain the significant differences T_w between gauging sites. Mean discharge, T_a and T_w data were separated into 15 different flow classes. Results showed mean discharge increased exponentially from the headwaters to the watershed outlet, and the differences between sites grew exponentially with every increase in flow class. Discharge did not significantly affect T_w at any flow class (p>0.5). Stream water temperature was, however, was significantly affected by cumulative urban land use percent in all flow classes >90% (p=0.03). Stream water temperature at urban sites #4 and #5 increased relative to other Hinkson Creek gauging with every increase in flow class, but the differences in T_w were not statistically significant (p>0.05) until the >90% flow class. These results provided additional evidence that T_w in Hinkson Creek was increased by heated urban stormwater runoff.

FINDINGS ON STREAM AND AIR TEMPERATURE RELATIONSHIPS

Time lag affected T_w / T_a relationships at every monitoring site in this study. Accounting for lag improved r^2 values at sub-daily time steps. Lag was greatest at site #1 and at site #5. Pooling buffered stream response to changes in air temperature at site #1. In general, time lag increased with stream distance from sites #2 to #5 because discharge increased with stream distance. Discharge buffered T_w response to meteorological conditions thereby increasing the lagged response of T_w to changes in T_a.

The second objective in this research was to compare T_w / T_a relationships between study stream sites. ANOVA analyses showed differences in T_w / T_a relationships

between study stream sites for flow classes >90%; thus, the null hypothesis was rejected (p=0.03). Independent and interacting natural processes and human impacts affected the strength of the T_w / T_a relationship. There was a general trend for T_w / T_a relationships to decrease with increasing stream distance and urban land use. Increased discharge buffered stream interaction with meteorological conditions decreasing r^2 values.

The effect of time scale on T_w / T_a relationships was also investigated because the third objective of this research was to compare T_w / T_a relationships at 15 minute, hourly, daily, weekly, monthly, and seasonal time scales. Results showed r^2 values significantly increased for linear and nonlinear models as time step increased (p<0.01). The null hypothesis was rejected. Linear coefficients were affected as time step increased from 15 minute to seasonal averages, but nonlinear coefficients were not affected. But, results showed a positive relationship in nonlinear relationships between alpha / beta coefficients, and an inverse relationship between gamma coefficients and alpha / beta coefficients.

The effects of discharge on the T_w / T_a relationship were investigated to complete the fourth objective, quantitatively characterize the significance of the effects of discharge in the T_w / T_a relationship. Mean discharge, T_a and T_w data were separated into 15 different flow classes. Linear regression analyses were performed for each flow class. The relationship between T_w and T_a was affected by discharge. As flow class increased, T_a explained significantly less variance in T_w (p<0.01). Stream water temperature regimes were controlled by meteorological conditions (e.g. solar radiation, and T_a), particularly during low flow periods. But, hydrologic factors (e.g. volume of water, source of water) dominate during high flow periods, in part, because of high heat capacity

137

of water and decreased residence time. Residence time decreased as discharge increased. As residence time decreased, stream interaction with the atmosphere decreased. These results reject the null hypothesis and show empirical T_w models that do not account for hydrology are not as accurate during stormflow periods.

FINDINGS ON STREAM WATER TEMPERATUIRE MODEL COMPARRISON

To test sub-daily linear and nonlinear regression T_w models with observed hydroclimatic data from five sites of the study stream for the fifth objective, results from sub-daily models were evaluated. The null hypothesis was rejected ($p<0.01$). The calibrated linear T_w model was the only model to produce realistic results at 15 minute and hourly time steps. Air temperature and stream water temperature data showed a sinusoidal period over a diel period. The crests and troughs over a diel period were greater in T_a compared to T_w. Thus, the T_a data appeared more "noisy". The difference in noise was, in part, due to the high heat capacity of water compared to air. The linear and nonlinear T_w models simulated T_w nearly equal to the noisy T_a between 5 °C and 20 °C. Conversely, calibrated linear T_w model outputs were visibly less noisy and thus closer to observed T_w at sub-daily time steps. Linear and nonlinear T_w models that require only T_a data to predict T_w should not be used at sub-daily time steps because they do not accurately simulate diel temperature fluctuations. But, the calibrated linear T_w models produce satisfactory results by adding two simple calibration parameters capable of decreasing the amplitude of the sinusoidal period observed in diel T_w.

The noise associated with diel variability in T_w and T_a data was lost in the averaging process when T_w and T_a data were reduced by averaging sub-daily data to a

daily time step. At a daily time step, T_w and T_a data are generally nearly equal between 5 °C and 20 °C. Thus, linear and nonlinear T_w models produce realistic results. Overall, the nonlinear T_w models performed better than all other T_w models evaluated at a daily time step. Nonlinear daily time step models account for cooling due to latent heat of vaporization observed in daily mean T_w data.

Results from the original SWAT T_w model, and the Ficklin et al. (2012) T_w model were compared to complete the sixth objective, test the daily T_w model utilized in the SWAT 2012, and the new T_w model developed by Ficklin *et al*. (2012) with observed hydroclimate data from five sites of the study stream.. Results failed to reject the null hypothesis. The Ficklin et al. (2012) T_w model yielded model evaluation numbers that were not significantly different than the original SWAT T_w model (p>0.05). Both T_w models yielded "Very good" results (i.e. $0.75 < NSE \leq 0.90; \pm 5 \leq PBIAS < \pm 10; 0.30 < RSR \leq 0.50$). The Ficklin et al. (2012) T_w model can be calibrated and accounts for hydrology, but the model was computationally demanding. The Ficklin et al. (2012) T_w model simulated accurate predictions when $T_w > 30$ °C during the summer. The original SWAT T_w model usually underestimated T_w during the summer. The original SWAT T_w model did not work well in the mountainous and coastal regions of the western United States because the process based Ficklin et al. (2012) T_w model is more transferrable to other regions than the original SWAT T_w model.

Results in this study showed equipping the SWAT model with the Ficklin et al. (2012) T_w model could produce T_w simulations as accurate as the original SWAT T_w model in the central U.S. Additionally, the SWAT model would better simulate in-stream water quality and biological processes dependent on T_w if the SWAT model was capable

of uploading observed T_w weather input data. Estimates involving in-stream water quality and biological processes that share a positive relationship with T_w are likely underestimated when T_a is above 20 °C using the original SWAT T_w model.

MANAGEMENT IMPLICATIONS

Results from this research provide baseline T_w information on the thermal regime in an EPA 303(d) listed urban stream located in an urbanizing watershed of the Lower Missouri Moreau River Basin (LMMRB). The study site for this research was important because Hinkson Creek watershed is representative of the LMMRB in regard to hydrologic processes, water quality, climate, and land use making the study site a useful tool for watershed restoration efforts focused on controlling nonpoint source pollution in the region (Hubbart et al. 2010). The nested scale experimental watershed study design was used to trace a diffuse pollutant (i.e. T_w surges). This information is useful to land managers faced with the task of remediating nonpoint source pollutants in the region.

Land managers concerned with the protection of aquatic ecosystem health should consider implementing management practices that attempt to cool heated stormwater in urban subbasins #3, #4, and #5 because of the relationship between increased T_w and urban land use associated with impervious surfaces observed in this research. Site #3 showed 5 days T_w was above "Critical Thermal Maximum" (>35 °C). Stream temperature surges >1 °C in a time span of 15 minutes were observed at site #3. The T_w surges observed in this research were fewer and of lesser magnitude and duration compared to other studies by Nelson and Palmer (2007) and Rice et al. (2011) considering the relationship observed by Nelson and Palmer (2007) between T_w surge frequency and

%impervious surface in the watershed draining to the sampling point, and the relationship

observed by Rice et al. (2001) between amount of impervious surface coverage within a

25 meter buffer and magnitude of and duration of T_w surges. Thus, terrestrial

development that involves increased impervious surfaces in the watershed is expected to

lead to more frequent T_w surges. Further, increases in impervious surface coverage within

a 25 meter buffer of Hinkson Creek or its tributaries should be avoided or T_w surges

could increase in magnitude and duration. Reviews by Webb et al. (2008) and Caissie

(2007) showed forested riparian zones help keep streams cool by providing shade that

reduces solar radiation at the stream surface. The T_w increase of approximately 4 °C at

site #5 that was not detected upstream at site #4 provided evidence that heated

stormwater entered Hinkson Creek in subbasin #5. The T_w of Flatbranch Creek should be

investigated because it enters Hinkson Creek approximately 1.3 linear km downstream of

site #4 in sub-basin #5 and drains the majority of high density urban land use in the City

of Columbia associated with increased imperious surfaces. Sudden increases in T_w like

the T_w surges observed during this work have been shown to impair aquatic ecosystem

health (Nelson and Palmer, 2007).

The 15 minute calibrated linear T_w regression models are useful for ecological

and water quality studies that need to estimate diel variability in T_w in Hinkson Creek.

The models are also good tools for land management that require estimates of T_w. The

validated T_w models from this research are useful to aid in the protection of water quality,

thereby providing local land managers with the knowledge to make informed

management decisions in the central United States. If RMSE of 3 °C for 15 minute T_w

model simulations is deemed an unacceptable amount of error, then T_w should be directly

measured. Practical T_w regression models dependent on T_a are an attractive choice, however, because of the costs associated with installing and maintaining instruments capable of measuring in-stream T_w.

ADVANCES TO SCIENCE

Information from this research advanced scientific understanding of T_w variability in a multi-land use watershed of the central United States by analyzing three water years of high resolution (15 minute) T_w data using a nested scale experimental watershed study design approach to elucidate the effects of discharge and land use on T_w variability. This research evaluated the efficacy of using linear and nonlinear T_w regression models at 15 minute, hourly, and daily time scales using six model evaluation criteria. The calibrated linear T_w models created and tested showed simple linear T_w regression models are capable of accurately estimating T_w with readily available T_a data at 15 minute and hourly time steps. While the linear T_w model used in the current version of SWAT (SWAT 2012) produced satisfactory estimates of T_w at a daily time step, however, the nonlinear T_w models tested at a daily time step performed significantly ($p<0.01$) better the linear T_w model currently used in SWAT. A newly proposed SWAT T_w model that was designed to work better than the original SWAT T_w model had not yet been tested in the central U.S. was evaluated and results showed the T_w model proposed by Ficklin et al. (2012) worked equally as well compared to the linear T_w model currently used in SWAT. Finding the Ficklin et al. T_w model worked well in this study is significant because the study site was cited to be representative of hydrologic processes, water quality, climate, and land use in the LMMRB making the Ficklin et al. T_w model useful tool for watershed

restoration efforts focused on controlling nonpoint source pollution in the region. Results from the daily T_w model analyses advance our ability to accurately predict T_w with SWAT, a highly used and robust hydrologic model.

CLOSING STATEMENT

Empirical techniques, such as the regression models created in this work, are often less computationally complex compared to analytical techniques (e.g. deterministic models). There will always be, however, a place for empirical theory in modeling (Rigler, 1982). The inclusions of more complex statistical analysis methods (e.g. time series analysis) in union with recent technological advances (statistical software, and process based simulation modeling) could help improve predictive modeling by reducing scale-dependencies and the explained variation in predictions (Pace, 2001). Scientific advances alone, however, will not improve prediction modeling. The future of prediction modeling in aquatic sciences also depends on the cooperation of multiple disciplines.

LITERATURE CITED

Akyuz FA, Market PS, Guinan PE, Lam JE, Oehl AM, Maune WC. 2004. The Columbia, Missouri, Heat Island Experiment (COHIX) and the Influence of a Small City on the Local Climatology. *Transactions of the Missouri Academy of Science* **38**: 5671.

Anderson WP, Storniolo RE, Rice JS. 2011. Bank thermal storage as a sink of temperature surges in urbanized streams. *Journal of Hydrology* **409**: 525-537.

Anka-Lufford L, Bets JD, Cooper AM, Daly AL, Soundariarajan S, Stingel AM, Winschel GA. 2007. A chemical and anthropogenic impact study of Lake Lonely. Skidmore College, Saratoga Springs, NY 12866.

Arnold JG, Moriasi DN, Gassman PW, Abbaspour KC, White MJ, Srinivasan R, Santhi C, Harmel RD, van Griensven A, Van Liew MW, Kannan N, Jha MK. 2012. SWAT: Model use, calibration, and validation, *American Society of Agricultural and Biological Engineers* **55** (4): 1491-1508.

Beitinger TL, Bennett WA, McCauley RW. 1998. Temperature tolerances of North American freshwater fishes exposed to dynamic changes in temperature, *Environmental Biology of Fishes* **58:** 237-275.

Bennett KD. 1990. Milankovitch Cycles and Their Effects of Species in Ecological and Evolutionary Time, *Paleobiology* **16**(1): 11 – 21.

Benyahya L, Caissie D, StHiaire A, Ouarda TBMJ, Bobee B. 2007. A review of statistical water temperature models. *Canadian Water Resources Association* **32** (3): 179192.

Bogan T, Stefan HG, Mohseni O. 2004. Imprints of secondary heat sources on the stream temperature/equilibrium temperature relationship, *Water Resources Research* **40:** 1-16.

Bond NR, Lake PS, Arthington AH. 2008. The impacts of drought on freshwater ecosystems: an Austrailian perspective. *Hydrobiologia* **600**: 3 – 16.

Bonett DG. 2002. Sample site requirements for estimating intraclass correlations with desired precision. *Statistics in Medicine* **21**: 1331 – 1335.

Boulton AJ. 2003. Parallels and contrasts in the effects of drought on stream macroinvertebrate assemblages. *Freshwater Biology* **48** (7): 1173 – 1185.

Brabec E, Schulte S, Richards PL. 2002. Impervious surfaces and water quality: a review of current literature and its implications for watershed planning. *Journal of Planning Litterature* **16** (4): 500 – 514.

Brown LE, Hannah DM, Milner AM. 2005. Spatial and temporal water column and streambed temperature dynamics within an alpine catchment: implications for benthic communities. *Hydrological Processes* **19**: 15851610.

Bulliner, 2011. Quantifying riparian canopy energy attenuation and stream temperature using An energy balance approach. Master's Thesis, The University of Missouri, Columbia, MO 65211.

Caissie D. 2006. The thermal regime of rivers: a review. *Freshwater Biology* **51**: 13891406.

Caissie D. Satish MG, ElJabi N. 2007. Predicting water temperatures using a deterministic model: Application on Miramichi River catchments (New Brunswick, Canada). *Journal of Hydrology* **336**: 303315.

Chapman SS, Omernik JM, Griffith GE, Schroeder WA, Nigh TA, Wilton TF. 2002. Ecoregions of Iowa and Missouri (color poster with map, descriptive text, summary tables, and photographs): Reston, Virginia, U.S. Geological Survey.

Dinan KF. 1992. Application of the stream network temperature model (SNTEMP) to the central Platte River, Nebraska. Professional Paper, Department of Fishery and Wildlife Biology, Colorado State University, Fort Collins, CO. 89 pp.

Dong J, Chen J, Brosofske KD, Naiman RJ. 1998. Modeling air temperature gradients across managed small streams in western Washington. *Journal of Environmental Management* **53**: 309321.

Dottori F, Martina MLV, Todini E. 2009. A dynamic rating curve approach to indirect discharge measurement. *Hydrology Earth System Sciences* **13**: 847863.

Doyle MW, Shields FD. 2012. Compensatory mitigation for streams under the clean water act: reassessing science and redirection policy. *Journal of the American Water Resources Association (JAWRA)* **48**: 494509.

Environmental Protection Agency (EPA) 2011. Region 7,Total Maximum Daily Load, Hinkson Creek (MO_1007 and _1008) Boone County, Missouri.

Erickson TR, Stefan HG. 2000. Linear air/water temperature correlations for streams during open water periods. *Journal of Hydrologic Engineering* 317-321.

Ficklin DL, Lou Y, Stewart IT, Maurer EP. 2012. Development and application of a hydroclimatological stream temperature model within the Soil and Water Assessment Tool, *Water Resources Research* **48**: 116.

Freeman, 2011. Quantifying suspended sediment loading in a Mid-Missouri urban watershed using laser particle diffraction. Master's Thesis, The University of Missouri, Columbia, MO 65211.

Furey PC, Nordin RN, Mazumder A, 2006. Littoral benthic macroinvertebrates under contrasting drawdown in a reservoir and a natural lake. *Journal of the North American Benthological Society* **25**: 19–31.

Gomi T, Moore RD, Dhakal AS. 2006. Stream water temperature response to clearcut harvesting with different riparian treatments, coastal British Columbia, Canada. *Water Resources Research* **42**: 111.

Herb WR, Janke B, Mohseni O, Stefan HG. 2008. Thermal pollution of streams by runoff from paved surfaces. *Hydrological* Processes **22**: 987999.

Herschy RW. 1985. Accuracy in streamflow measurements. *Elsevier*. Amsterdam.

Hester ET, Bauman KS. 2012. Stream and Retention pond thermal response to heated summer runoff from urban impervious surfaces, *Journal of the American Water Resources Association* **49**(2): 328-342.

Hubbart JA. 2011. Urban floodplain management: understanding consumptive water – use potential in urban forested floodplains. *Stormwater* **12**(6): 56 – 63.

Hubbart JA, Freeman GW. 2010. Sediment laser diffraction: a new approach to an old problem in the central U.S. *Stormwater Journal* **11**(7): 3644.

Hubbart JA, and Zell C. 2013. Considering streamflow trend analyses uncertainty in urbanizing watersheds: a baseflow case study in the central United States. *Earth Interactions* **17**(5): 1 – 28.

Hubbart JA, Link TE, Gravelle JA, William EJ. 2007. Timber harvest impacts of water yield in the continental/maritime hydroclimatic region of the United States. *Forest Science* **53**(2): 169180.

Hubbart JA, Holmes J, Bowman G. 2010. Integrating science based decision making and TMDL allocations in urbanizing watersheds. *The Watershed Science Bulletin* **01**: 1924.

Hubbart JA, Muzika RM, Huang D, Robinson A. 2011. Bottomland hardwood forest influence on soil water consumption in an urban floodplain: potential to improve

flood storage capacity and reduce stormwater runoff. *The Watershed Science Bulletin* **Fall**: 3443.

Hubbart JA, Kellner E, Freeman G. 2013. A case study considering the comparability of mass and volumetric suspended sediment data. *Environmental Earth Science* 71: 40514060.

Hubbart JA, Kellner E, Hooper L, Lupo AR, Market PS, Guinan PE, Stephan K, Fox NI, Svoma BM. 2014. Localized climate and surface energy flux alterations across an urban gradient in the central U.S. *Energies* 7: 17701791.

Hutchinson VH, 1961. Critical thermal maxima in salamanders. *Physiological Zoology* **34**:97-125.

Krashnikikov SA. 1987. About Optimal Approximation for Stage Discharge Relationship. *Proceedings of the State Hydrological Institute* **328**: 5869.

Kaushal SS, Likens GE, Jaworski NA, Pace ML, Sides AM, Seekell D, Belt KT, Secor DH, Wingate RL. 2010. Rising Stream and River Temperatures in the United States. *Research Communications* **8**(9): 46166.

Lin C, Chen F, Huang JC, Chen WC, Liou YA, Chen WN, SC Liu. 2008. Urban heat island effect and its impact on boundary layer development and land– sea circulation over northern Taiwan. *Atmospheric Environment* **42**: 56355649.

McClain ME, Bilby RE, Triska FJ. 1998. Nutrient cycles and response to disturbance. p. 347367. *In: River ecology and management* R. J. Naiman and R. E. Bilby (eds.). Springer Verlag, New York.

MDNR. 2006. Stream Survey Sampling Report. Phase III Hinkson Creek Stream Study, Columbia, Missouri, Boone County. Prepared by the Missouri Department of Natural Resources, Field Services Division, Environmental Services Program, Water Quality Monitoring Section.

MDNR, 2011. Total Maximum Daily Load for Hinkson Creek Boone County, Missouri. Prepared by the Missouri Department of Natural Resources Water Protection Program.

Missouri Resource Assessment Program (MRAP). 2005. Land use/Land Cover Data.

Mohseni O, Stefan HG, Erickson TR. 1998. A nonlinear regression model for weekly stream temperatures. *Water Resources Research* **34**(10): 2685692.

Mohseni O, Erickson TR, Stefan HG. 1999. Sensitivity of stream temperatures in the United States to air temperatures projected under a global warming scenario. *Water Resources Research*. **35**(12): 3723733.

Moore R, Spittlehouse D, Story A. 2005. Riparian microclimate and stream temperature response to forest harvesting: a review. *Journal of the American Water Resources Association* **41**: 813834.

Monk WA, Wood PJ, Hannah DM, Wilson DA. 2008. Macroinvertebrate community response to interannual and regional river flow regime dynamics. *River Research and Applications* **24**: 9981001.

Moriasi DN, Arnold JG, Van Liew, Bingner RL, Harmel, Veith TL. 2007. Model evaluation guidelines for systematic quantification of accuracy in watershed simulations. *American Society of Agricultural and Biological Engineers* **50**(3): 885900.

Nelson KC, Palmer MA. 2007. Stream water temperature surges under urbanization and climate change: data, models, and responses. *Journal of the American Water Resources Association* **43**(2): 44052.

Neitsch, SL, Arnold JG, Kiniry JR, Williams JR, and King KW. 2005. Soil and Water Assessment Tool Theoretical Documentation: Version2005, Texas Water Resources Institute, College Station, TX.

Nigh TA, Schroeder WA. 2002. Atlas of Missouri ecological sections. Missouri Department of Conservation.

Pace ML. 2001. Prediction and the aquatic sciences. *Canadian Journal of Fisheries and Aquatic Sciences* **58**: 63-72.

Peck R, Devore JL. 2012. *Statistics: The Exploration and Analysis of Data*, Boston: Brooks/Cole, Cengage Learning, 2012. Print.

Perkins B. 1995. Temporal variability in a Midwestern stream during spring. Master's Thesis, The University of Missouri, Columbia, MO 65211.

Poole GC, Berman CH. 2001. An Ecological Perspective on In-Stream Temperature: Natural Heat Dynamics and Mechanisms of Human Caused Thermal Degradation. *Environmental Management* **27**(6): 787802.

Qi C, Grunwald S. 2005. GIS-based hydrologic modeling in the Sandusky watershed using SWAT, *American Society of Agricultural Engineers* **48**(1): 169-180.

Rice JS, Anderson WP, Thaxton CS. 2011. Urbanization influences on stream temperature behavior within low-discharge headwater streams. *Hydrological Research Letters* **5**: 27-31.

Rigler, FH. 1982. Recognition of the possible: an advantage of empiricism in ecology. *Canadian Journal of Fisheries and Aquatic Sciences* **39**: 1323-1331.

Rivers-Moore NA, Lorentz S, 2004. A simple, physically-based statistical model to simulate hourly water temperatures in a river. *South African Journal of Science*. **100**: 331-333.

Scollan DP. 2011. A multiconfiguration evaluation of the Soil and Water Assessment Tool (SWAT) in a mixed land use watershed in the central U.S.A. Master's Thesis, The University of Missouri, Columbia, MO 65211.

Shiklomanov AI, Yakovleva TI, Lammers RB, Karasev IP, Vorosmarty CJ, Linders E. 2005. Cold region river discharge uncertainty estimates from a large Russian river. *Journal of Hydrology* **326**: 231256.

Sinokrot BA, Gulliver JS. 2000. Instream flow impact on river water temperatures. *Journal of hydrologic research* **38**: 339349.

Silva L, Williams D. 2001. Buffer zone versus whole catchment approaches to studying land use impact on river water quality. *Water Resources* **35**(14): 34623472.

Smith K. 1972. River water temperature – an environmental review. *Scottish Geographical Magazine* **88**: 211 – 220.

Smith K, Lavis ME. 1975. Environmental influences on the temperature of a small upland stream. *Oikos* **26**(2): 228 – 236.

Stefan HG, Preud'homme EB. 1993. Stream water temperature estimation from air temperature. *Water Resources Bulletin* **29**(1): 27 – 45.

Stoline MR. 1981. The status of multiple comparisons: Simultaneous estimation of all pairwise comparisons in oneway ANOVA designs. *The American Statistician*, **35**(3): 134141.

Subehi L, Fukushima T, Onada Y, Mizugaki S, Gomi K, Kosugi K, Hiramatsu S, Kitahara H, Kuraji K, Terajima T. 2010. Analysis of stream water temperature changes during rainfall events in forested watersheds. *Limnology* **11**: 11524.

Sutron Corporation. *Accubar Constant Flow Bubble Gauge/Recorder 560133*. 8 Feb. 2008. Operations and Maintenance Manual. 21300 Ridgetop Circle, Sterling, Virginia.

United States Census Bureau (USCB). 2011. U.S. Census Bureau Delivers Missouri's 2010 Census Population Totals, including First Look at Race and Hispanic Origin Data for Legislative Redistricting, Accessed March 22, 2011. Available on line at: http://2010.census.gov/news/releases/operations/cb11cn49.html.

United States Core of Engineers (USCE), 1962. Statistical Methods in Hydrology. U.S. Corps of Engineers Institute for Water Resources Hydrologic Engineering Center, Davis, California.

Wahr JM. 1998. The Earth's rotation, *Annual of Review of Earth and Planetary Sciences* **16:** 231-249.

Ward JV. 1985. Thermal characteristics of running waters. *Hydrobiologia* **125**: 31 – 46.

Webb BW, Walling DE. 1993. Longer-term water temperature behavior in an upland stream. *Hydrological* Processes **7**: 1932.

Webb BW, Nobilis F. 1997. A long-term perspective on the nature of the air – water temperature relationship: a case study. *Hydrological Processes* **11**: 137 – 147.

Webb BW, Zhang Y. 1997. Spatial and seasonal variability in the components of the river heat budget. *Hydrological Processes* **11**: 79 – 101.

Webb BW, Zhang Y. 1999. Water temperatures and heat budgets in Dorset chalk water courses, *Hydrological Processes* **13**: 309 – 321.

Webb BW, Zhang Y. 2004. Intra-annual variability in the non advective heat energy budget of Devon streams and rivers. *Hydrological Processes* **18**: 21172146.

Webb BW, Zhang Y, Nobilis F. 1995. Scale related water temperature behavior, *Effects of Scale on Interpretation and Management of Sediment and Water Quality*, (Proceedings of a Boulder Symposium). International Association of Hydrological Sciences Publication No. 226; 231 – 239.

Webb BW, Clack PD, Walling DE. 2003. Water – air temperature relationships in a Devon River system and the role of flow. *Hydrological Processes* **17**: 30693084.

Webb B, Hannah D, Moore R, Brown L, Nobilis F. 2008. Recent advances in stream and river temperature research. *Hydrological Processes* **22**: 902918.

White ED, Easton ZM, Fuka DR, Collick AS, Adgo E, McCarney M, Awulachew SB, Selassie YG, Steenhuis TS. 2010. Development and application of a physically based landscape water balance in the SWAT model, *Hydrological Processes* **25**(6): 915-925.

Yu B. 2000. A systematic over estimation of flows. *Journal of Hydrology* **233**: 258262.

Zachos J, Pagani M, Sloan L, Thomas E, Billups K. 2001. Trends, Rhythms, and aberrations in global climate 65 Ma to present, *Science* **292:** 686-693.

Zhou B, He HS, Nigh TA, Schulz JH. 2012. Mapping and analyzing change of impervious surface for two decades using multitemporal Landsat imagery in Missouri, International *Journal of Applied Earth Observation and Geoinformation,* **18**: 195206.

APPENDIX A

CLIMATE DURING THE STUDY PERIOD
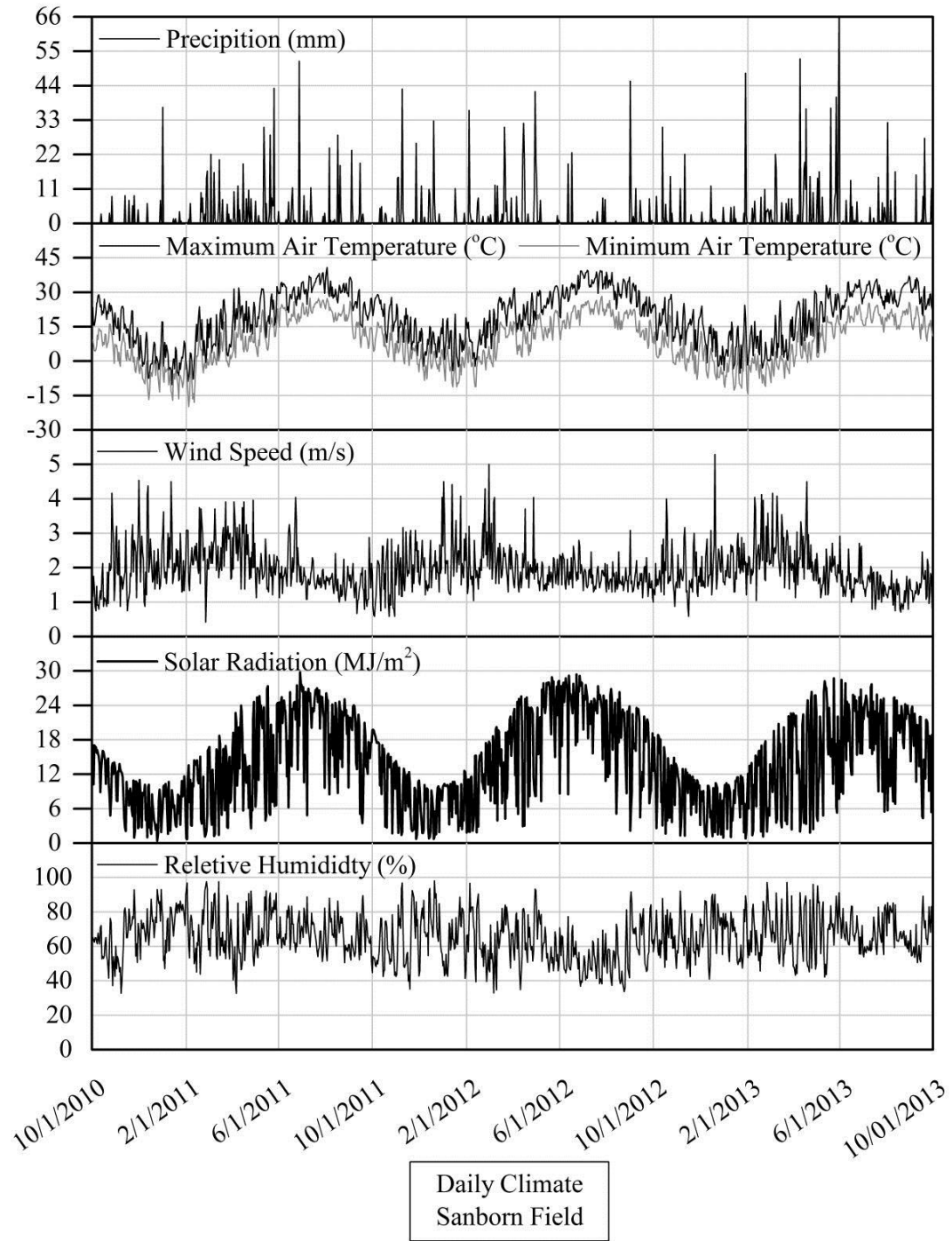
A1. Climate during the study period (WY 2010 – 2013) recorded at Sanborn Field climate station located in Hinkson Creek Watershed, Missouri, USA.
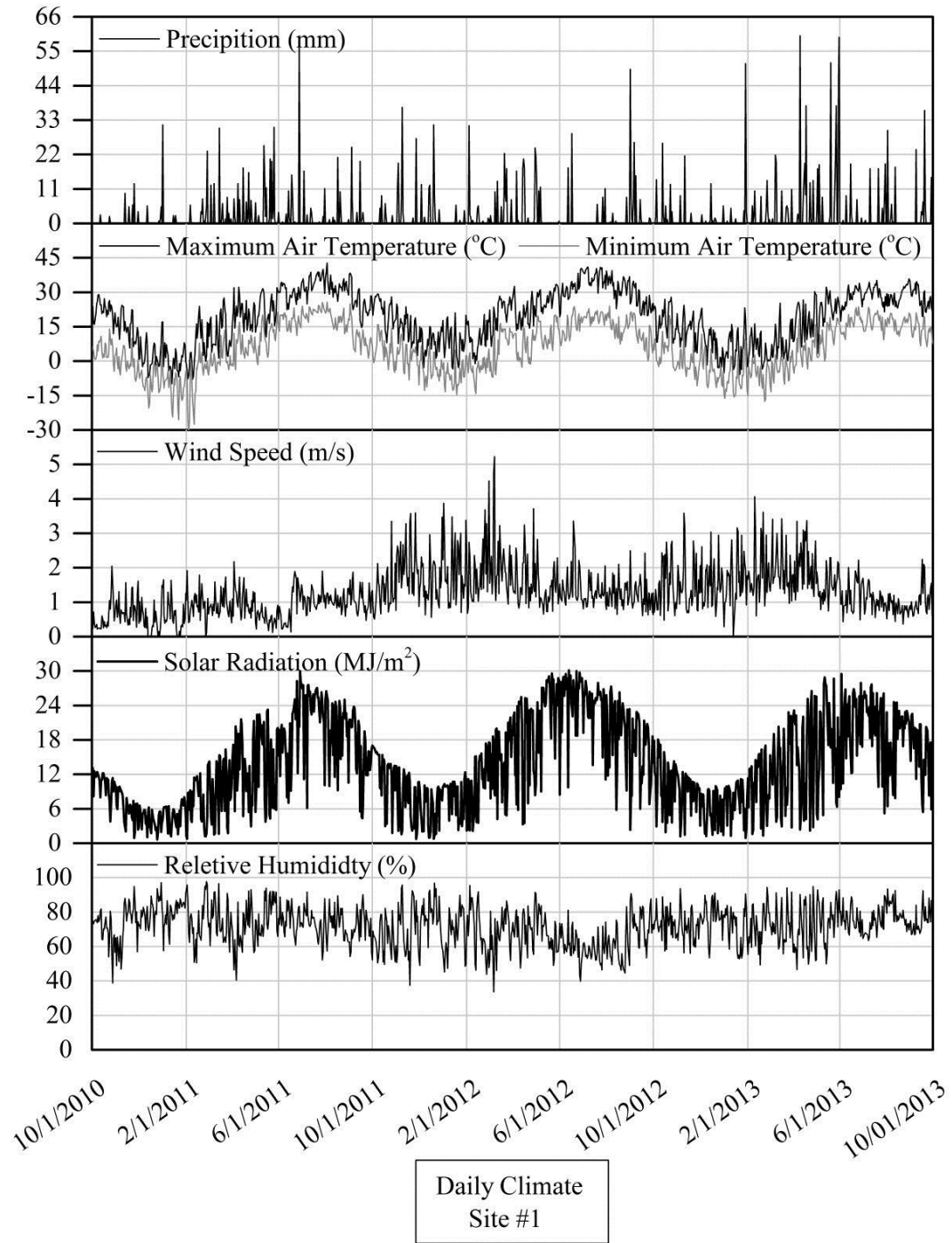
A2. Climate during the study period (WY 2010 – 2013) recorded at the site #1 climate station located in Hinkson Creek Watershed, Missouri, USA.

A3. Climate during the study period (WY 2010 – 2013) recorded at the site #2 climate station located in Hinkson Creek Watershed, Missouri, USA.

A4. Climate during the study period (WY 2010 – 2013) recorded at the site #3 climate station located in Hinkson Creek Watershed, Missouri, USA.
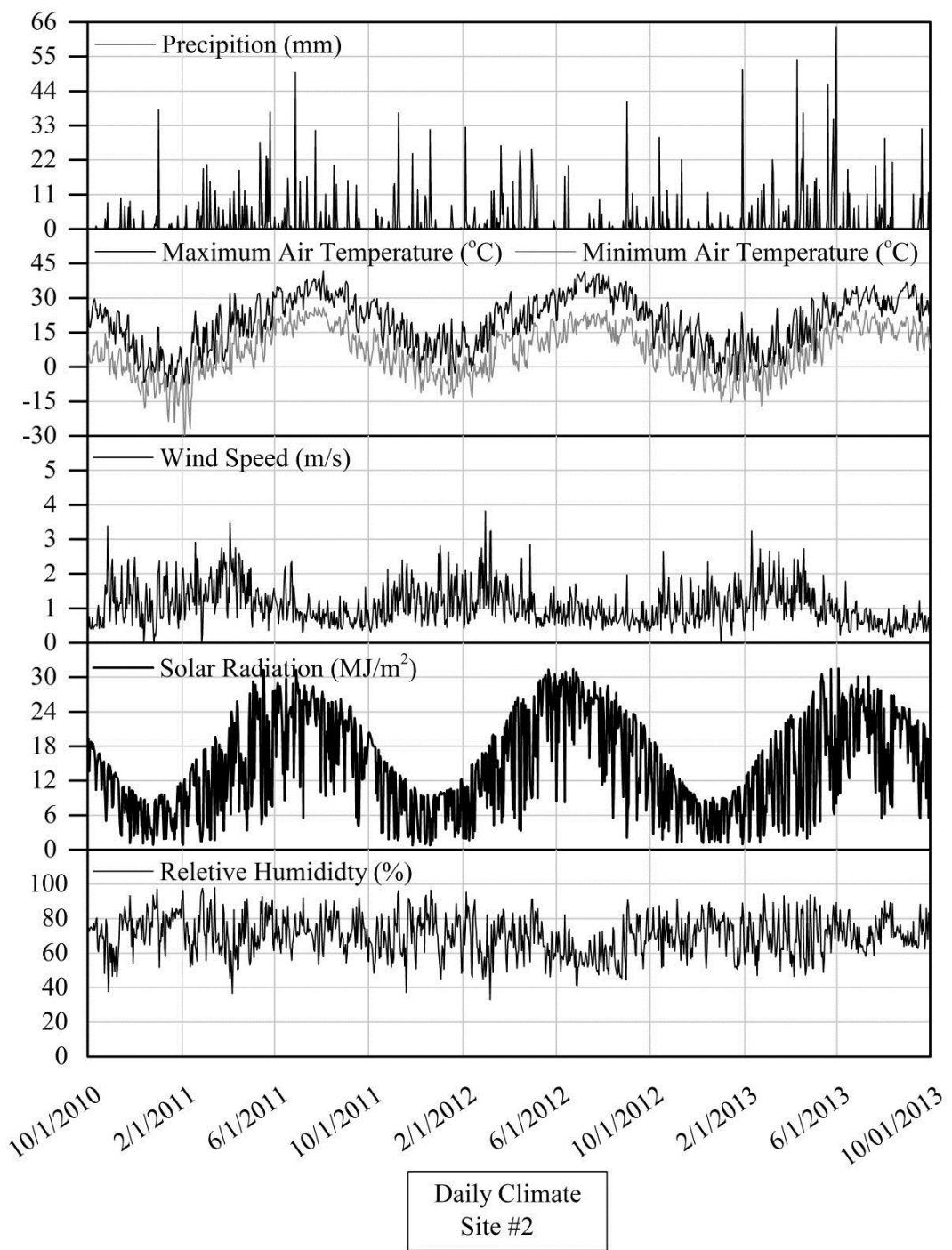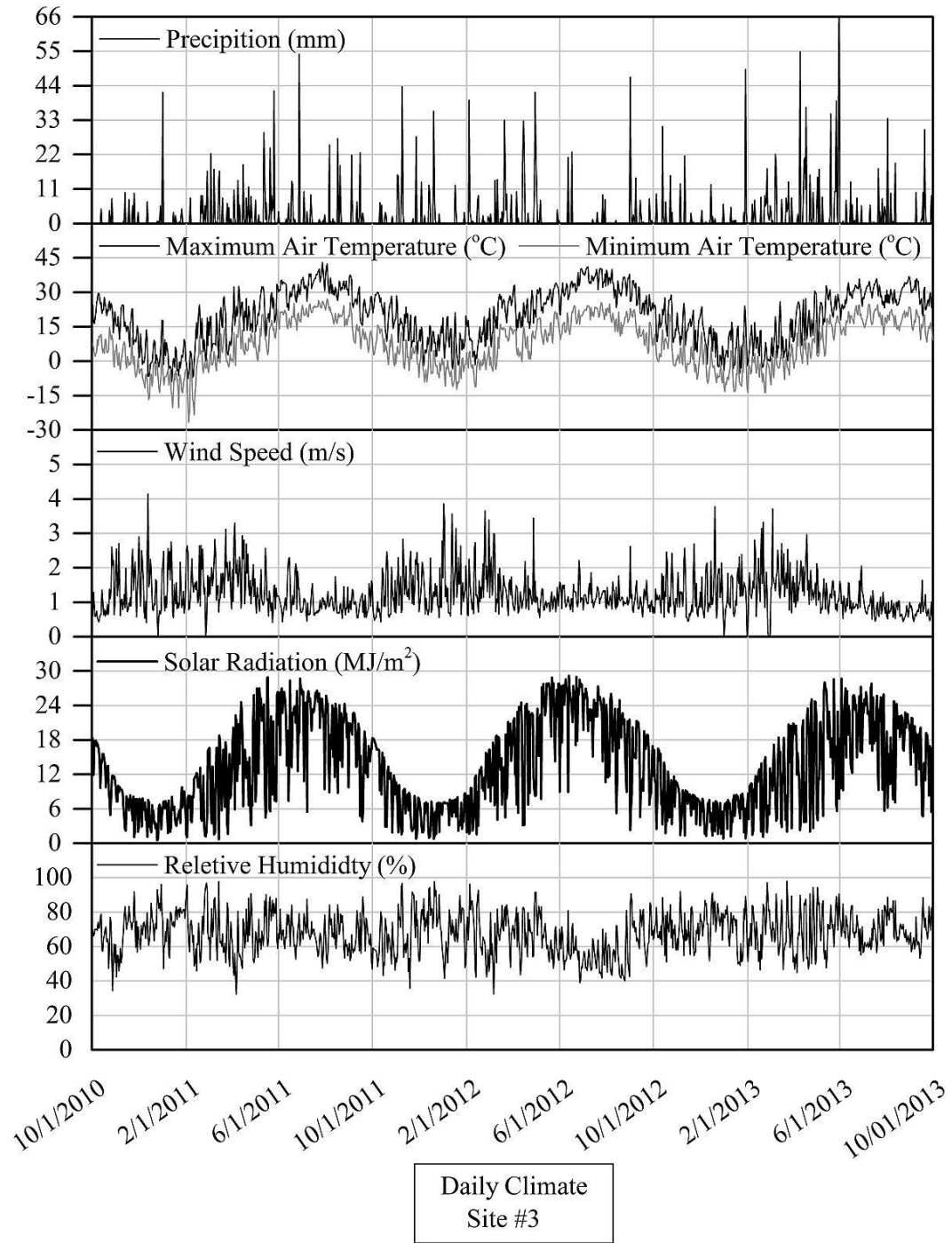
A5. Climate during the study period (WY 2010 – 2013) recorded at the site #4 climate station located in Hinkson Creek Watershed, Missouri, USA.
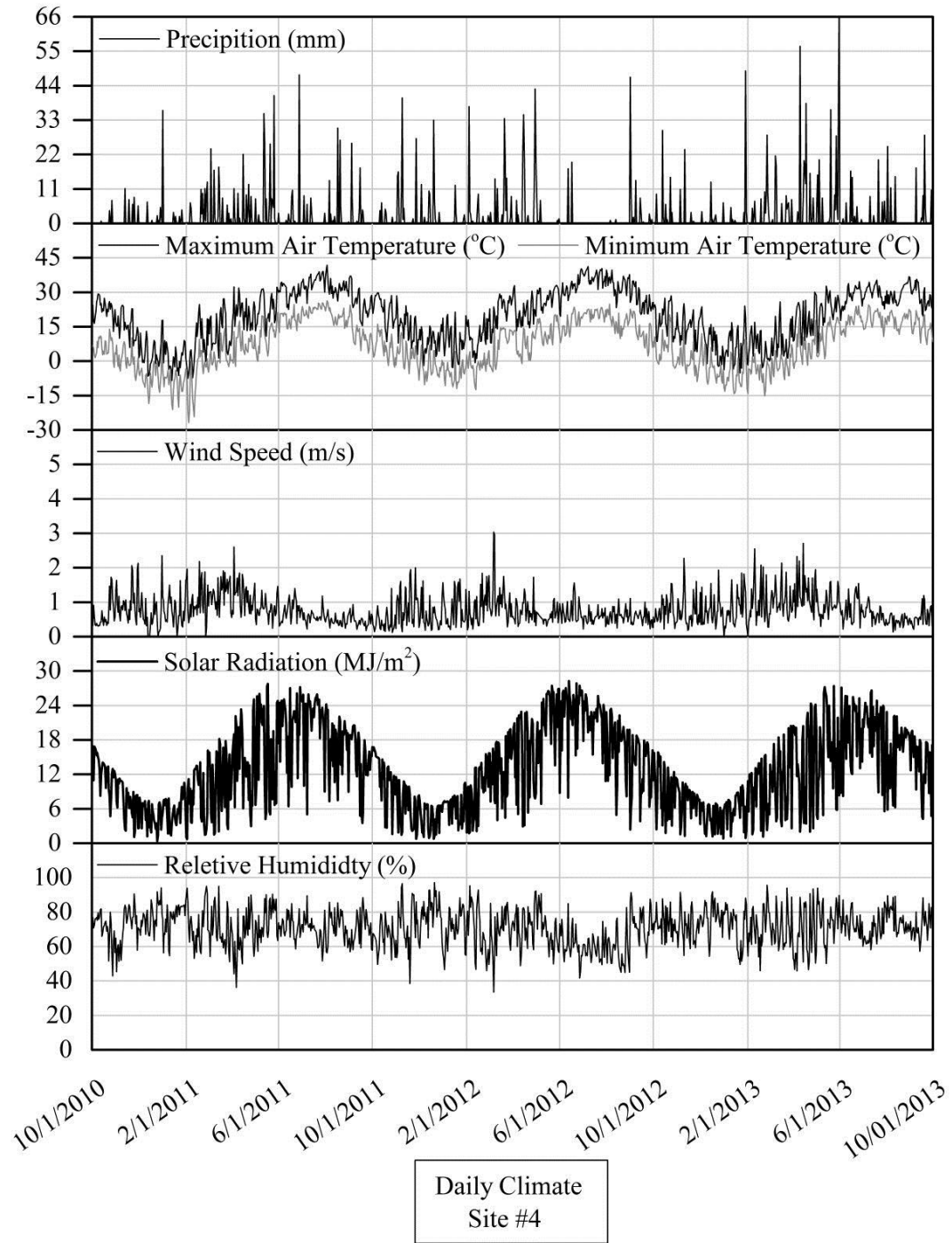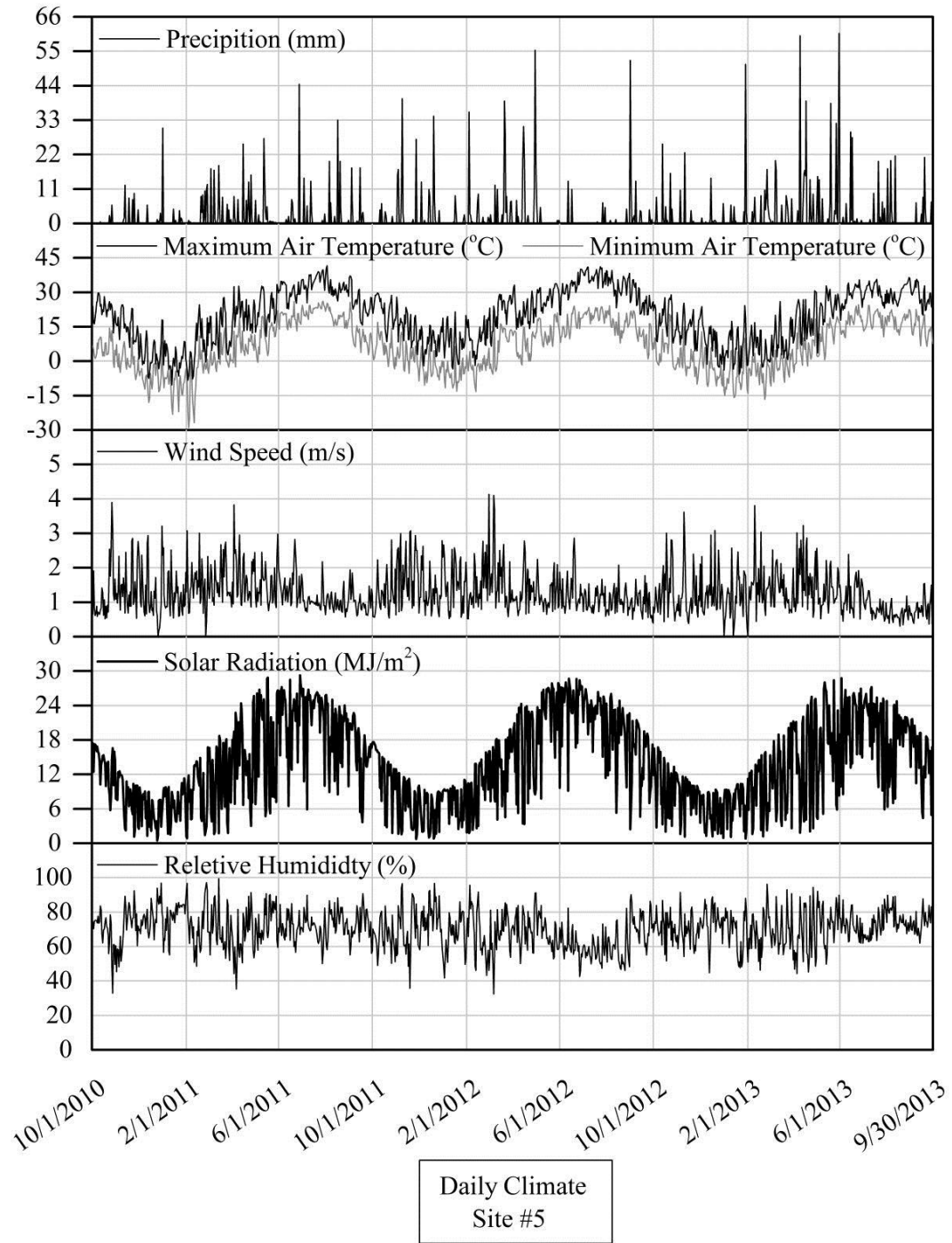
A6. Climate during the study period (WY 2010 – 2013) recorded at the site #5 climate station located in Hinkson Creek Watershed, Missouri, USA.

STREAM WATER TEMPERATURE MODEL EVALUATION RESULTS

B1. Summary of 15 minute linear stream water temperature model evaluation results during calibration and validation periods for five gauging sites in Hinkson Creek Watershed, USA.

15 Minute Linear Stream Water Temperature Model						
Statistic	Site #1	Site #2	Site #3	Site #4	Site #5	All sites
Calibration						
NSE	0.82	0.86	0.86	0.83	0.80	0.83
PBIAS (%)	0.33	0.45	2.75	2.02	0.94	0.02
RSR	0.43	0.38	0.37	0.41	0.44	0.41
MAE (°C)	2.99	2.88	2.80	3.11	3.21	3.00
MSE (°C)	14.37	13.98	12.88	16.02	16.85	14.82
RMSE (°C)	3.79	3.74	3.59	4.00	4.11	3.85
Validation						
NSE	0.79	0.85	0.86	0.82	0.80	0.83
PBIAS (%)	0.23	1.94	1.52	2.14	1.11	0.69
RSR	0.46	0.38	0.37	0.42	0.45	0.42
MAE (°C)	3.02	2.82	2.78	2.98	3.23	2.97
MSE (°C)	14.28	14.06	13.02	14.92	17.17	14.69
RMSE (°C)	3.78	3.75	3.61	3.86	4.14	3.83

NSE is Nash-Sutcliffe efficiency, PBIAS is percent bias, RSR is ratio of root mean square error to the standard deviation of observed data, MAE is mean absolute error, MSE is mean square error, RMSE is root mean square error.

B2. Summary of 15 minute nonlinear stream water temperature model evaluation results during calibration and validation periods for five gauging sites in Hinkson Creek Watershed, USA.

15 Minute Nonlinear Stream Water Temperature Model						
Statistic	Site #1	Site #2	Site #3	Site #4	Site #5	All sites
Calibration						
NSE	0.83	0.86	0.87	0.83	0.81	0.84
PBIAS (%)	0.35	1.07	2.98	1.01	0.27	0.62
RSR	0.42	0.38	0.36	0.41	0.44	0.40
MAE (°C)	2.90	2.89	2.81	3.09	3.18	2.97
MSE (°C)	13.65	13.76	12.51	15.75	16.55	14.44
RMSE (°C)	3.69	3.71	3.54	3.97	4.07	3.80
Validation						
NSE	0.81	0.87	0.87	0.83	0.81	0.84
PBIAS (%)	0.71	1.61	1.34	1.44	0.91	0.38
RSR	0.43	0.37	0.36	0.41	0.44	0.40
MAE (°C)	2.74	2.72	2.69	2.84	3.09	2.81
MSE (°C)	12.88	12.94	11.94	14.20	16.35	13.66
RMSE (°C)	3.59	3.60	3.46	3.77	4.04	3.69

NSE is Nash-Sutcliffe efficiency, PBIAS is percent bias, RSR is ratio of root mean square error to the standard deviation of observed data, MAE is mean absolute error, MSE is mean square error, RMSE is root mean square error.

B3. Summary of 15 minute calibrated linear stream water temperature model evaluation results during calibration and validation periods for five gauging sites in Hinkson Creek Watershed, USA.

15 Minute Calibrated Linear Stream Water Temperature Model						
Statistic	Site #1	Site #2	Site #3	Site #4	Site #5	All sites
Calibration						
NSE	0.91	0.91	0.91	0.94	0.90	0.91
PBIAS (%)	3.37	2.94	0.62	3.01	1.93	2.37
RSR	0.30	0.30	0.31	0.25	0.31	0.29
MAE (°C)	1.88	1.96	1.34	1.07	2.05	1.66
MSE (°C)	6.56	7.48	4.96	3.80	8.11	6.18
RMSE (°C)	2.56	2.74	2.23	1.95	2.85	2.46
Validation						
NSE	0.89	0.88	0.91	0.90	0.89	0.89
PBIAS (%)	4.08	6.57	2.41	5.38	4.08	4.50
RSR	0.34	0.35	0.30	0.31	0.34	0.33
MAE (°C)	2.29	2.28	2.24	2.24	2.29	2.26
MSE (°C)	9.45	8.49	8.73	8.28	9.45	8.88
RMSE (°C)	3.07	2.91	2.95	2.88	3.07	2.98

NSE is Nash-Sutcliffe efficiency, PBIAS is percent bias, RSR is ratio of root mean square error to the standard deviation of observed data, MAE is mean absolute error, MSE is mean square error, RMSE is root mean square error.

B4. Summary of hourly linear stream water temperature model evaluation results during calibration and validation periods for five gauging sites in Hinkson Creek Watershed, USA.

Hourly Linear Stream Water Temperature Model						
Statistic	Site #1	Site #2	Site #3	Site #4	Site #5	All sites
Calibration						
NSE	0.82	0.86	0.87	0.83	0.81	0.84
PBIAS (%)	0.02	0.95	0.82	0.29	0.51	0.52
RSR	0.43	0.38	0.36	0.41	0.44	0.40
MAE (°C)	2.97	2.87	2.67	3.13	3.20	2.97
MSE (°C)	14.28	13.99	12.13	16.01	16.79	14.64
RMSE (°C)	3.78	3.74	3.48	4.00	4.10	3.82
Validation						
NSE	0.79	0.85	0.87	0.82	0.80	0.83
PBIAS (%)	0.62	3.66	2.13	0.49	0.69	1.27
RSR	0.45	0.38	0.36	0.42	0.45	0.41
MAE (°C)	3.01	2.85	2.61	2.99	3.22	2.93
MSE (°C)	14.20	14.24	12.13	14.77	17.08	14.48
RMSE (°C)	3.77	3.77	3.48	3.84	4.13	3.80

NSE is Nash-Sutcliffe efficiency, PBIAS is percent bias, RSR is ratio of root mean square error to the standard deviation of observed data, MAE is mean absolute error, MSE is mean square error, RMSE is root mean square error.

B5. Summary of hourly nonlinear stream water temperature model evaluation results during calibration and validation periods for five gauging sites in Hinkson Creek Watershed, USA.

Hourly Nonlinear Stream Water Temperature Model						
Statistic	Site #1	Site #2	Site #3	Site #4	Site #5	All sites
Calibration						
NSE	0.83	0.86	0.87	0.83	0.81	0.84
PBIAS (%)	0.36	0.40	0.39	0.03	0.23	0.14
RSR	0.42	0.37	0.36	0.41	0.44	0.40
MAE (°C)	2.90	2.87	2.72	3.13	3.22	2.97
MSE (°C)	13.64	13.61	12.23	15.69	16.79	14.39
RMSE (°C)	3.69	3.69	3.50	3.96	4.10	3.79
Validation						
NSE	0.81	0.86	0.87	0.83	0.80	0.84
PBIAS (%)	0.81	3.28	2.07	0.59	0.76	1.18
RSR	0.43	0.37	0.36	0.41	0.44	0.40
MAE (°C)	2.74	2.73	2.60	2.86	3.13	2.81
MSE (°C)	12.83	13.07	11.78	13.94	16.36	13.60
RMSE (°C)	3.58	3.61	3.43	3.73	4.04	3.68

NSE is Nash-Sutcliffe efficiency, PBIAS is percent bias, RSR is ratio of root mean square error to the standard deviation of observed data, MAE is mean absolute error, MSE is mean square error, RMSE is root mean square error.

B6. Summary of hourly calibrated linear stream water temperature model evaluation results during calibration and validation periods for five gauging sites in Hinkson Creek Watershed, USA.

Hourly Calibrated Linear Stream Water Temperature Model						
Statistic	Site #1	Site #2	Site #3	Site #4	Site #5	All sites
Calibration						
NSE	0.91	0.92	0.92	0.92	0.90	0.91
PBIAS (%)	3.49	3.57	2.26	3.41	1.86	2.92
RSR	0.30	0.29	0.28	0.29	0.31	0.29
MAE (°C)	1.98	2.15	1.97	2.09	2.16	2.07
MSE (°C)	6.93	8.25	7.17	7.82	8.47	7.73
RMSE (°C)	2.63	2.87	2.68	2.80	2.91	2.78
Validation						
NSE	0.88	0.91	0.92	0.90	0.89	0.90
PBIAS (%)	6.57	2.72	2.64	5.38	4.07	4.28
RSR	0.35	0.30	0.29	0.31	0.33	0.32
MAE (°C)	2.27	2.19	2.08	2.23	2.27	2.21
MSE (°C)	8.44	8.56	7.60	8.22	9.29	8.42
RMSE (°C)	2.90	2.93	2.76	2.87	3.05	2.90

NSE is Nash-Sutcliffe efficiency, PBIAS is percent bias, RSR is ratio of root mean square error to the standard deviation of observed data, MAE is mean absolute error, MSE is mean square error, RMSE is root mean square error.

B7. Summary of daily linear stream water temperature model evaluation results during calibration and validation periods for five gauging sites in Hinkson Creek Watershed, USA.

Daily Linear Stream Water Temperature Model						
Statistic	Site #1	Site #2	Site #3	Site #4	Site #5	All sites
Calibration						
NSE	0.91	0.92	0.93	0.91	0.90	0.92
PBIAS (%)	-1.15	0.21	-1.37	-1.24	-1.29	-0.97
RSR	0.30	0.28	0.26	0.29	0.31	0.29
MAE (°C)	1.96	2.05	1.83	2.07	2.13	2.01
MSE (°C)	6.92	7.39	6.29	7.66	8.19	7.29
RMSE (°C)	2.63	2.72	2.51	2.77	2.86	2.70
Validation						
NSE	0.88	0.91	0.92	0.90	0.88	0.90
PBIAS (%)	0.97	-1.12	-1.35	0.85	0.30	-0.07
RSR	0.35	0.30	0.28	0.31	0.34	0.32
MAE (°C)	2.20	2.22	1.96	2.19	2.34	2.18
MSE (°C)	8.15	8.45	6.99	8.04	9.62	8.25
RMSE (°C)	2.85	2.91	2.64	2.83	3.10	2.87

NSE is Nash-Sutcliffe efficiency, PBIAS is percent bias, RSR is ratio of root mean square error to the standard deviation of observed data, MAE is mean absolute error, MSE is mean square error, RMSE is root mean square error.

B8. Summary of daily nonlinear stream water temperature model evaluation results during calibration and validation periods for five gauging sites in Hinkson Creek Watershed, USA.

Daily Nonlinear Stream Water Temperature Model						
Statistic	Site #1	Site #2	Site #3	Site #4	Site #5	All sites
Calibration						
NSE	0.92	0.92	0.93	0.93	0.90	0.92
PBIAS (%)	-0.38	-0.73	-0.74	-0.67	-0.66	-0.64
RSR	0.29	0.28	0.26	0.26	0.31	0.28
MAE (°C)	1.92	2.03	1.90	1.89	2.19	1.99
MSE (°C)	6.47	7.11	6.29	5.78	8.18	6.77
RMSE (°C)	2.54	2.67	2.51	2.40	2.86	2.60
Validation						
NSE	0.90	0.92	0.93	0.93	0.89	0.91
PBIAS (%)	1.48	-2.46	-1.20	1.01	0.46	-0.14
RSR	0.32	0.28	0.27	0.26	0.33	0.29
MAE (°C)	1.94	2.04	1.87	1.85	2.26	1.99
MSE (°C)	6.88	7.46	6.42	5.55	9.06	7.07
RMSE (°C)	2.62	2.73	2.53	2.36	3.01	2.65

NSE is Nash-Sutcliffe efficiency, PBIAS is percent bias, RSR is ratio of root mean square error to the standard deviation of observed data, MAE is mean absolute error, MSE is mean square error, RMSE is root mean square error.

B9. Summary of daily calibrated linear stream water temperature model evaluation results during calibration and validation periods for five gauging sites in Hinkson Creek Watershed, USA.

Daily Calibrated Linear Stream Water Temperature Model						
Statistic	Site #1	Site #2	Site #3	Site #4	Site #5	All sites
Calibration						
NSE	0.92	0.95	0.96	0.95	0.94	0.94
PBIAS (%)	3.46	3.56	2.25	3.40	1.84	2.90
RSR	0.28	0.22	0.21	0.23	0.25	0.24
MAE (°C)	1.89	1.99	1.78	1.99	2.07	1.94
MSE (°C)	6.22	6.94	5.73	7.10	7.83	6.76
RMSE (°C)	2.49	2.63	2.39	2.66	2.80	2.60
Validation						
NSE	0.88	0.92	0.93	0.91	0.89	0.91
PBIAS (%)	6.57	2.74	2.66	5.38	4.08	4.29
RSR	0.34	0.28	0.26	0.31	0.33	0.30
MAE (°C)	2.19	2.06	1.85	2.18	2.21	2.10
MSE (°C)	7.86	7.37	6.13	7.83	8.88	7.61
RMSE (°C)	2.80	2.72	2.48	2.80	2.98	2.75

NSE is Nash-Sutcliffe efficiency, PBIAS is percent bias, RSR is ratio of root mean square error to the standard deviation of observed data, MAE is mean absolute error, MSE is mean square error, RMSE is root mean square error.

B10. Summary of original SWAT stream water temperature model evaluation results during calibration and validation periods for five gauging sites in Hinkson Creek Watershed, USA.

Statistic	Site #1	Site #2	Site #3	Site #4	Site #5	All sites
Original SWAT Stream Water Temperature Model						
Calibration						
NSE	0.90	0.90	0.90	0.89	0.89	0.90
PBIAS (%)	-4.60	-2.92	-6.28	-3.55	-5.87	-4.64
RSR	0.32	0.32	0.31	0.33	0.34	0.32
MAE (°C)	2.05	2.39	2.21	2.38	2.35	2.28
MSE (°C)	7.73	9.47	8.82	9.45	9.88	9.07
RMSE (°C)	2.78	3.08	2.97	3.07	3.14	3.01
Validation						
NSE	0.87	0.88	0.89	0.88	0.87	0.88
PBIAS (%)	-3.18	-5.65	-7.92	-2.74	-5.48	-4.99
RSR	0.36	0.34	0.34	0.34	0.37	0.35
MAE (°C)	2.21	2.64	2.42	2.46	2.52	2.45
MSE (°C)	8.62	11.10	10.01	9.65	11.13	10.10
RMSE (°C)	2.94	3.33	3.16	3.11	3.34	3.17

NSE is Nash-Sutcliffe efficiency, PBIAS is percent bias, RSR is ratio of root mean square error to the standard deviation of observed data, MAE is mean absolute error, MSE is mean square error, RMSE is root mean square error.

B11. Summary of Ficklin et al. (2012) stream water temperature model evaluation results during calibration and validation periods for five gauging sites in Hinkson Creek Watershed, USA.

Ficklin et al. (2012) Stream Water Temperature Model						
Statistic	Site #1	Site #2	Site #3	Site #4	Site #5	All sites
Calibration						
NSE	0.91	0.92	0.93	0.91	0.90	0.91
PBIAS (%)	4.20	4.76	0.88	3.80	1.46	3.02
RSR	0.31	0.28	0.27	0.30	0.32	0.30
MAE (°C)	2.08	2.05	1.86	2.11	2.18	2.06
MSE (°C)	7.33	7.45	6.44	8.13	8.72	7.61
RMSE (°C)	2.71	2.73	2.54	2.85	2.95	2.76
Validation						
NSE	0.86	0.91	0.92	0.89	0.88	0.89
PBIAS (%)	8.23	5.27	2.53	7.41	4.58	5.60
RSR	0.37	0.29	0.28	0.33	0.35	0.32
MAE (°C)	2.37	2.12	1.87	2.32	2.36	2.21
MSE (°C)	9.16	7.97	6.79	9.10	10.21	8.65
RMSE (°C)	3.03	2.82	2.61	3.02	3.20	2.93

NSE is Nash-Sutcliffe efficiency, PBIAS is percent bias, RSR is ratio of root mean square error to the standard deviation of observed data, MAE is mean absolute error, MSE is mean square error, RMSE is root mean square error.

B12. Coefficients of determination (r^2) from stream water temperature model evaluation results during the study period (WY 2011 to 2013) for five gauging sites in Hinkson Creek Watershed, USA.

| Time Scale	T_w Model	Site #1	Site #2	Site #3	Site #4	Site #5
15 minute	Linear	0.811	0.859	0.870	0.832	0.810
	Nonlinear	0.823	0.863	0.874	0.837	0.813
	Calibrated	0.908	0.918	0.924	0.918	0.906
Hourly	Linear	0.812	0.860	0.874	0.834	0.812
	Nonlinear	0.823	0.864	0.872	0.834	0.806
	Calibrated	0.909	0.918	0.924	0.916	0.901
Daily	Linear	0.904	0.923	0.931	0.918	0.904
	Nonlinear	0.914	0.924	0.931	0.919	0.900
	Calibrated	0.916	0.927	0.936	0.922	0.907
	Original SWAT	0.899	0.918	0.925	0.908	0.896
	Ficklin et al. (2012)	0.904	0.925	0.931	0.913	0.901

APPENDIX C

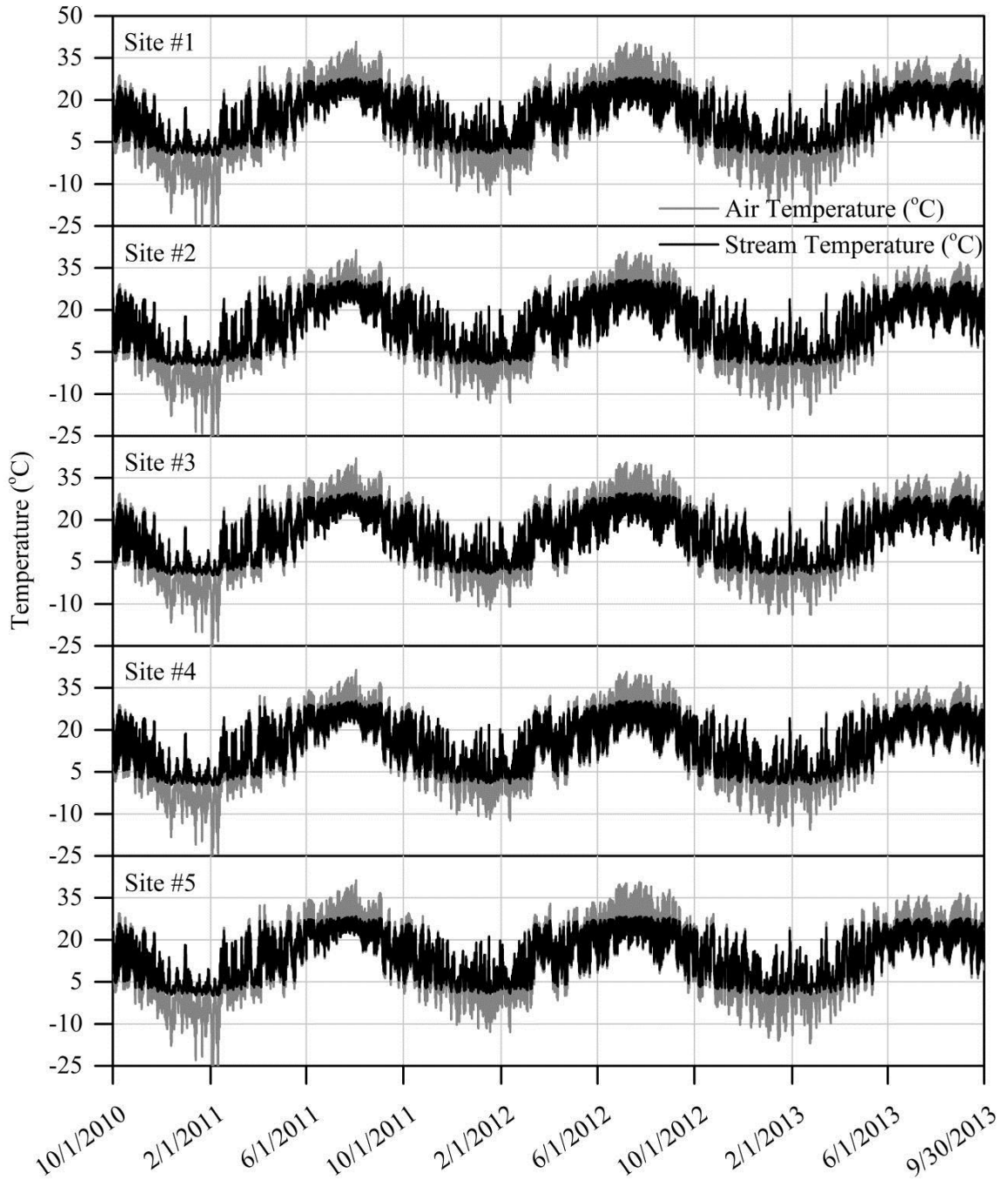STREAM WATER TEMPERATURE MODEL EVALUATION RESULTS
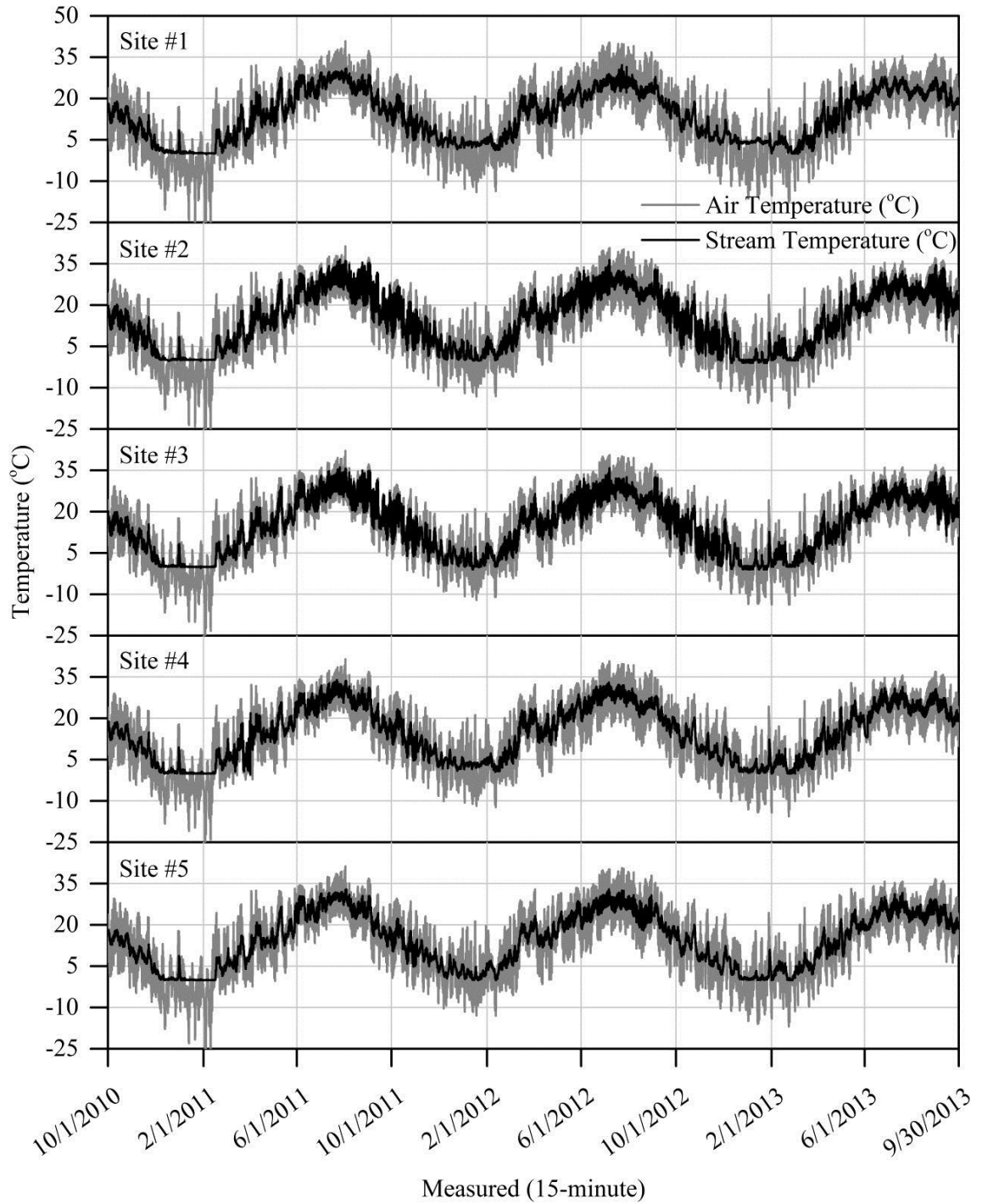
C1. Measured 15 minute time series air and stream water temperature from five gauging sites in Hinkson Creek for the three year study period.
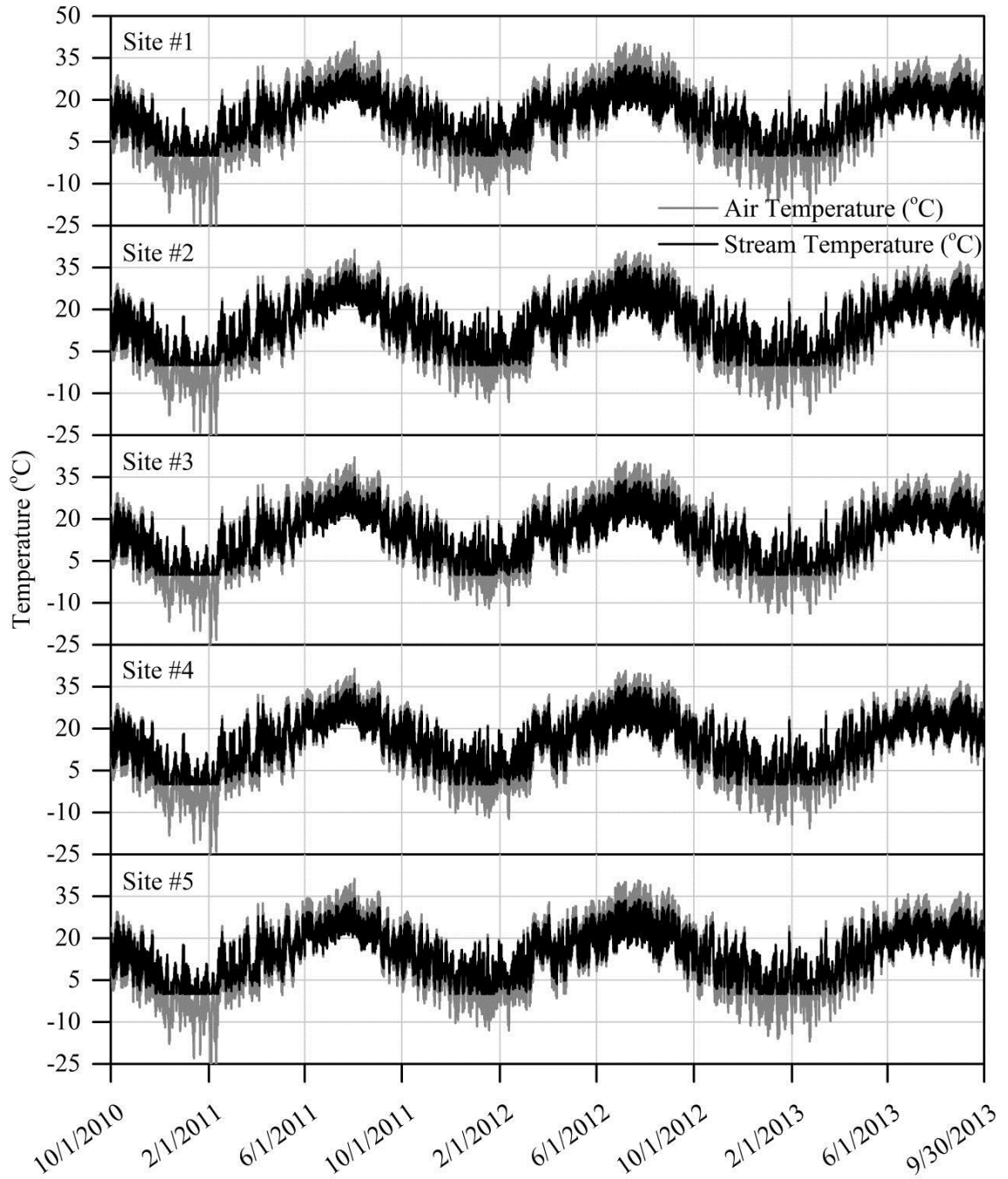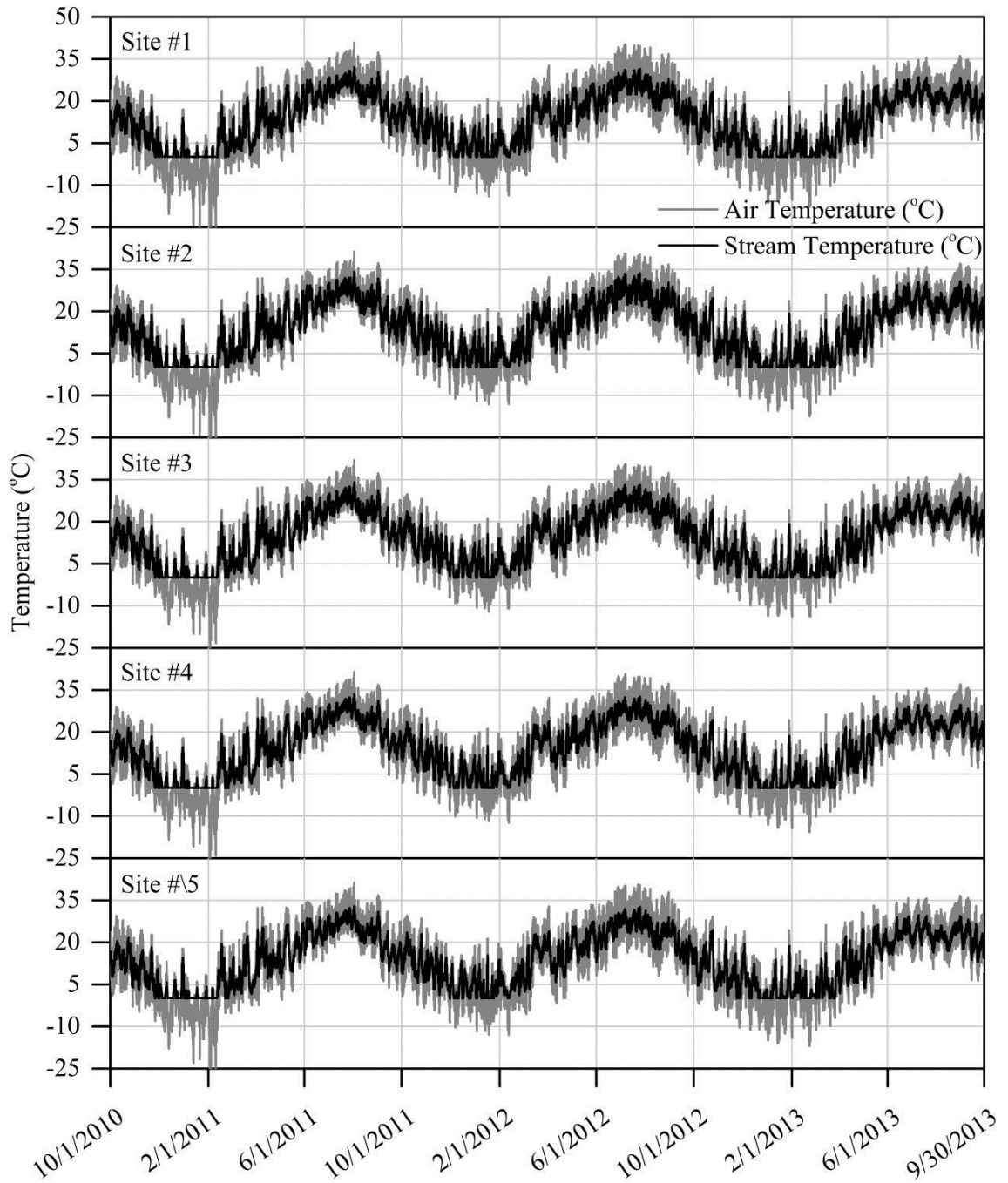
Linear (15-minute)

C2. Results from linear regression model simulations showing 15 minute time series stream water temperature from five gauging sites in Hinkson Creek for the three year study period. Measured air temperature data are shown as a refrence.
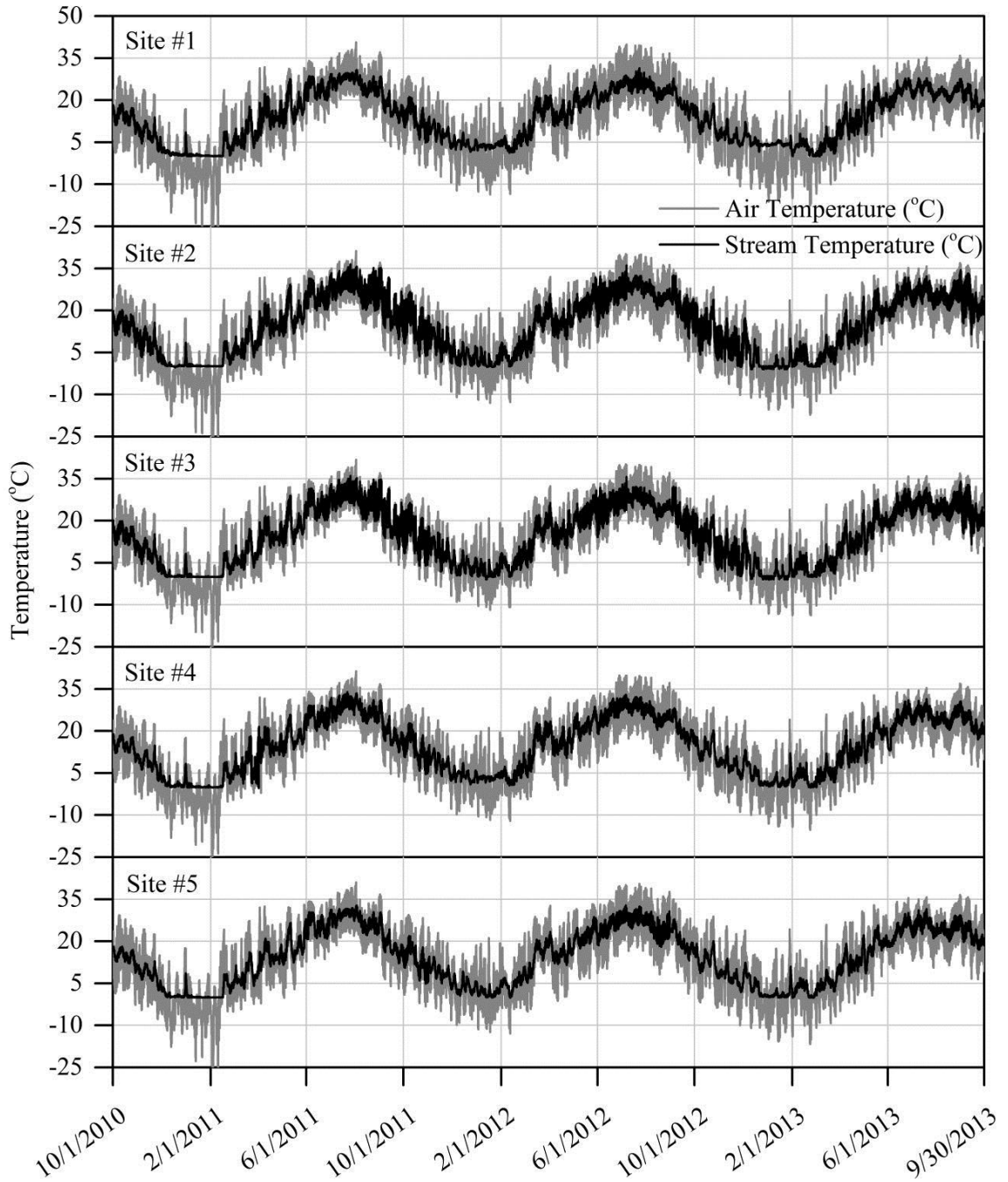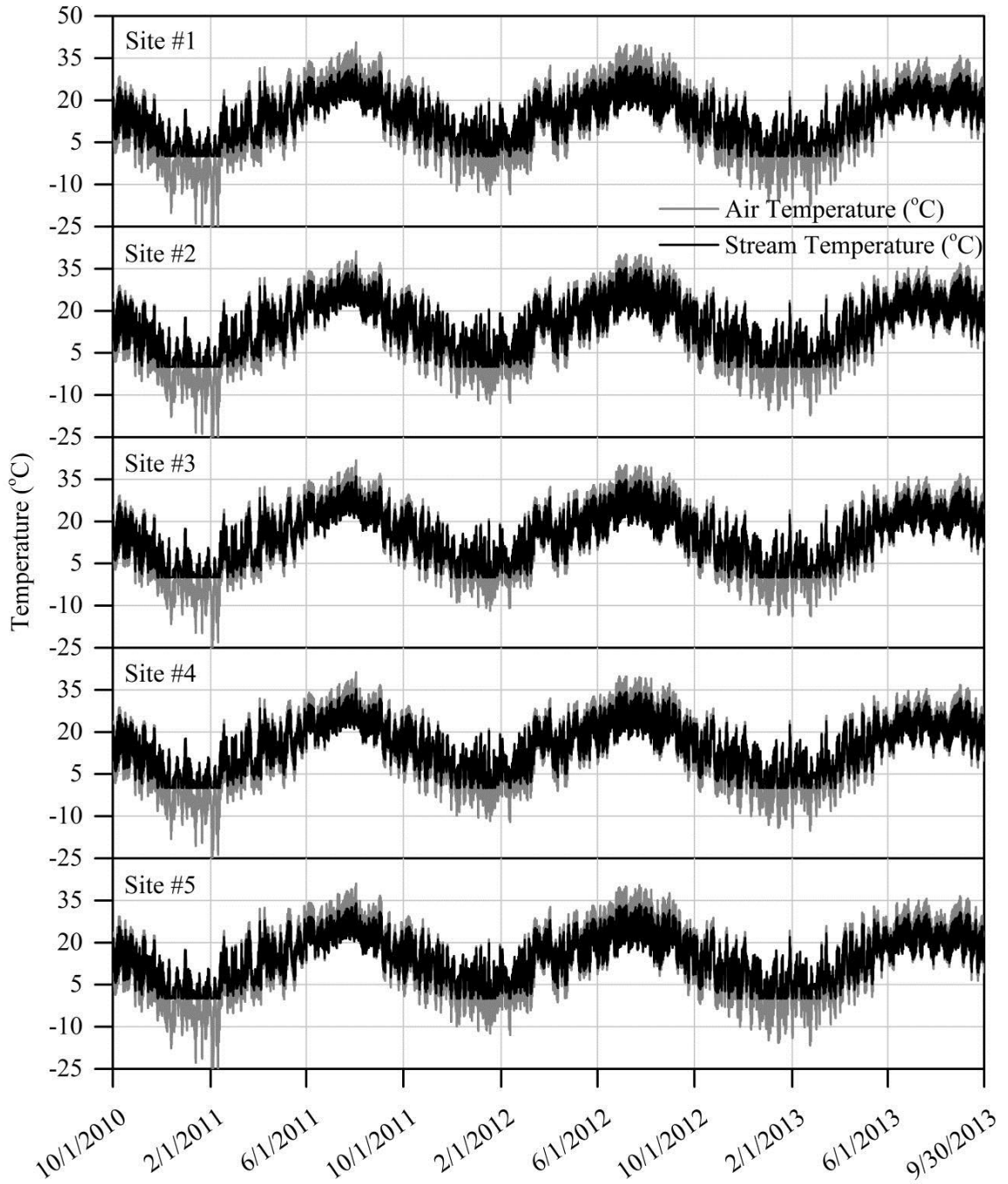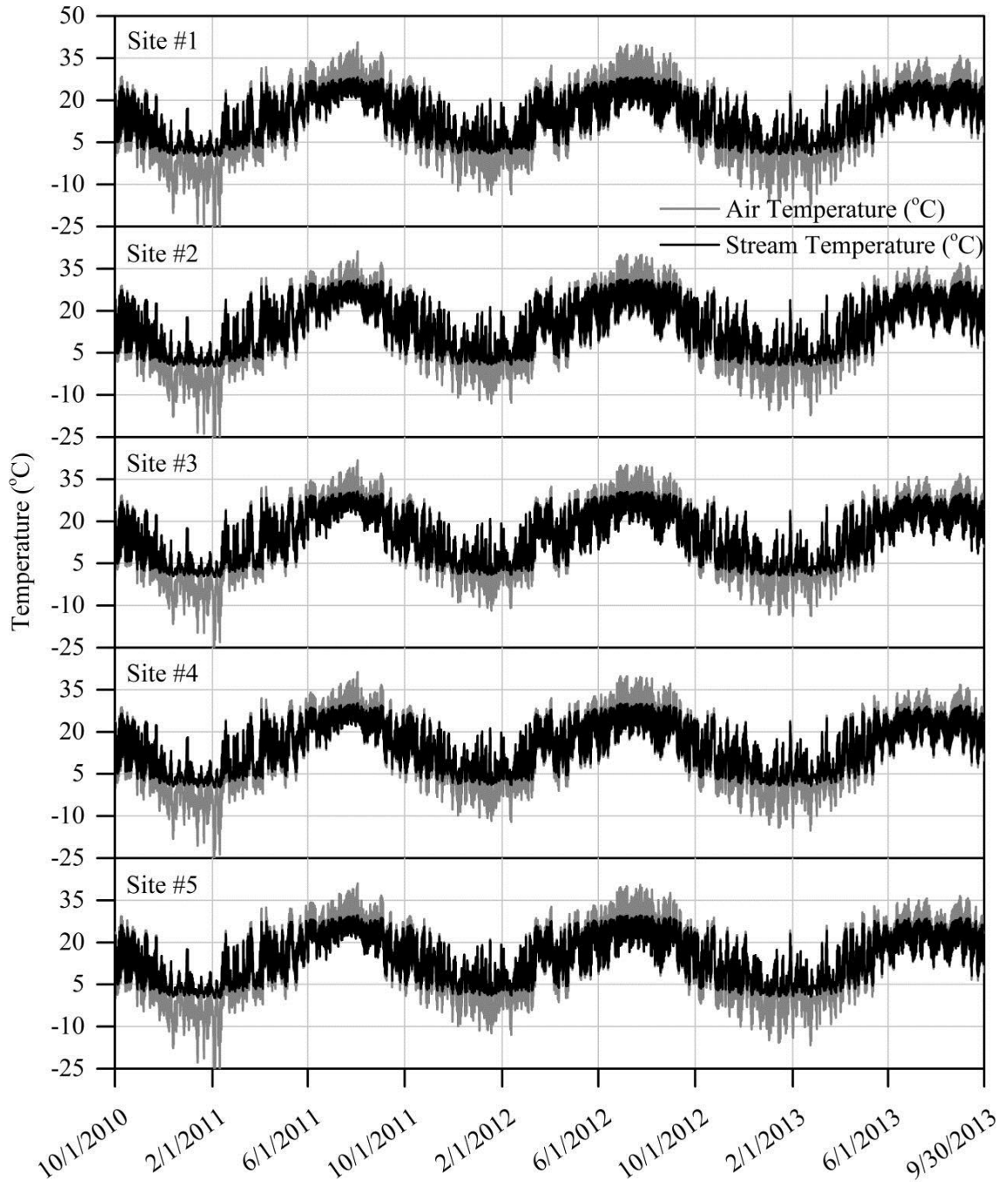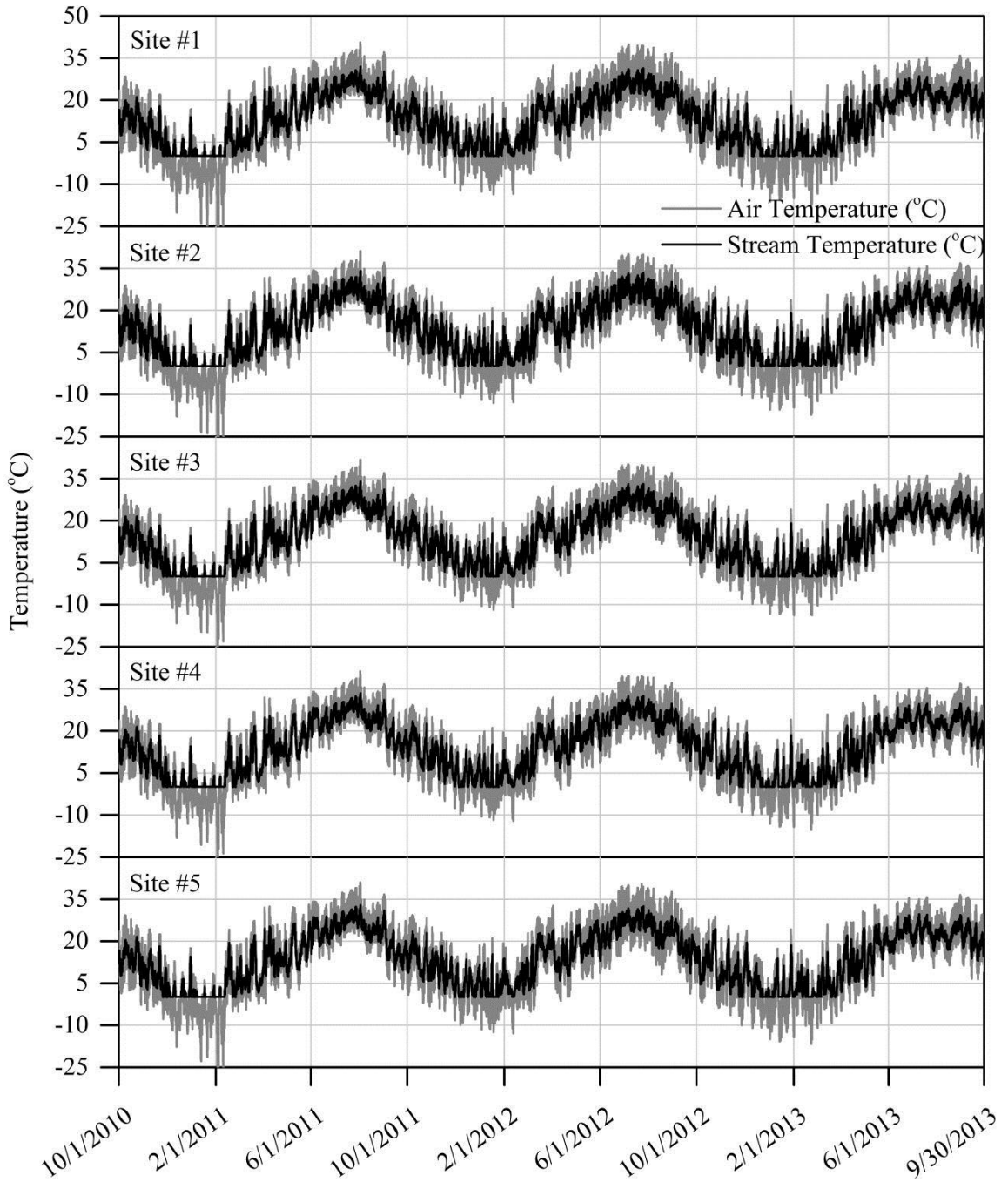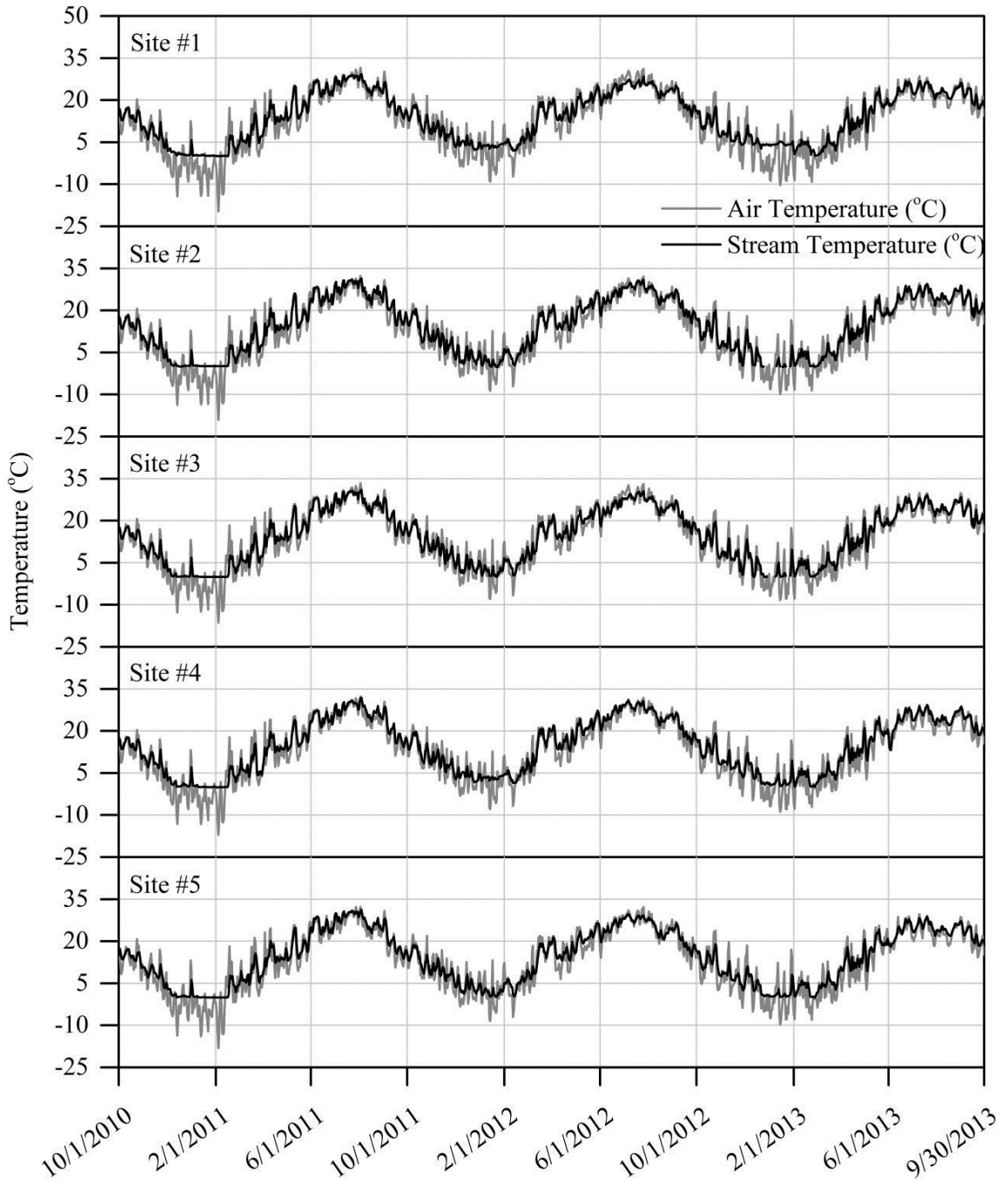
C3. Results from nonlinear regression model simulations showing 15 minute time series stream water temperature from five gauging sites in Hinkson Creek for the three year study period. Measured air temperature data are shown as a refrence.

C4. Results from calibrated linear regression model simulations showing 15 minute time series stream water temperature from five gauging sites in Hinkson Creek for the three year study period. Measured air temperature data are shown as a refrence.

C5. Measured hourly time series air and stream water temperature from five gauging sites in Hinkson Creek for the three year study period.
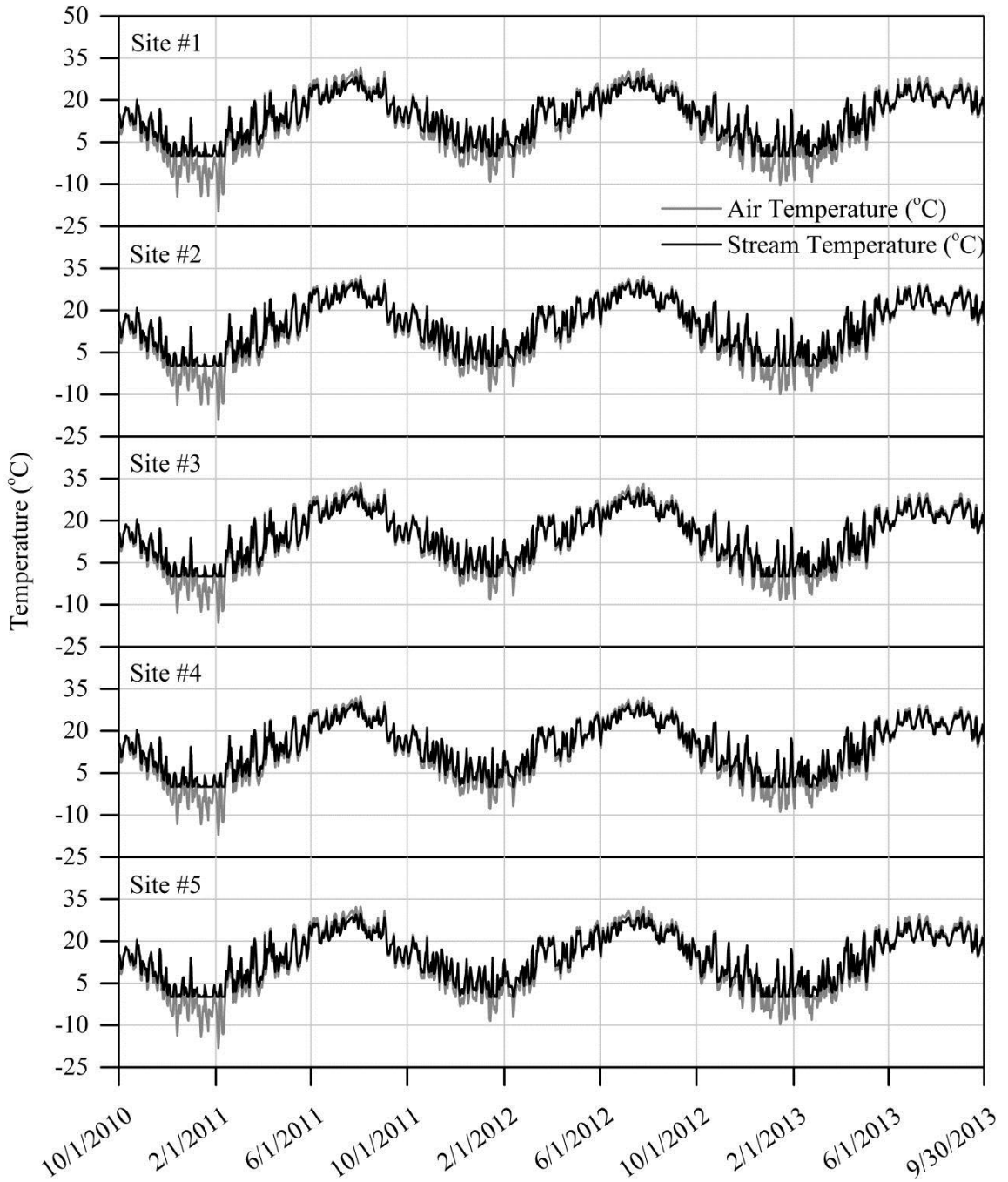
C5. Results from linear regression model simulations showing hourly time series stream water temperature from five gauging sites in Hinkson Creek for the three year study period. Measured air temperature data are shown as a refrence.
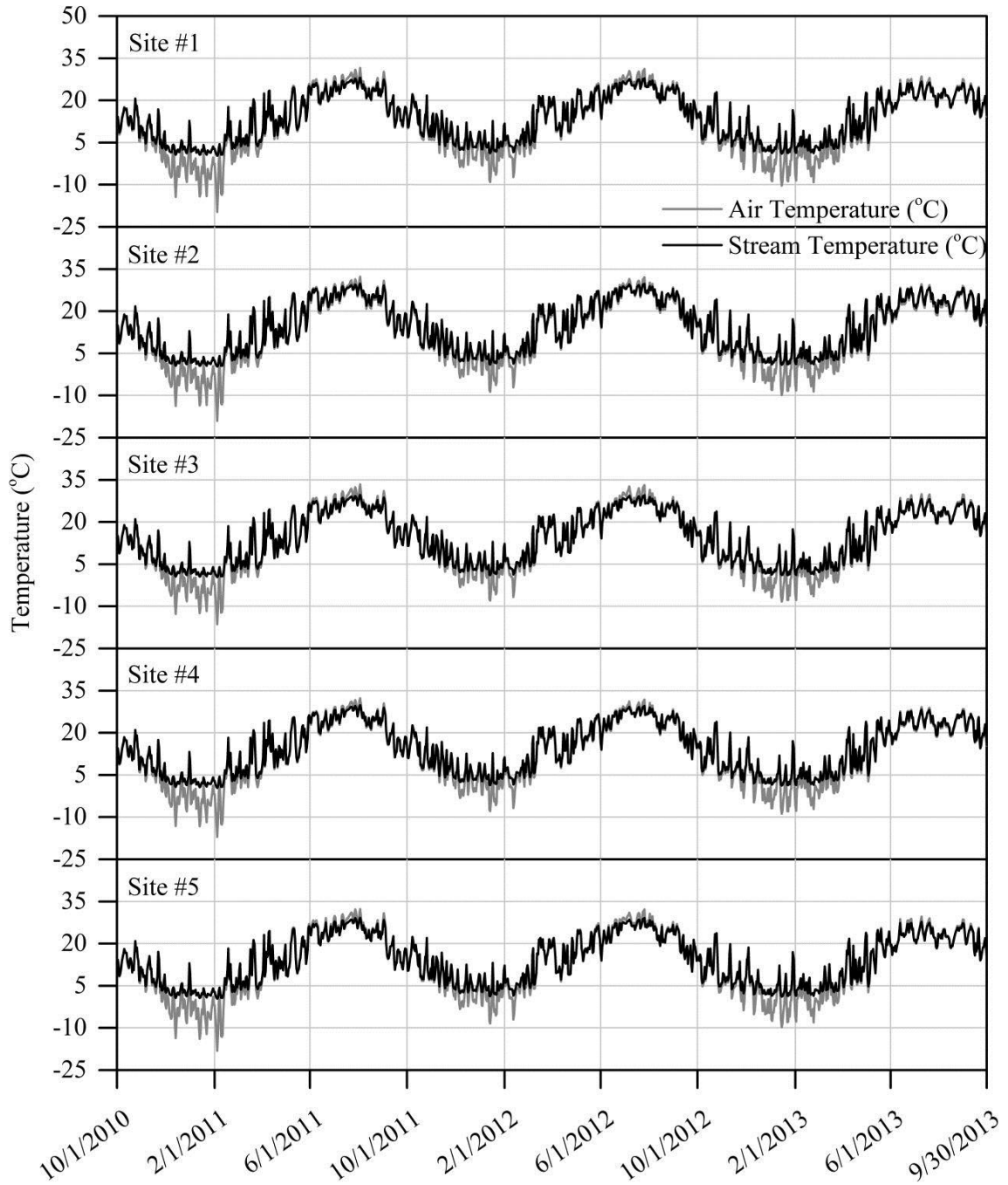
C6. Results from nonlinear regression model simulations showing hourly time series stream water temperature from five gauging sites in Hinkson Creek for the three year study period. Measured air temperature data are shown as a refrence.

177

C7. Results from calibrated linear regression model simulations showing hourly time series stream water temperature from five gauging sites in Hinkson Creek for the three year study period. Measured air temperature data are shown as a refrence.

C8. Measured daily time series air temperature and stream water temperature from five gauging sites in Hinkson Creek for the three year study period.
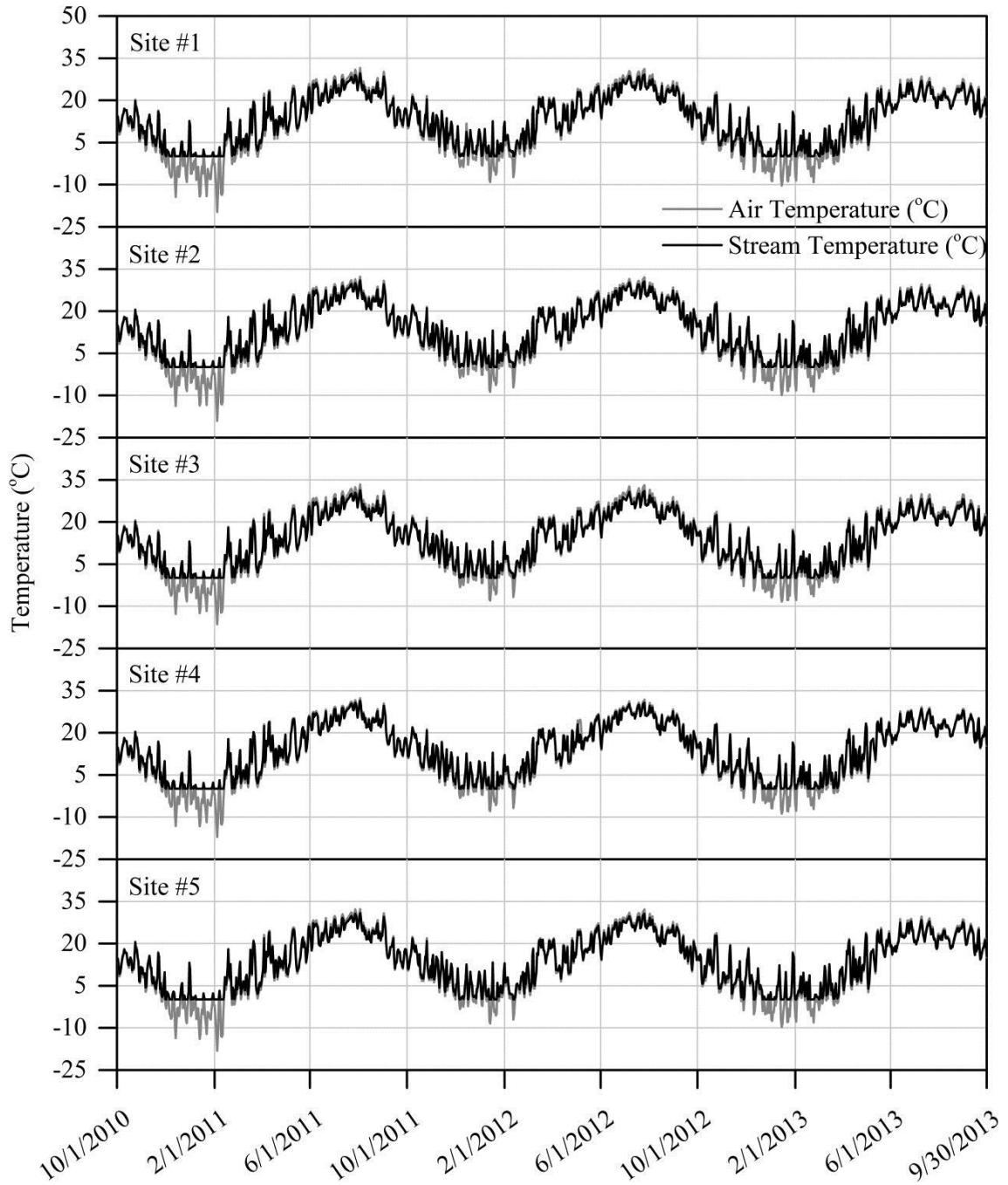
179

C9. Results from linear regression model simulations showing daily time series stream water temperature from five gauging sites in Hinkson Creek for the three year study period. Measured air temperature data are shown as a refrence.
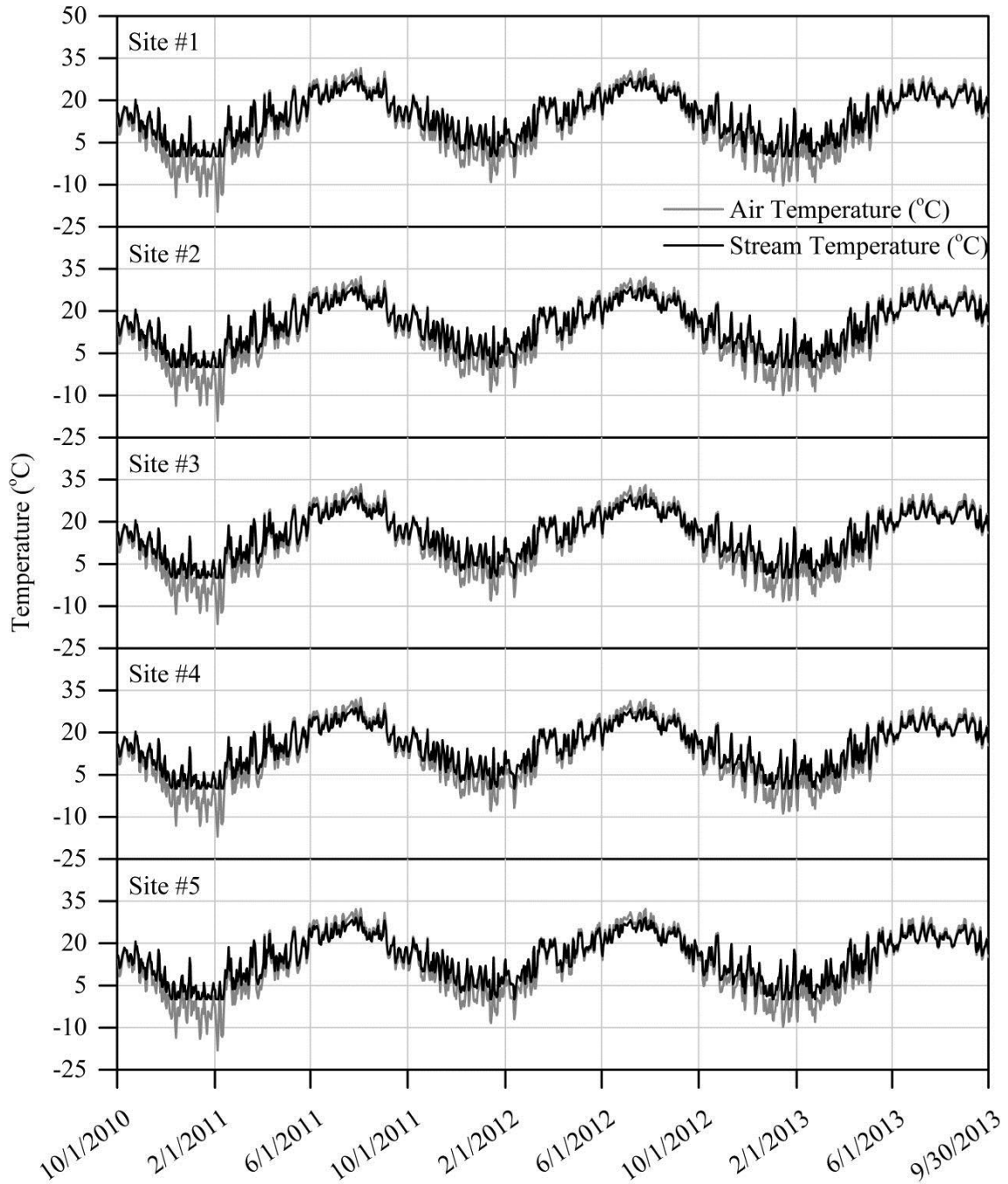
C10. Results from nonlinear regression model simulations showing daily time series stream water temperature from five gauging sites in Hinkson Creek for the three year study period. Measured air temperature data are shown as a refrence.
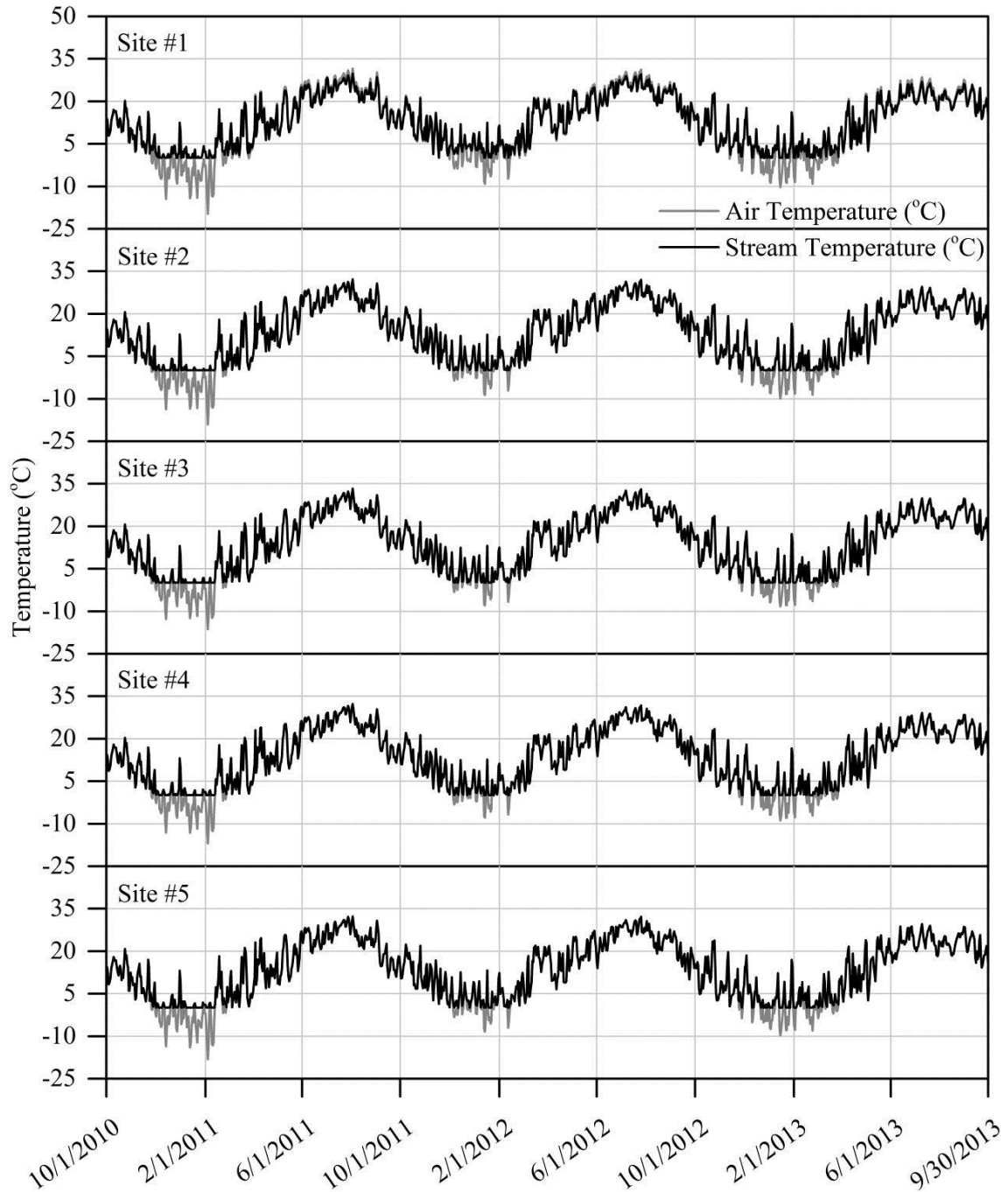
C11. Results from calibrated linear regression model simulations showing daily time series stream water temperature from five gauging sites in Hinkson Creek for the three year study period. Measured air temperature data are shown as a refrence.

Original SWAT Model (Daily)

C12. Results from the original SWAT stream water tempeature model simulations showing daily time series stream water temperature from five gauging sites in Hinkson Creek for the three year study period. Measured air temperature data are shown as a refrence.

Ficklin *et al.* (2012) Model (Daily)

C13. Results from Ficklin et al. (2012) stream water temperature model simulations showing daily time series stream water temperature from five gauging sites in Hinkson Creek for the three year study period. Measured air temperature data are shown as a refrence.

184